

– An international journal for New Concepts in Global Tectonics –

NCGT JOURNAL

Editor-in-Chief: Bruce LEYBOURNE (leybourneb@iascc.org)



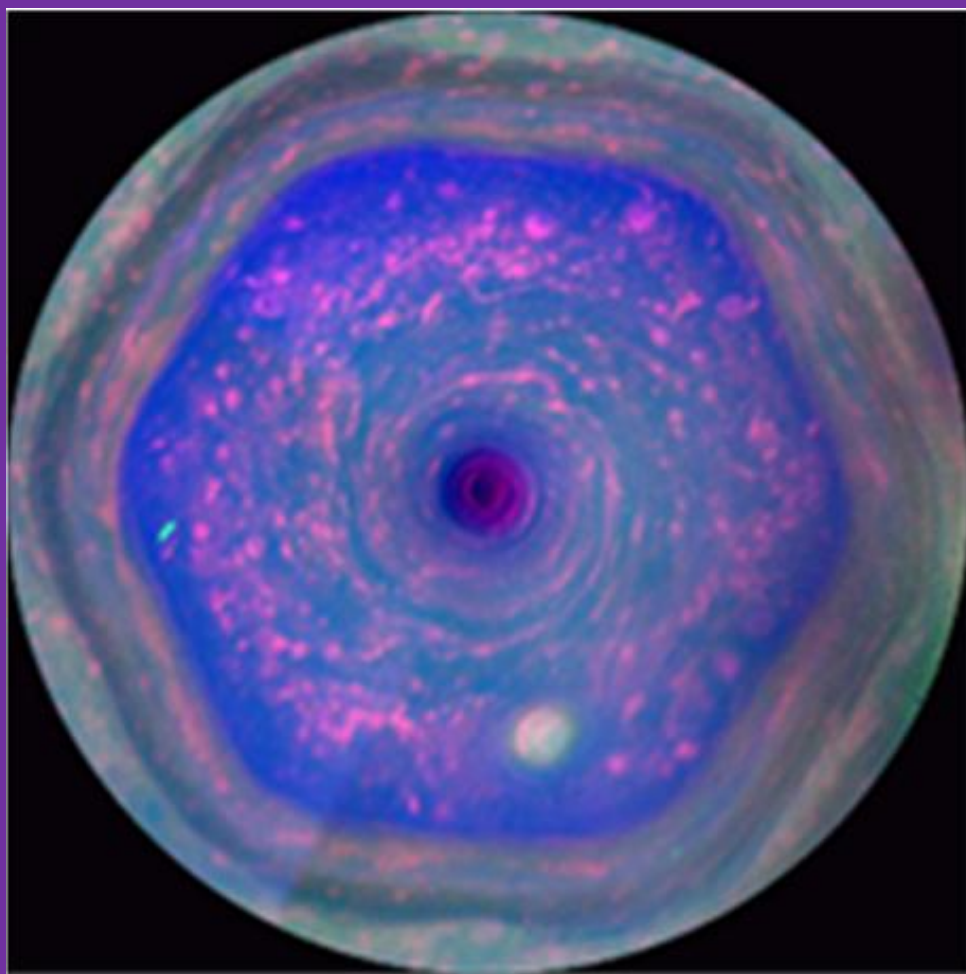
 NCGT Journal
New Concepts in Global Tectonics

Volume 14, Number 4
April 2026

Part 2

ISSN 2202-0039

WWW.ncgtjournal.com



Saturn's streaming hexagon

“In full view: This colorful view from NASA's Cassini mission is the highest-resolution view of the unique six-sided jet stream at Saturn's North Pole known as ‘the hexagon’. Image obtained on December 10, 2012 and released December 4, 2013.

Credit: NASA/JPL-Caltech/SSI/Hampton.” Figure and captions after Anonymous (2018f). NASA copyright free policy.

This issue : Fig .12 in The solar cycle and MiniMax - Effects on other planets. P 363.

Special Issue on
Air-Earth Currents

A collage of three images. The top left shows a view of Earth from space, showing the blue atmosphere and white clouds. The bottom left shows a volcanic eruption with bright orange and red lava flows. The right side shows the aurora borealis in shades of green and blue against a dark sky.

 NCGT Journal
New Concepts in Global Tectonics

Earth & Space

NCGT International Conference

September 21-24, 2026
Parma (Italy)

– *An international journal for New Concepts in Global Tectonics* –

NCGT



JOURNAL

Volume 14, Number 4, April 2026. ISSN 2202-0039.

EDITORIAL BOARD

Editor-in-Chief: Bruce LEYBOURNE, USA (leybourneb@iascc.org)
Co-Editor-in-Chief: Valentino STRASER, Italy (valentino.straser@gmail.com)
Masahiro SHIBA, Japan (shiba@dino.or.jp)
Giovanni P. GREGORI, Italy (giovannipgregori38@gmail.com)
Louis HISSINK Australia (louis.hissink@outlook.com)
Per MICHAELSEN, Mongolia (perm@must.edu.mn)
Biju LONGHINOS, India (biju.longhinos@gmail.com)
Vladimir ANOKHIN, Russia (vladanokhin@yandex.ru)

CONTENTS

PART 2

EDITOR'S CORNER - Comments by Editor in Chief - Bruce Leybourne.....	318
Announcements on Upcoming Conferences - "CALL FOR PAPERS"	318
Letters to the Editor.....	320
Online Book.....	321
Company Profiles.....	322
Article:	
The solar cycle and MiniMax: Giovanni Pietro Gregori, Bruce Allen Leybourne.....	323
The solar cycle and MiniMax - Effects on other planets: Giovanni Pietro Gregori, Bruce Allen Leybourne.....	362
About the NCGT Journal	388

For donations, please feel free to contact the Research Director of the Geoplasma Research Institute, Mr. Bruce Leybourne, at leybourneb@iascc.org. For contact, correspondence, or inclusion of material in the NCGT Journal please use the following methods: *NEW CONCEPTS IN GLOBAL TECTONICS*. 1. E-mail: leybourneb@iascc.org (files in MS Word or ODT format, and figures in gif, bmp or tif format) as separate files; 3. Telephone, +61 402 509 420. **DISCLAIMER**: The opinions, observations and ideas published in this journal are the responsibility of the contributors and do not necessarily reflect those of the Editor and the Editorial Board. *NCGT Journal* is a refereed quarterly international online journal and appears in March, June, September and December. ISSN number; ISSN 2202-0039.

EDITOR'S CORNER: - Comments by Editor in Chief - Bruce Leybourne**Announcements on Upcoming Conferences - "CALL FOR PAPERS"****21-24 September 2026 – NCGT in Italy****Organized by Valentino Straser (valentino.straser@gmail.com)****Timetable for participating in the conference:**

Open abstract March 1, 2026

Abstract acceptance May 31

Payment due by June 15, 2026 (To organizing committee)

Publication of conference and abstract book September 1, 2026

September 21-24, 2026, International NCGT Conference - Parma, Italy

**Regarding information for authors:**

Abstract: 150 words (maximum)

Short CV: 300 words (maximum) and a photo.

For formatting and fonts, use NCGT Journal.

Abstract submission opens March 15, 2026

Conclusion: May 31, 2026

Confirmation of abstract acceptance: June 15, 2026

Information website about the city of Parma and its province:[homepage - Informazioni turistiche su Parma e provincia](#)

Attempting for hotel with a meeting room in the center of Parma less than 500 meters from the train station.

"Earthquake Forecasting with Space Weather between Heaven and Earth" summarizes the contents of the NCGT 2026 Conference scheduled in Parma from September 21 to 24, 2026. The NCGT team returns after fifteen years, to discuss Earth model innovations and scenarios for understanding geophysical processes and space weather effects. And, more traditionally, new models of Global Tectonics.

Understanding the Earth today means looking beyond the traditional boundaries of geology and geophysics, combining expertise ranging from electromagnetism to atmospheric physics to space weather. The "Earth & Space" conference was born with this objective: to propose an integrated interpretation of geophysical phenomena, exploring the role of electromagnetic signals as potential precursor indicators of seismic events and analyzing the contribution of new technologies for data observation and interpretation.

In recent decades, studies inspired by the global electric circuit model, a concept developed from the insights of scientists in recent decades, have highlighted how the Earth's atmosphere, ionosphere, and planetary surface constitute an electrically connected system. From this perspective, processes occurring in the lithosphere, including those preceding an earthquake, could produce measurable variations in electromagnetic fields and ionospheric properties.

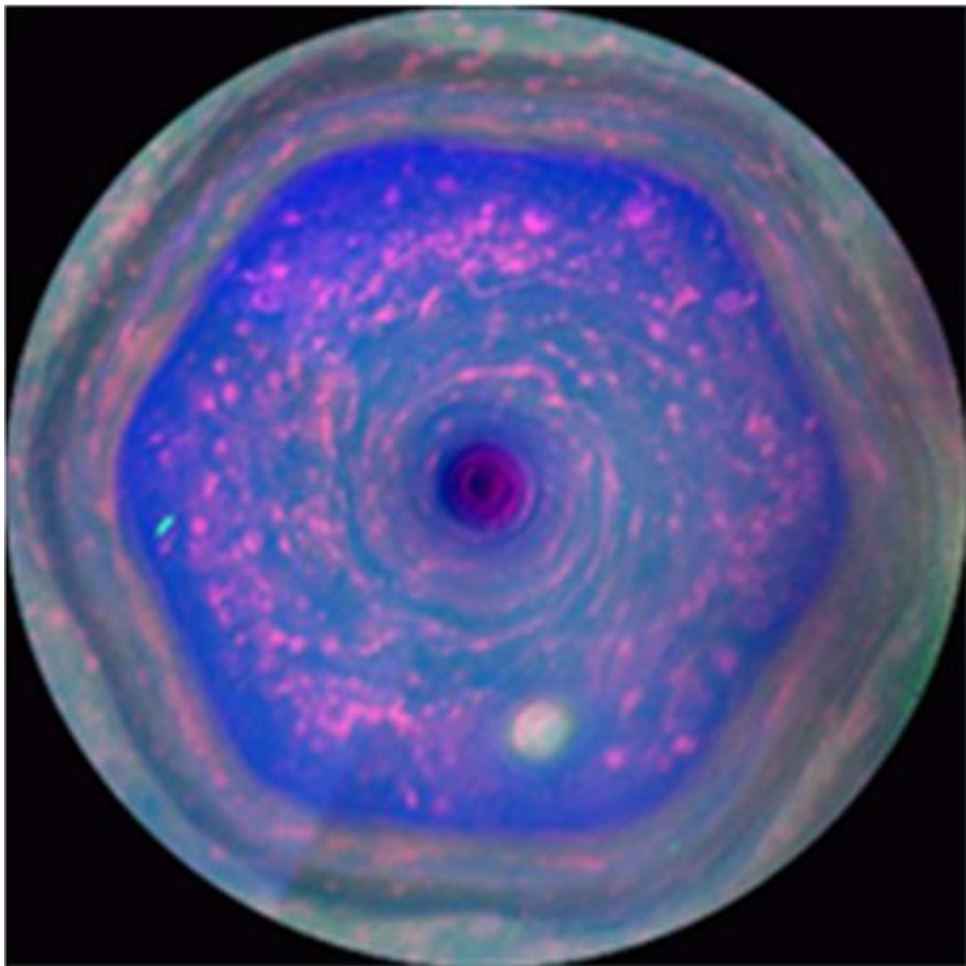
The conference aims to further analyze the so-called "candidate seismic precursors" of electromagnetic nature, evaluating their potential and limitations considering the latest scientific evidence. The integration of highly sensitive ground-based sensors, satellite networks, and ionospheric monitoring systems opens new perspectives in multi-parametric data collection and modeling of phenomena.

Special focus will be on the role of the Sun. Solar activity monitoring from NASA missions and international space weather programs, indicate influences in the ionosphere and Earth's magnetic field, have potential implications for climate and geodynamic systems. Understanding the interactions between the solar wind, the magnetosphere, and Earth's internal processes represents a crucial frontier for interpreting complex geophysical events from a systemic perspective. "Earth & Space" therefore proposes new interpretative concepts, encouraging us to move beyond compartmentalized visions to embrace a dynamic and interconnected model of the planet. Earth's evolution is not merely the result of endogenous forces but can be interpreted as the product of a continuous dialogue between space and the surface, between solar energy and deep-seated processes.

The conference is aimed at researchers, professionals, administrators, and citizens interested in understanding how new technologies and interdisciplinary models can contribute to a more advanced understanding of natural phenomena. It will provide an opportunity for scientific and cultural exchange to explore the future challenges of prevention, sustainability, and risk management on an increasingly complex planet.



- 1.) Straser - EQ forecasting (Abstracts requested)
- 2.) Leybourne - Stellar Transformer - Global Space Weather interactions (6 Abstracts in Editor's Corner within New Concepts in Global Tectonics Journal - Volume 12, Number 4, December 2024)
- 3.) Anokhin - Lake Ladoga - Siberia (2 Abstracts in Editor's Corner within New Concepts in Global Tectonics Journal - Volume 13, Number 1, March 2025 pp. 5-8, more abstracts requested)
- 4.) Longhinos - Indian Tectonics (Abstracts requested)



Cover Image : Saturn's streaming hexagon: "In full view: This colorful view from NASA's Cassini mission is the highest-resolution view of the unique six-sided jetstream at Saturn's North Pole known as 'the hexagon'. Image obtained on December 10, 2012 and released December 4, 2013. Credit: NASA/JPL-Caltech/SSI/Hampton." Figure and captions after Anonymous (2018f). NASA copyright free policy. **This issue : Fig. 12 in The solar cycle and MiniMax - Effects on other planets. P 363.**

Letters to the Editor: Giovanni Gregori discusses research papers

In the present series of papers on air-earth currents, the set is composed of:

Gregori, G. P., B. A. Leybourne, and G. Paparo†. Introduction – Anomalous lesser air-earth phenomena,

Gregori, G. P., and B. A. Leybourne. The electrostatic Sun

Gregori, G. P., B. A. Leybourne, and J. R. Wright. The solar cycle and MiniMax

Gregori, G. P., and B. A. Leybourne. The solar cycle and MiniMax - Effects on other planets

The first paper discusses a few items that are generally considered of lesser interest, although they are strictly pertinent to the discussion of air-earth currents. Since they were not included while dealing with other facets of our discussion, they are here outlined for the sake of completeness.

The second paper deals with the electrical charge of the Sun and of the solar wind that, at present, are erroneously assumed having a neutral charge. In contrast, a correct discussion leads to an unprecedented and clear explanation of the sunspot cycle, and this is an essential aspect for several items related to air-earth currents.

The last two papers present a concise reminder about phenomena related to some anomalies of the sunspot cycle, which imply peculiar effects either on the Earth or on planets, mostly on the large gaseous planets.

The next special issue of NCGT will contain an important historical witness by Prof. Martin T. Hovland, and a large synopsis of all recently appeared papers that, either directly or indirectly, deal with several aspects of air-earth currents. Altogether these papers are a “monograph” (of over 1,700 pages) dealing with a topic that was lacking since the time of Gauss. We hope by this having fulfilled an important gap for a correct understanding of several crucial features of solar-terrestrial relations.

New Book

G. P. Gregori (born 1938), Degree in Physics (1961, Univ. of Milan),

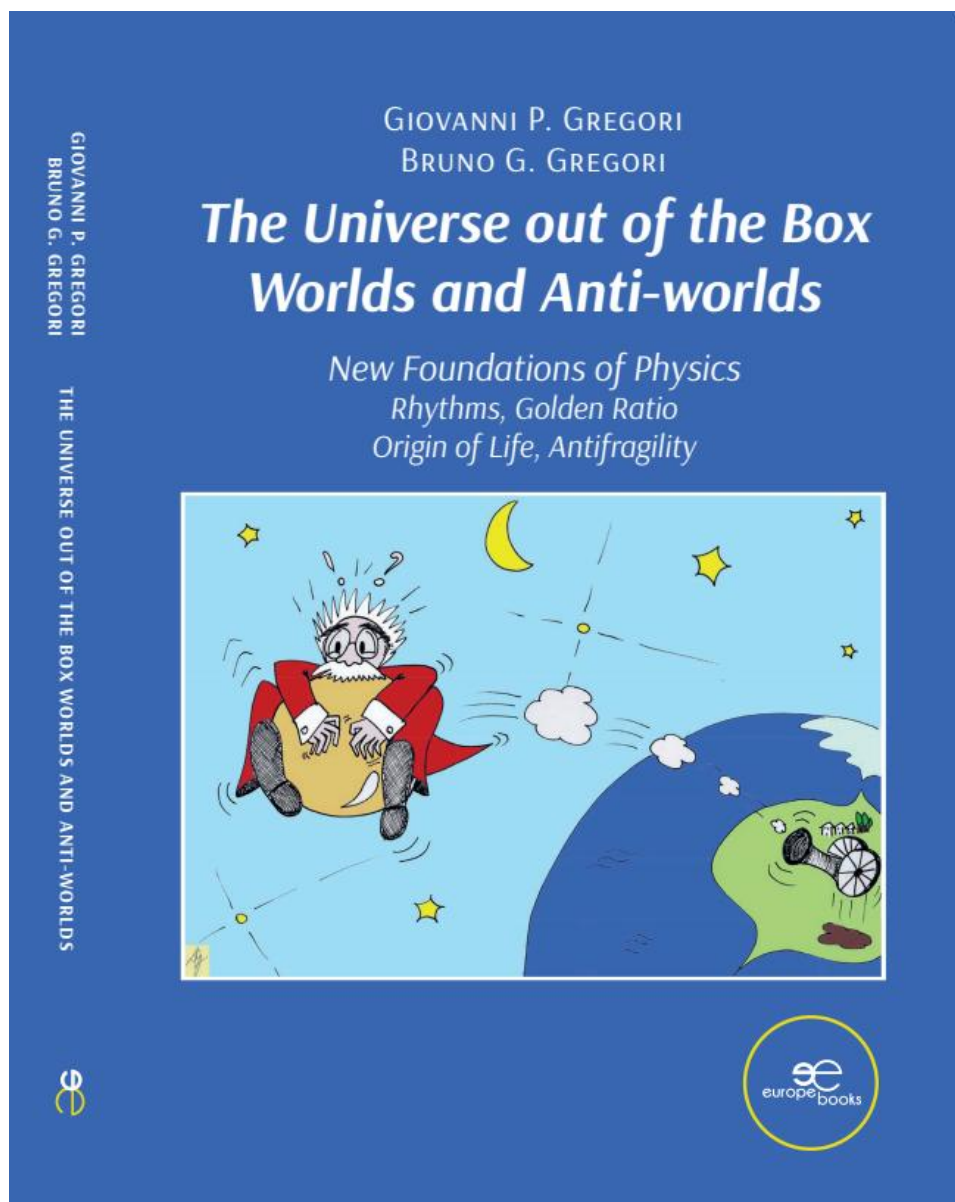
B. G. Gregori (born 1967), Degree in Medicine and Surgery (1992) and Specialization in Neurology (1999)

Science is suffering an identity crisis. Our “widespread scientific knowledge” is “static”.

Our mind dislikes uncertainty. Not relying on the mainstream is uncomfortable, but we gain better awareness of the world and of ourselves. This book is challenging. It stimulates the reader also on a psychological level, and tries to explain concepts that to most people consider abstruse. It is a journey where mind can dance between quantum physics, cosmology, theology, Greek philosophy and the mystery of life and death. Science is logic, and a scientist can never give up. Many present unsolved paradoxes can find a solution.

At present, we are biased by: 3 “original sins” in Newton’s principles, by an Einstein’s mistake, and by a misconception of “absolute” time and of the perception of time passing. A new formulation is presented, which is a substantial advancement compared to Galileo, Newton, Maxwell and Einstein.

<https://www.europebookstore.com/products/the-universe-out-of-the-box-worlds-and-anti-worlds-g-p-gregori-and-b-g-gregori/>



Company Profiles:

Tesla 3D, Inc. is an independent research and development company with a strong applied science foundation, enabling rapid and practical innovation in the energy and exploration sectors. While not a large enterprise, Tesla 3D, Inc. stays well informed about breakthroughs in electrical generation, storage, and mining technologies. When called upon, the company can comprehend complex challenges and develop strategic, real-world plans that effectively navigate regulations, funding mechanisms, and policies. Tesla 3D, Inc. actively contributes to national and industry advancement through volunteer leadership, including participation in the Homeland Security Taskforce focused on energy resilience and EMP (electromagnetic pulse) threats. The company also set a precedent by independently qualifying for federal Innovation (R&D) Tax Credits; demonstrating that small, agile innovators can leverage these incentives to streamline regulatory solutions and tackle critical infrastructure challenges. This involvement underscores Tesla 3D, Inc.'s commitment to advancing energy security and shaping the transformative role of technology in resource development. Founded: 2011 Colorado by R. Miller.

Geo-Transect LLP (www.tgeo.co.in) Geo-Transect LLP is a knowledge-driven geoscience consultancy, specializing in subsurface exploration and environmental intelligence across India. With core expertise in subsurface mapping, groundwater zonation, aquifer recharge quantification, coastal and shoreline analysis, landscape and topological planning, and island conservation, the firm delivers data-driven insights that empower sustainable planning and development. Representing the forefront of India's earth-science services sector, Geo-Transect blends scientific precision with advanced technologies to support governmental, industrial, and research-based initiatives across southern India and beyond. Integrating indigenous knowledge with global best practices, the firm is committed to environmental stewardship and responsible resource management. Guided by the ethos "With Wisdom in Nature," Geo-Transect envisions a future where scientific understanding harmonizes development with the natural world.

Stellar Transformer Technologies (<https://stellartransformertechnologies.com/>) is a private geophysical modeling company specializing in modeling the dynamic electro-magnetic Stellar Transformer interactions between Earth-Sun and planets within our solar system. Original research started in 1995 by the current owner and founder during investigations of the seafloor as a geophysicist with the Naval Oceanographic Office at Stennis Space Center. Leading to an understanding and application of new tectonic theories. Later research confirmed dynamic links to space weather affecting a myriad of environmental factors: such as everyday weather; hurricanes; tornadoes; sever weather outbreaks; earthquakes; global climate-change; and certain types of wildfire outbreaks from passing coronal mass ejections induced by internal core generated Electro-Magnetic Pulses (EMP). Current and planned services include mapping of Stellar Transformer circuits; innovative modeling of deep earth magnetics, forecasting Earth's natural hazards listed above; database development and more. Combining big data and AI to find inter-relationships. Developing algorithm inputs for forecasting, data visualization and simulations. All leading to new forecasting technologies. We are actively assisting the EMP Task Force power grid protection efforts with direct input and evaluation of EMP threats. Our company comprehends the complex challenges of geophysical modeling and development of real-world forecasting applications. Electro-magnetic or magnetic induction is the production of an electromotive force, or voltage, across an electrical conductor in a changing magnetic field. The Stellar Transformer Concept contends that simple step-down energy induction occurs between Sun and Earth, much like the transformer process that steps down your household energy from higher voltage transmission lines sourced from the power company. The Sun represents a large coil from the power company, while the Earth represents the smaller coil to your home. The larger coil element generally excites current into the smaller coil element by induction of "step down energy", although lesser feedback mechanisms occur due to the action/reaction principles. Layers within the Earth hold and release charge acting as condensers, or capacitance layers. Thus, the Earth operates somewhat like a battery where energy is either stored or released through time-change of state-of-matter. We combine new Geophysical Intelligence with AI for a winning combination of innovations that will bring new mitigation strategies for space weather to the forefront. Bringing a paradigm shift to the business community for global environmental forecasting based on solar and planetary effects. This will save lives and mitigate property damage using new science and innovative technologies. Many of these ideas were first presented at EU2015 - Electric Universe (<https://www.youtube.com/watch?v=IoggZhbxxhU>). Followed up at EU2016 with discussions on geometrical modeling applications, adhering to golden ratio principles (<https://www.youtube.com/watch?v=Q355Haapq-0>). Founded: 2023 in Colorado by Bruce Leybourne – Owner/Operator.

The solar cycle and MiniMax

Giovanni Pietro Gregori^{1,2}, Bruce Allen Leybourne², John Ricken (Rickmo) Wright⁴

¹*IDASC-Istituto di Acustica e Sensoristica O. M. Corbino (CNR), Roma, now merged into IMM-Istituto per la Microelettronica e Microsistemi (CNR) and ISSO-International Seismic Safety Organization, Italy*

²*GeoPlasma Research Institute-(GeoPlasmaResearchInstitute.org), Aurora, CO 80014, USA*

⁴*Emeritus Professor of Chemistry, Southeastern Oklahoma State University*

Corresponding Author: G. P. Gregori, *IDASC-Istituto di Acustica e Sensoristica O. M. Corbino (CNR), Roma, now merged into IMM-Istituto per la Microelettronica e Microsistemi (CNR)*;
Email:
giovannipgregori38@gmail.com
leybourneb@iascc.org
rw4946594@gmail.com

Abstract: Sunspots and sunspot cycle are the object of a gigantic old literature. We focus here on four items. Two items deal with the old-fashioned and largely subjective definition of sunspots and their trend vs. time. One “old-fashioned” analysis deals with the solar cycle length (SCL) according to studies carried out by the Tang MaoCang school in China, which is generally poorly known in the western world. The second “old-fashioned” analysis is the seemingly most updated study available in the literature. Conversely, a third item deals with a much more objective and rigorous probabilistic approach by means of machine learning (ML) and artificial intelligence (AI), i.e. generalized wavelet analysis, combined with Bayesian statistics. This monumental innovative approach implies a substantial improvement of understanding of the observational interpretation of sunspots and of the solar magnetic fields. The fourth item deals with the anomalous very low (minimum) of the maximum of the solar cycle (MiniMax), which seems to have a significant impact on climate. This impact is here briefly discussed. Every cycle is characterized by a cycle amplitude, and by a cycle duration. The physical mechanisms are also discussed that can eventually support the electrostatic model of the solar cycle, which is discussed in an accompanying paper (Gregori et al., 2025s). On a statistical basis, a low solar activity is reported, unanimously correlated with a comparatively milder climate. This conclusion seems, however, contradicted by the recent MiniMax cycle. This inference agrees with the expected dominant dependence on the time-delay between endogenous heat production by the TD dynamo, and energy release at Earth’s surface through air-earth currents. In fact, the MiniMax occurred during a heartbeat of the Earth’s electrocardiogram, when the time delay is null. Conversely, during the entire time span of human history and of several proxies, the time-delay was varying, even up to ~27.4 Ma. Hence, the seemingly higher impact on climate during active Sun derives from the time-delay of the release of endogenous energy. If this is correct, no direct correlation must be expected between a single solar cycle and climate, unless observations are carried out during a maximum of an Earth’s heartbeat. A leading factor of climate is thus represented by the encounters of the Solar System with clouds of interstellar matter, which control the solar dynamo and activity, hence the cycle morphology due to a modulation of the solar wind, in a perspective of Galaxy-Sun-Earth relations.

Keywords: sunspot cycle (amplitude and duration) – standard subjective definition – artificial intelligence analysis - MiniMax — climate proxies – solar magnetic field – impact on climate - dependence on the time-delay between endogenous energy production and release at Earth’s surface

Introduction

The physics of the Sun and of stars is a huge discipline started when Larmor (1919, 1919a, 1920) proposed the explanation of the solar magnetic field B by means of what was later called an MHD dynamo powered by endogenous thermonuclear reactions. The focus of the present paper is rather on the control by MiniMax on the atmospheric electrical circuit, hence on air-earth currents and on climate.

A previous paper (Gregori et al. 2025s) illustrated the electrostatic model of the Sun, and of the solar cycle. The present paper is an attempt to understand how that standard

approach to the solar cycle – by means of sunspots and other proxies – can match with the electrostatic nature of the Sun.

A warning, however, is that the literature mixes the role of the total length of a solar cycle, and of the amplitude or intensity of the sunspot cycle, plus other minor morphological details. The overall picture results therefore somewhat confused, and often controversial.

In addition, the same definition of sunspot group must be considered. The historical standard way is largely subjective, while a more recent and rigorous approach relies on artificial intelligence (AI). The analysis is bottom-up, i.e. one relies on observations, and attempts to interpret their implications, in terms of a presumed repetitive cyclic

morphology. A fundamental bias is, however, related to the inhomogeneity of the available historical data series. The old-fashioned standard approach is based on “reasonable” assumptions of uniformity of the data series, and some arbitrary criteria are used for comparing information by different authors, using different instruments and assumptions. In contrast, the approach by means of *AI* and of Bayesian statistics is strictly objective, and – indeed – it represents a recent substantial improvement, also concerning the connection between sunspot observation and solar magnetic fields.

From the huge literature dealing with the old-fashioned approach, we report only the analysis carried out on the solar cycle length (*SCL*) carried out by the Tang MaoCang school in China, as these investigations are generally poorly known in the western world. In addition, we highlight some seemingly better updated investigations according to the old fashioned standard approach. Then, we report the most recent and rigorous approach by means of *AI* including the inferred much improved evidence of the temporal trend of solar activity. The final topic is the connection of solar cycle with climate, which is the object of a huge and extensive literature. We focus on the recent singular anomalous MiniMax.

MiniMax is the name given to cycle 24, which displayed an anomalous minimal height of the maximum amplitude of the sunspot cycle. MiniMax is suspected to have close relationships with climate anomalies.

Therefore, a concise reminder is first given about some historical items concerned with the definition of the solar cycle, which is the needed prerequisite to discuss the MiniMax. On the other hand, the investigations on the sunspot cycle is an old classical discipline and a whole devoted volume should be needed to review this item. We focus here only on a few items required for the discussion of MiniMax.

A subsequent paper (Gregori et al. 2025u) deals with the impact of MiniMax on the other planets that can operate like probes suited to monitor the state of the solar wind at large distances from the Sun.

The sunspot cycle – Some historical items

The concept of sunspot number is often misunderstood, as it is only a simple index referring to some unknown phenomena that are in progress inside the Sun. In contrast, we evaluate the sunspot index relying on observations that depend on the available instrument. Hence, the role is fundamental of the empirical constraint. Sunspot observations had therefore an evolution *vs.* time, and it is difficult to compare one another the information provided by different observers at different epochs.

In this respect, we stress that, similarly to human observations *vs.* time, the analysis of every proxy datum – such e.g., a tree ring – is biased by several disturbances. However, unlike for men’s observations, the tree ring or

every other natural “detector” is always the same *vs.* time. Hence, a proxy datum deals with an objective and uniform information that is independent of the epoch – as far as the datum, i.e. tree rings or other, can be clearly detectable.

Only during a comparatively recent time, a series of a few devoted workshops (see e.g. Cliver et al., 2015 and Clette et al., 2016, and references therein) were concerned with the critical analysis that must be systematically carried out of the original, old-fashioned historical data and methods. The target is to provide a final assessment of this index, which in any case is a unique available historical long series of direct observation referring to the Sun and to its evolution.

The most recent, and more rigorous and objective approach in terms of *AI* is later discussed relying on the extensive and far-looking gigantic study carried out by Velasco Herrera et al. (2021, 2022). Concerning the old-fashioned database, a reference paper is Clette et al. (2014) that contains a long and detailed discussion of sources and methods. Only their conclusion is here reported.¹ Clette et al. (2014) begin and describe the standard, classical, definition of sunspot number (*SN* or *SSN*). The classical definition by R. Wolf (1851, 1856)² is

$$R = k(10 \times N_g) + N_s \quad (1)$$

where N_s is the total number of sunspots, N_g is the number of sunspot groups, k is called scaling coefficient, or also personal coefficient of the observer. The personal coefficient is aimed to obviate to the arbitrariness of every observer (depending on telescope aperture, local seeing, personal experience) when he estimates the number of recorded sunspots, and also of how he defines and splits groups of sunspots. Wolf was conventionally associated with the $k = 1$ personal coefficient. Wolf called R the “relative sunspot number”. This R is often also called “Zürich sunspot number”, or W in honor of Wolf. Other standard names are R_z and R_i corresponding, respectively, to the periods before and after 1981.

In the 1970s a new index became fashionable, i.e., the $F10.7\text{cm}$ background radio flux. In fact, somebody contended the subjectivity of purely visual and manual sunspot counts, in contrast with an objective instrumental record. Note, however, that every index refers to one facet of a multifaceted phenomenon. No two indices can *per se* refer to the identical aspects of the physical system. No two indices will result exactly correlated each other, as every index deals with physically distinct information. Thus, every couple of indices has a partially correlated and a partially uncorrelated component. In addition, the prize of a data series is the total span of the available time interval. In this respect, the *SN* time series is the only available direct historical record capable to retrace the long-term evolution of the solar cycle. Therefore, in this respect, it is nonsensical to abandon the old-fashioned *SN*.

In addition, as mentioned *passim* in the present set of papers on air-earth currents, and very often in the literature,

of astronomy at both the *University of Zürich* and the *Federal Institute of Technology* in Zürich.

¹ A shorter account is given by Vaquero et al. (2016).

² Johann Rudolf Wolf (1816-1893), Swiss astronomer and mathematician. After 1855 he was appointed Professor

other proxies (such as tree-rings, or glacier layers, or in general several sedimentary layers of various kind) can provide with longer data series.

In some way, these proxies are even more objective than manmade observations and reports. On the other hand, every datum has some intrinsic bias. However, in general, the comparison of different evidence can help to discriminate between different drivers and effects.

Several studies rely on the standard SN series that can be reconstructed and expanded by means of a mixture of different composite time series assembled by means of some inhomogeneous proxies. Therefore, the accuracy of the solar cycle reconstruction decreases as we go back in time.

Mostly, before the 19th century the observational database is scant. Hence, owing to the poor available information prior to 1700, Wolf missed the important Maunder minimum episode.

A new long-term series was assembled by Hoyt and Schatten (1998a, b). In fact, Schaefer (1993) had warned that the SN is largely proportional to the group count alone. Hence, Hoyt and Schatten defined the group number as

$$R_G = \frac{12.08}{N} \sum k_i N_{gi} \quad (2)$$

where N_{gi} is the number of sunspot groups recorded by the i th observer, k_i is the personal scaling factor of the i th

observer, N is the number of observers used to compute the daily value, and the constant 12.08 is empirically defined in order to standardize the new GN series to the same scale as SN . Hoyt and Schatten (1998a, b) relied on the Greenwich sunspot catalog, which is constructed by means of the Greenwich photographic plate collection spanning the interval 1874-1976 (Willis et al., 2013). In addition, Hoyt and Schatten integrated the database with the visual *USAF/SOON* group counts, spanning 1976-1995. Thus, Hoyt and Schatten afforded to derive daily, monthly and yearly means during 1610-1995.

An additional improvement was made by Hoyt et al. (1994) by means of clever interpolations between sparse observations. The number of recovered observations was thus approximately doubled, and the series was extended until the very first telescopic observations.

In addition to a long discussion of sources and methods, Clette et al. (2014) consider advantages and points of weakness of the SN vs. GN data series. In fact, before ~AD 1880 a substantial discrepancy was found between the SN and GN series, as R_G falls ~40% below R_Z . Only the final result is here shown in Fig. 1 (after Cliver et al., 2015), but see also Clette et al. (2016) who briefly consider the different more recent sunspot data-series that were computed by different authors.

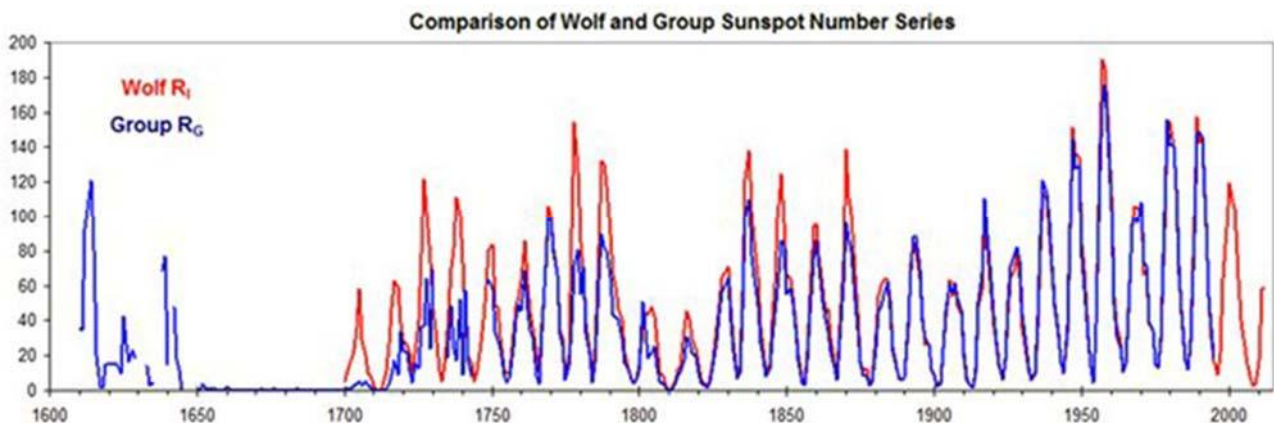


Fig. 1. Comparison of yearly mean values of the Wolf number R_I with the Group R_G SSN time series. The figure, adapted from Hoyt and Schatten, 1998b) was published also in Cliver et al. (2015). With kind permission of the *Observatory*.

With reference to the evidence discussed by Gregori and Leybourne (2026b), the distinction between low and large SN is not related to solar “activity” in terms of released solar energy. In fact, the so-called “quiet” Sun periods display fewer sunspots and a few groups of sunspots. In contrast, the phenomenon shows only a concentration of all sunspots into a few groups, or even in one group alone. This is shown also by the coalescence of filaments and by the lognormal distribution of sunspots. That is, several huge “electron guns” or “van de Graaff generators” coalesce into a few or a unique giant “van de Graaff generator”. Therefore, maybe, the released energy is either the same or, perhaps, even larger. Differently stated, it seems that, after migrating to heliocentric latitude as per the well-known butterfly diagram, several “electron guns” merge and coalesce into a unique giant “van de Graaff generator”.

In any case, the solar corona expansion, and the solar wind, are accordingly influenced. Hence, the low-frequency of the electromagnetic (e.m.) signal transported by the solar wind is substantially changed. Differently stated, the most common observed configuration of the Parker’s spiral pattern of B_{int} is divided into 4 sectors (i.e., $+ \rightarrow - \rightarrow + \rightarrow -$) (see Fig. 3 of Gregori and Leybourne, 2026b). Conversely, when all sunspots coalesce into a unique large group, the Parker’s spiral B_{int} pattern is modified into 2 sectors (i.e., $+ \rightarrow -$). Hence, upon considering an average 27 days rotation period of the Sun, during standard solar activity the leading period of the e.m. induction by B_{int} in the deep Earth’s or planetary interiors is $\sim 27/2$ days. Instead, with “quiet” Sun the leading period is ~ 27 days. Hence, the skin-depth of penetration of the e.m. induction is deeper, hence the control is more efficient on the TD (tide

driven) dynamo, either of the Earth or of every planetary object (see Gregori and Leybourne, 2021 and references therein).

Clette et al. (2014) summarize as follows the main conclusion of their careful analysis. Before AD 1800, the available sunspot records are biased by poor observations. In contrast, the better series for the more recent epoch is mainly characterized by three main inhomogeneities, i.e. during 1880-1915 for *GN* and in 1947 in 1980-2014 for *SN*. Some additional corrections were therefore computed and some inferences were thus achieved concerning solar activity during the last 400 years.

A progressive decline of solar activity is evident before the onset of the Maunder Minimum. As well, the slowly rising trend is strongly reduced, which characterized solar activity after the Maunder Minimum. Hence, by the middle of the 18th century, solar activity had already recovered to the intensity comparable to the more recent solar cycles of the 20th century.

Additional discussion borrowed after Clette et al. (2014) is given below concerning the MiniMax. However, note that, at present, upon considering the comparatively recent proposal of the *GN* series, the whole literature - which is here mentioned - in general often relies on the old-fashioned *SN* series.

In any case, the intrinsic logical limit ought to be taken into account of any kind of a 1D index. In fact, owing to definition, an index is always *per se* a self-limiting indication, suited for a first-order approximate characterization of a natural system - with no real physical implication other than being suited for characterizing some more or less "anomalous" apparent behavior of the system. As far as the present study is concerned, these items about solar indices must be better considered within the framework of the discussion of solar processes, which are outside the target of Earth's sciences. According to the aforementioned rationale, this sunspot solar cycle can be the evidence of an electrostatic cycle, associated with the non-vanishing total Coulomb charge of the solar wind (Gregori and Leybourne, 2026b).

In contrast, the physical explanation that was extensively investigated in the literature deals exclusively with a Larmor dynamo, and with its instabilities. The Larmor dynamo certainly seems to be the most likely mechanism for the generation of the solar **B**, with all its observed features. The concern is, rather, about the primary perturbation that triggers an instability capable to reverse the Sun's **B**. This can be, e.g., either a tidal action originated by the whole planetary system on the Sun, or even by an electrostatic unbalance, or by both these causes that sometimes can, perhaps, eventually exchange their leading role. In fact, they can be eventually co-responsible for the trigger. In other words, in principle several concurrent different causes can be responsible for the morphology of solar activity, including also the encounters of the Solar System with interstellar matter - as stressed in Gregori (2002) and Gregori and Leybourne (2021).

Upon mentioning only the conclusion, the feeble tidal influence on the Sun must, perhaps, be considered that is

caused by all its planets. This item has been debated, and is somewhat controversial, but Figs 2 and 3 seem to prove that the effect is real and concrete. These figures plots vs. time the *CMSS* (center of mass of the Solar System) and the *SCMSS* (speed of the center of mass of the Solar System).

For the sake of completeness, some intriguing case histories were investigated by astrophysicists concerning stars affected by a large tidal perturbation, caused either by a large close planet, or by a companion star. The observed magnetic field **B** of these stars is therefore a convenient natural laboratory to test theoretical expectation.

In any case, more or less seldom in the literature, some authors revive the hypothesis of a possible tidal influence by the planets on the Sun. The effect is certainly very faint in terms of energy content. In some respects the effect is almost negligible, but the phenomenon exists. Maybe, it is responsible for triggering an instability on the Sun, whenever the Sun is eventually close to becoming unstable. This inference applies to the Sun, independent of the mechanisms that determine its state and evolution (i.e., either appealing to an electrostatic phenomenon as it is here guessed, or to any other kind of physical process, *MHD*, or gravitational, etc.). This effect, if it plays a real and concrete role, gives justice for the physical significance of solar cycles of period much longer than the best-known sunspot cycle. That is, solar physics is not only controlled by the erratic encounters of the Solar System with interstellar clouds of matter (as stressed in Gregori, 2002 and Gregori and Leybourne, 2021).

An objective and more far-looking analysis relies on *AI*, combined with a probabilistic approach relying on Bayesian statistics, which represents a new benchmark in the analysis of the solar cycle.

We discuss therefore first the analysis of the *SCL* according to a study implemented by the Tang MaoCang school in China. Then, we discuss the seemingly most recent inference based on the standard old-fashionable approach.

Then, we discuss the rigorous formal and more objective analysis in terms of *AI*, and we show how the newly available evidence can fit or not with the ancient results.

The last item deals with the discussion of the climate impact as inferred by MiniMax.

A discussion of the changes of solar cycle length (*SCL*)

The way must be considered by which the solar cycle can be computed. The simplest way is by direct visual inspection of the plot of sunspot number vs. time. A more formal approach is discussed by Lockwood and Fröhlich (2007, 2007a). They superpose different diagrams, and every diagram was obtained by applying - to the unsmoothed data series - a filtering by means of a moving average. That is, they used a square-box filter, i.e., an unweighted mean over a moving constant-amplitude interval. Owing to the role played by aliasing, the superposition of these different plots gives clear evidence for the solar cycle length (*SCL*) and of its variation.

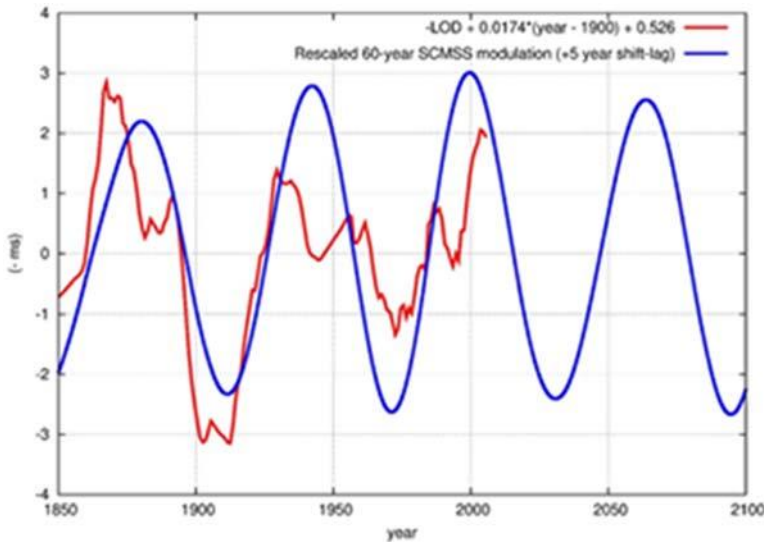


Fig. 2. Length of the day (red) vs. the 60 year modulation of the SCMSS (blue), which is derived from the Jupiter's and Saturn's combined orbits. The SCMSS is shifted by +5 years and opportunely rescaled for a better visual comparison. The *l.o.d.* is inverted and detrended of the linear trend. The correlation between the two records is evident. A black-and-white version of this figure is shown by Scafetta (2010). The present improved figure is reproduced by courtesy, and with kind permission, of the author.

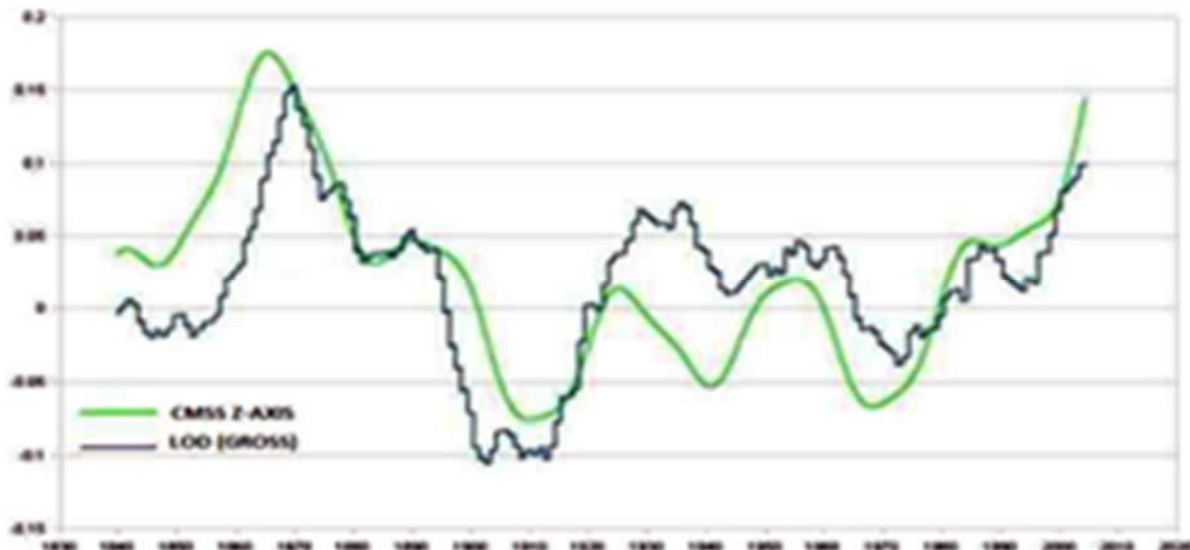


Fig. 3. “z-axis motion of the CMSS relative to the solar equatorial plane plotted against the length of the day (*l.o.d.*) (Gross, 2007) 1840-2005.” Figure and captions after Tattersall (2013a). With kind permission of *Pattern Recognition in Physics* (“Open Access”) and of Roger Tattersall.

Lockwood and Fröhlich (2007, 2007a) comment that their estimate of the temporal variation of SCL “does not appear as similar to the inverse of the global temperature anomaly as has been reported elsewhere (Friis-Christensen and Lassen, 1991). This is because it has not been smoothed with the long time-scale filter used in those studies.” In fact, this former well-known result by Friis-Christensen and Lassen (1991) triggered several subsequent analogous studies, which raised however controversial evidences and debates. The former evidence showed a good correlation between the variable period of the ~ 11 year sunspot cycle and the mean temperature at the Earth's surface over the Northern Hemisphere (NH) during 1865- 1985.³ The origin of these discrepancies was probably associated to different

filtering techniques, whereby the aliasing played a different role.

Let us only remind about some information⁴ on the investigations carried out by the school of the late Professor Tang MaoCang (see also Gregori et al. 2026e, 2026f, 2026g, 2025 h).

Feng and Tang (1997) considered a single SCL series, spanning over 2500 years (Fig. 4), with a mean SCL of 11.07 years, and investigated whether this curve can be correlated with climate temperature in China. They carried out a power spectrum analysis of the SCL series and found significant periodicities, respectively, at 200, 76.9, 50, 41.6, 22, 11.1 and 5.6 years.

³ No systematic review of this topic is here given. Refer e.g. to Lassen and Friis-Christensen (1995), or as an example of opponents, e.g., to Schröder and Treder (1996).

⁴ We are indebted to Dong WenJie and to Gao Xiaoqing for providing some crucial information that we updated by means of subsequent literature, eventually relying only on the English abstracts of papers written in Chinese.

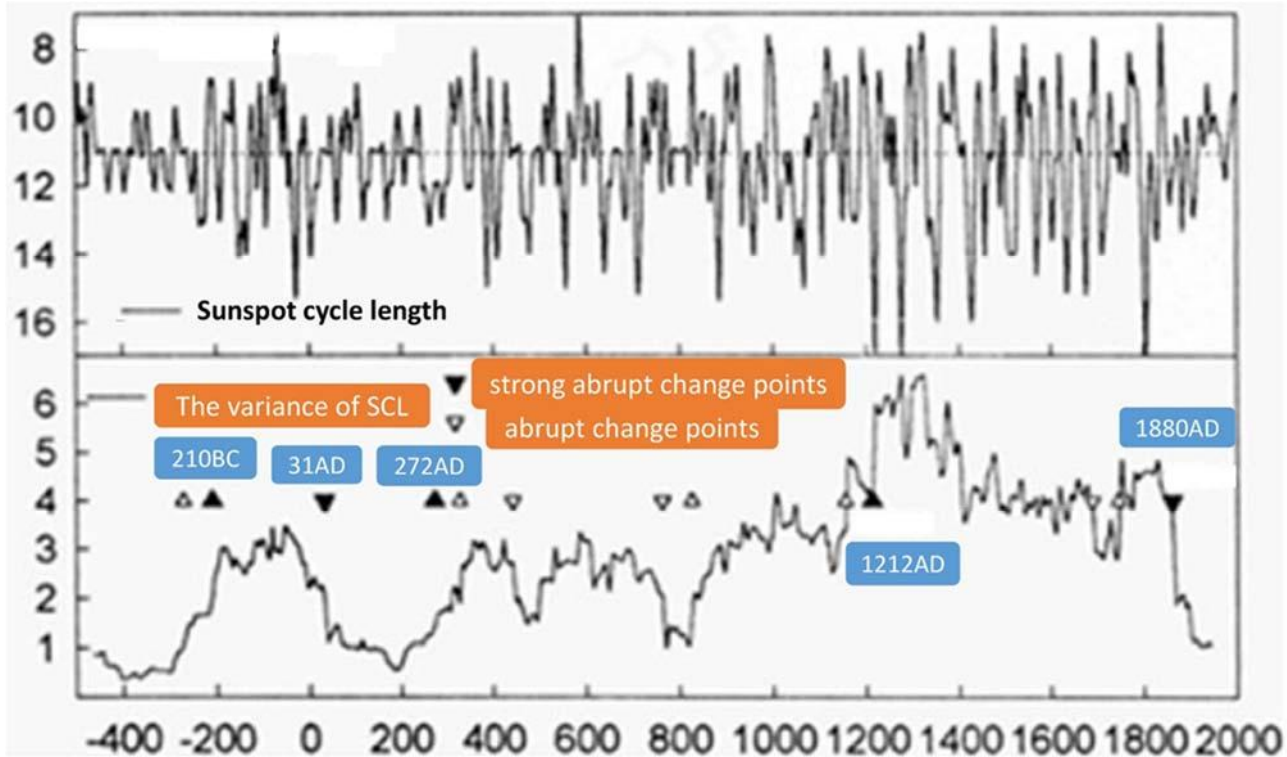


Fig. 4. The SCL and its variance during the last 2500 years. After a preliminary note by Feng Song and Tang Maocang. Unpublished figure.

The 200 and 76.9 years periods are close to the well-known centennial time-scale solar periods, i.e., the Suess-de Vries cycle (210 year) and the Gleisberg cycle (between ~ 80 – 90 year), respectively. However, a reminder is also about the vaguely evidenced periodicity of roughly ~ 60 years in geomagnetic records, often reported in a large literature (not here listed for brevity purpose). Error bars in different data series play a devastating role in their respective period definition.

The 41.6 years period is close to the intriguing roughly ~ 40 – 45 years period found in several climatic series, i.e. the ~ 42.7 years that was found in the series of climate anomalies in the Tanaro valley (a right affluent of Po) and the possible relation with volcanic activity, or the 42.85 year periodicity in the historical Hungarian aurora, or in the Hudson Bay beach (no details are here given for brevity purpose). If this is a real phenomenon - since climate looks sensible to this period alone, better than to others - according to the rationale of the present study this means that the Earth's TD geodynamo has a resonance - or relative maximum performance - tuned at this period, in addition to the 6th harmonic of the ~ 22 years Hale solar cycle (Alessandrini et al., 1987). Note, however, that also every higher harmonic of some other cycle is more or less amplified depending on whether the Earth resonates on it, or not.

These phenomena ought to be considered in the framework of the Fibonacci's regularity of the Solar System envisaged by the Tattersall's (2013, 2013a, 2013b) analysis of the gravitational interaction inside the Solar System (see Gregori et al., 2022).

Feng and Tang (1997) applied a 15 point running mean and identified 10 short cycle and 9 long cycle stages, respectively. In addition, they claim that 3 maxima and 6 minima stages of solar activity - that were derived by ¹⁴C - more or less agree with the short and long period SCL stages. They guess therefore that the SCL time series can be considered reliable also on the longer time range.

Then, they searched for possible relations with three temperature curves – two of them derived from ice cores ($\delta^{18}O$)-related to climate in Eastern China, i.e., the “Zhu's temperature series” Tibet Plateau (Guliya ice core), and Arctic region (Greenland ice core), respectively. They found the following results.

- i. Longer SCL are correlated with colder Earth's temperature. The shortest (longest) episodes of SCL coincide with the warm (cold) periods. The corresponding (number of episodes) ratios are for Zhu's temperature 14/19, for the Guliya ice core $\delta^{18}O$ 12/15, and for Greenland's ice sheet $\delta^{18}O$ 14/15, respectively. Hence, they concluded that the temperature fluctuation in the Arctic region appears particularly sensitive to solar activity. By the way, this is consistent with the location of a vertex of the tetrahedron under the North Pole that must therefore be expected to be particularly sensible to the modulation by a varying e.m. induction by the solar wind into deep Earth (Gregori and Leybourne, 2021).
- ii. The shorter are the short SCL episodes, the shorter are also the warm periods of Earth's temperature. Symmetrically, the longer are the long SCL episodes, the longer are also the cold periods of Earth's

temperature. Upon comparing the central years of either the *SCL* episodes or the climate temperature periods, almost all central years of the short (long) *SCL* periods anticipate the central years of warm (cold) period of Earth's temperature. The number of case histories that satisfy this rule are, respectively, in the three aforementioned temperature series, 8/8, 11/12, 10/12, and their corresponding mean advance years are 10.6, 25, 12.5 *years*, respectively.

iii. In addition, they claim that the *SCL* data series seems to be suited to describe also lesser temperature fluctuations in China. In this respect, they mention the following case histories.

Although it was relatively warm during $\sim 300 - 44$ BC, a cold climate occurred during the Qin dynasty (221 – 207 BC) and the middle Han dynasty (206 BC – AD 220), while in the same period of time the *SCL* was relatively long (consistently with an expected cold climate as per above).

It was very cold during $\sim 200 - 500$ AD, particularly in $\sim 280 - 289$ AD, while the average *SCL* during $\sim 247 - 290$ AD was 12.5 *years*, i.e. ~ 1.5 *years* longer than the mean *SCL* value over the entire 2500 *years* time span.

There was a cool 19th century in China, but a warm decade occurred in the 1850s. The mean *SCL* during 1829-1848 was 9.3 *years*, i.e., this was the shortest observed *SCL* value.

That is - as expected - "climate" cannot be identified or described by *SCL* alone. According to the rationale of the present study, a longer *SCL* implies a comparatively deeper amount of e.m. induction (due to the skin depth effect). This affects the *TD* dynamo, as the currents induced in the mantle are equivalent to the stator of an elementary dynamo, while the rotating coil is represented by the relative displacement of various ionized components of the solid Earth, due to a differential tidal action applied by the Moon and by the Sun. Therefore, a difference of e.m. induction currents into the mantle - at the frequencies that are relevant for the *TD* dynamo performance - implies a different performance of the *TD* dynamo. In the case here of concern, the *TD* dynamo seems to be comparatively less effective. Therefore, there is less electric current supply to sea-urchin spikes worldwide, hence to Joule heat that supplies geothermal flux, volcanism, and geodynamics. Thus, a smaller amount of endogenous energy is transferred to "climate".

In addition, the *SCL* periods anticipate the central years of climate periods by a mean advance of 10.6, 25, 12.5 *years*, respectively, for the three aforementioned data series. This means that the time delay - between a change of dynamo performance and the appearance at Earth's surface - of its effect is in the range of $\sim 10 - 25$ *years*. The delay depends on site, and is, roughly, some kind of mean time needed for the transfer at Earth's surface of a change of endogenous energy production.

It is important, however, to consider that, according to the implication of the Earth's electrocardiogram (Gregori, 2002; Gregori and Leybourne, 2021) such a time delay is much variable, and it can be much longer, between zero and

27.4 *Ma*, which is the pace of the Earth's electrocardiogram. At present we are close to the top of a heartbeat, and it is fairly possible that the time delay changed vs. time during the time lag of several centuries investigated by means of historical solar cycle data.

Therefore, it can be concluded that this analysis on *SCL* is consistent with the mechanism that is here envisaged. It can be stated that, at every time, every variation of a suitable long-period component of solar activity originates a "climate" effect, which is manifested at the Earth's surface with a $\sim 10 - 25$ *years* delay.

On the other hand, one must consider that changes in jet stream patterns related to north-south ridge e.m. induction effects are almost instantaneous (Wu and Leybourne 2020; Wu, 2025), while longer term - vertical *TD* driven e.m. induction internal Joule heat related to volcanism - may have these lags. Climate change is related to both and many other inputs. That is, in principle no unique thumb rule can be defined.

Hence, if the aforementioned inference is correct, at every given time we can use a several decades record of solar activity before that given instant of time. In this way, we assess whether the *TD* dynamo was more or less effective some $\sim 10 - 25$ *years* in advance. By this we can get an indication on whether "climate" is to be expected to be more or less "cold" or "warm". This is a modest early step, but it might be a beginning towards the achievement of the old "dream" of long-range "climate" forecast. Note, however, that this is a general indication of trend, not a forecast. Neither it is possible to expect any better indication by means of one index alone.

In this same respect, consider that a greater availability of endogenous energy is associated with a greater geodynamic activity, hence a greater seismicity and volcanism (Gregori, 2002, Gregori and Leybourne, 2021).

Then, Feng and Tang (1997) interpolated the *SCL* series and obtained a regular series of annual values. They considered the Chinese annual air temperature (*CAAT*) series and searched for formal time-delayed correlation. They found, during 1875-1988, a correlation coefficient -0.762 when the *SCL* was shifted by 1 *year* in advance compared to *CAAT*.

They also searched for a regression equation between *CAAT* and *SCL*, thus explaining $\sim 57.8\%$ of the *CAAT* variance. Thus, they constructed, by means of such a regression curve, the climate temperature in China during 2500 *years* and correlated it with the two (Zhu's and Greenland) of the three aforementioned data series. They found, respectively, correlation coefficients 0.441 and 0.459, although they claim they are significant at a 0.001 level. However, the correlations found by Feng and Tang (1997) did not look clear. They concluded that the variations of *SCL* are probably co-responsible for the temperature fluctuation in China during the last 2500 *years*, but they stress that also other drivers must be considered.

Tang et al. (2001) divided the last 2500 *years* into periods of good climatic condition (*GCC*) and bad climatic condition (*BCC*), according to the state of *SCL*. Droughts are more frequent during *BCC*, while *GCC* are identified

with warm climate. Tang and Tang (2002) associated *GCC* with the comparably more peaceful times in the Chinese history, and *BCC* with the comparably more troubled times.⁵

Tang et al. (2002) considered the $\Delta^{14}\text{C}$ data series since ~ 15,000 years ago and compared it with the *SCL* data series for the last 2600 years. They found a close agreement.

Then, they considered the stability of the *SCL* datum. A stable *SCL* period lasted typically ~ 300 years during the last two millennia. At present *SCL* seems to be stable since 1910. Hence, they guess that the future climate ought to be at the start of a “*millenarian warm period*”.

Wang et al. (2002) simulated the temperature in China during the past 2000 years. They claim that their results look consistent with the previous studies, mainly during the last 700 years. They also simulated the temperature curve for the *NH* during the last 120 years. They concluded that, on the decade time scale, solar activity seems to be a driver for temperature variations, but also greenhouse gases must be considered.

Tang et al. (2003) specifically addressed climate forecast in Northwestern China, which is particularly important for social needs. They considered the climate periodicities in Northwestern China, *SCL* data, pollen and ice cores, and they inferred that in that area climate has now completed the transition from a cold to a warm stage. Hence, a millenarian wet period ought to start beginning from the 22nd century, while after 2020 the climate in the eastern part of Northwestern China ought to turn wet.

Wang et al. (2003), which is a paper written in English, report about an analysis of the natural disasters (drought, flood, and strong earthquakes) that hit China during the last 108 years, and about their apparent relations with *SCL*. They claim that the *SCL* appears to be “*a useful indicator for drought/flood and strong earthquakes*”. They claim that when solar activity strengthens, *SCL* shortens, while more floods occur in Southern China, and frequent strong earthquakes happen in the Tibet Plateau. In contrast, droughts in East China - as well as the strong earthquakes in Taiwan and at the western boundary of China - are very few. The opposite effect occurs when solar activity weakens.

Note that, according to the rationale of the present study, when solar activity strengthens, *SCL* shortens, the *TD* geodynamo intensifies and a greater amount of endogenous heat is generated. There is, however, some time delay as the delay is very short on top every sea-urchin spike. A greater amount of energy in the atmosphere originates a greater Cowling dynamo effect (Gregori et al., 2026d), hence larger precipitation and storminess. In addition, the thermal expansion of crust and lithosphere favors a greater geodynamic activity, hence the occurrence of eventual earthquakes.

This expectation agrees with Southern China and the Tibet Plateau. In contrast, concerning East China, Taiwan

and the eastern boundary of China, the opposite correlation ought to be explained by some suitable secondary effects caused by atmospheric dynamics and tectonic patterns. This is consistent, e.g., with the analysis of wildfire propagation discussed in Gregori and Leybourne (2025i), where a branch of crustal stress is envisaged that moves from Indochina (maybe from the Banda Sea) through the eastern coast of China until a “flash” that occurs north of Beijing.

In any case, this is a confirmation of the fact that no global wet and dry periods of time occur, neither warm or cold periods, rather periods of greater scatter with respect to mild climate trend. That is, floods and droughts occurs during the same period of time in different areas. Therefore, it is correct to state that when *SCL* is shorter a greater storminess occurs with all its unwanted extreme consequences, due however to a time delay between *SCL* and impact on climate.

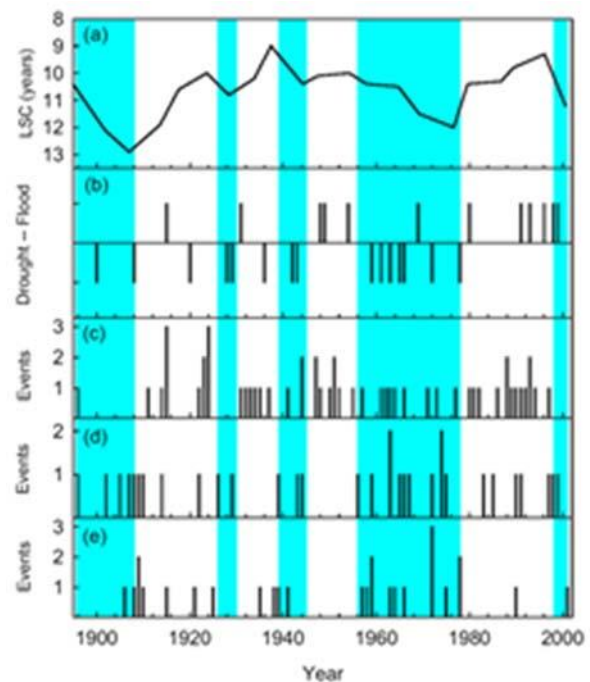


Fig. 5. “*SCL and natural disasters in China during the last 108 years. For (c), (d), and (e), the ordinate is the frequency of disastrous events. The shading represents weakening solar activity (WS) stages. (a) SCL, (b) floods in South China (upright bars) and droughts in East China (upside-down bars), (c) strong earthquakes ($M > 6.5$) in the Tibetan Plateau, (d) strong earthquakes ($M > 6.25$) in the China-Afghanistan-Pakistan boundary region, and (e) strong winter earthquakes ($M > 7.0$) in the Taiwan region.*” Figure and captions after Tang et al. (2003). With kind permission of *Chinese Journal of Glaciology and Cryopedology*.

Wang et al. (2003) conclude that there are indications that solar activity can play an important role in determining both climate extremes and the behavior of the lithosphere. Their data are shown in Fig. 5.

while they state that they expect a forthcoming *GCC*, although they warn about possible perturbations by overlapping *BCC* periods.

⁵ They also divided the Chinese emperors into 4 categories: “*virtuous, sage, mediocre and atrocious*”, and associated them with *GCC* or *BCC*. They appear happy

As a general comment, all these inferences rely on uneven series of proxy data that are affected by relevant and unknown error bars and data gaps. Nevertheless, they are observational matters-of-fact that reflect the objective occurrence of some large-scale phenomena. Neither they require any preconceived and more or less oversimplifying model. Additional information about palaeoclimate and archæo-climate variations in China is given in Gregori et al. (2026g, 2025h). Concerning the relations between climate, seismic activity, and other geophysical phenomena, see also the discussion reported in Gregori et al. (2026d, 2026e, 2026f).

A general comment seems to apply dealing with the case histories that do not fit into every given aforementioned rationale - such as the *SCL* indicator for climate, or the often-reported scatter concerning the association of quiet Sun with a cooler climate etc. In fact, according to the rationale of the present study, other parameters must be considered as follows.

Consider that solar-terrestrial relations occur through either the “external” or the “internal way” (see Gregori, 1997, 2002; Gregori and Leybourne, 2021). The “external” way coincides with the standard and fashionable “space weather” model that envisages an effect propagating downward from interplanetary space through the Earth’s atmosphere until Earth’s surface. Conversely, the “internal” way considers the e.m. induction into the Earth’s mantle, which affects the performance of the *TD* geodynamo, hence the generation of endogenous heat. The varying release of endogenous energy controls geodynamics, volcanism, and climate. However, the release of endogenous energy occurs with a largely varying time-delay, related to the temporary more or less developed sea-urchin spike pattern (Gregori, 2002, Gregori and Leybourne, 2021). Consider also as e.m. dynamics is related to tectonic micro-gravity process of air-earth currents within the global pressure oscillation teleconnections as explained in “*El Niño tectonic modulation in the Pacific Basin*” (Leybourne and Adams, 2020).

The “external” energy source leads to comparably uniform or smoothly varying effects on the ocean/atmosphere system. In contrast, the “internal” energy source is well-known to be associated with large space- and time-gradients and inhomogeneities. Inhomogeneities generate “vorticity” in the ocean and in the atmosphere, i.e., rearrangement of jet stream patterns related to flooding and drought.

Call $w_{ext}(t)$ and $w_{int}(t)$ the power contributed to the ocean/atmosphere system at a given time t through the “external” and “internal way”, respectively. Call $w_{ext,a}$, $w_{int,a}$, $w_{ext,q}$ and $w_{int,q}$ some indicative “mean” power that is typical of active and quiet Sun time (according to the index a or q , respectively). Since the “internal” way is more important, the crucial parameter is:

$$p_{int}(t) = \frac{w_{int}(t)}{w_{int}(t) + w_{ext}(t)} \quad (3)$$

In fact, the larger $p_{int}(t)$, the greater the global “vorticity” of the atmosphere, the more relevant the role of the Cowling

dynamo (Gregori et al., 2026d), the greater the activity of atmospheric electricity, the greater the condensation of water vapor, the greater the global cloud coverage, the greater the amount of atmospheric precipitations, the thicker the blanket of water vapor, the greater the Earth’s albedo, the lesser the solar energy captured by the Earth, the cooler gets climate, although the greenhouse effect may be eventually greater.

In the ultimate analysis, the result depends on a delicate equilibrium between difference forcing agents. For instance, Knorr et al. (2011) investigated the warm climate of the Late Miocene and claim that “*energy balance estimates suggest that a reduction in the planetary albedo and a positive water vapor feedback in a warmer atmosphere are the dominating mechanisms to explain the temperature increase.*” That is, in any case no “simple” model can apply to every case history, and every lesser change of the role of any one given driver can have consequences that can hardly be realistically foreseen.

Therefore, owing to the complicated feedback by different drivers, the result can eventually appear scattered, when it is compared to every “simple” rule that attempts to correlate one given observational parameter with some generally defined “mean global climate temperature”.

Remind, however, also about the rationale of Fig. 6 of Gregori et al. (2026a) and Fig. 6, by which during higher solar activity a higher endogenous heat flow must be expected.

All this, however, is only indicative. Indeed, “climate” after 2010 has been particularly “anomalous”. Also, the solar cycle has been particularly anomalous – as shown by Fig. 7 that displays the solar MiniMax of cycle 24 - and this climate anomaly occurred even though it was during years of active Sun.

In any case, note that the solar cycle and its length cannot be treated in terms of simple mathematical facts. Solar physics is controlled by the encounters of the Solar System with clouds of interstellar matter (Gregori, 2002; Gregori and Leybourne, 2021). However, owing to the empirical constraint, the distribution through space is poorly known of matter encountered by the Sun. Hence, as far as our knowledge is concerned, the phenomenon seems erratic. Owing to this reason, no clear pattern can be recognized of any stable deterministic chaos in the solar cycle (e.g., Weiss, 1988), as this is a mathematical concept relying on specific assumptions. In contrast, the phenomenon is deterministic, depending on the physical distribution and dynamics of interstellar matter.

The solar MiniMax and the old-fashioned approach

The MiniMax period (see Fig. 7) was carefully analyzed in detail by Clette et al. (2014) by means of the *GN* series. Owing to the strong climatic anomalies occurred after ~2010, this long-range trend of the solar cycle deserves a particular concern and is the main focus of the present paper.

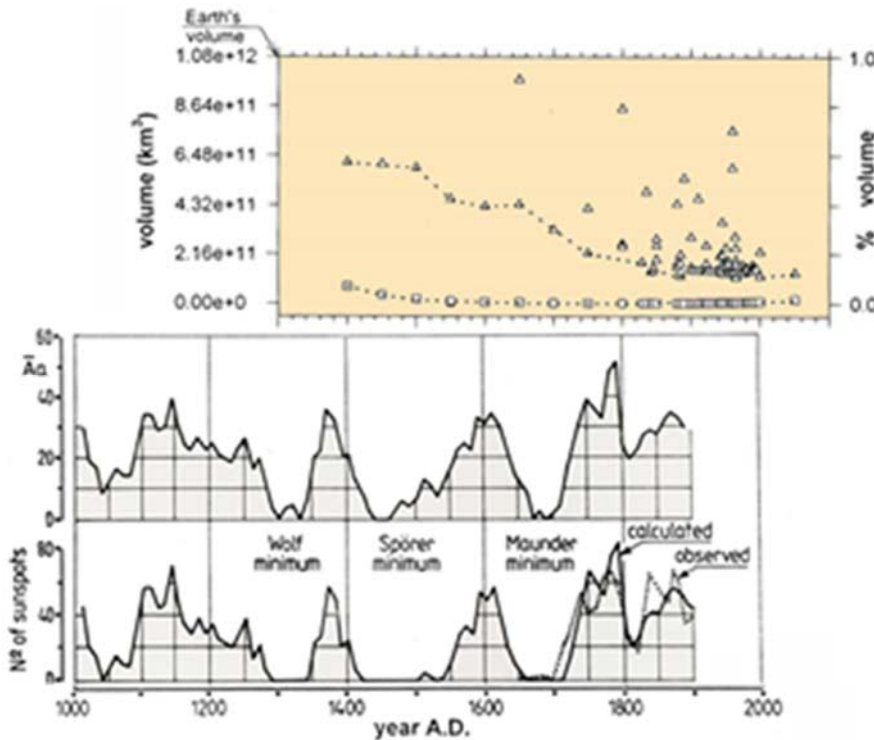


Fig. 6. Fig. 6 of Gregori et al. (2026a) is re-plotted in order to show the solar control on the radius of the core-mantle boundary (CMB). Refer to the captions of Fig. 6 of Gregori et al. (2026a) and see text. Note that the plateau in the CMB radius corresponds to a peculiar enhanced solar activity. These results were formerly obtained in cooperation with Fabrizio T. Gizzi. Unpublished figure.

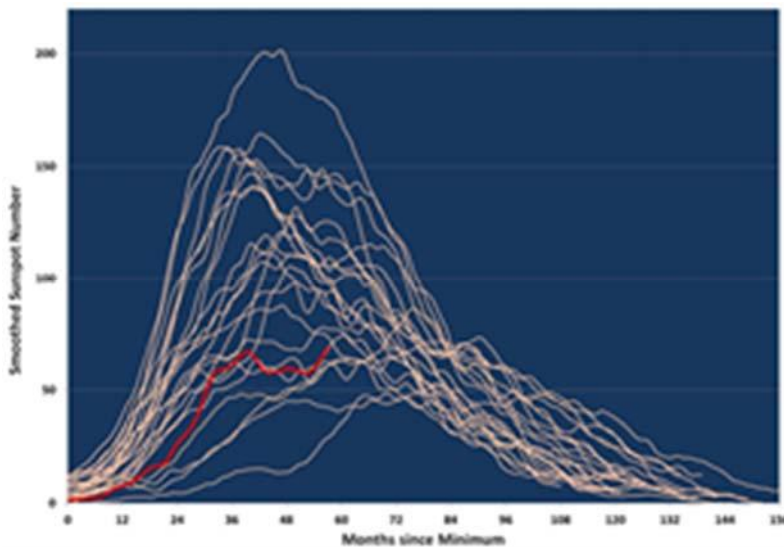


Fig. 7. “This plot prepared by Ron Turner of Analytic Services, Inc., shows the smoothed sunspot number of Cycle 24 (red) vs. the previous 23 cycles since 1755.” Figure and captions after Phillips (2014e). NASA copyright free policy.

Consider that, in principle, according to the rationale of the present study, the crucial physical information deals with the time-varying component of solar activity – hence of the e.m. interaction of the solar wind – that resonates inside the Earth’s mantle (Gregori, 2002, Gregori and Leybourne, 2021 and references therein). In this way, this solar signal influences the yield of the TD geodynamo, hence the generation of endogenous heat. The endogenous heat is then released – with a suitable time delay – and it injects energy in the ocean/atmosphere system, thus affecting its dynamics. Therefore, in principle, a dynamic power spectrum ought to be computed of the solar activity signal (whether its SN or GN series). Then, a correlation ought to be found between the total spectral power inside a suitable frequency band with a suitably time-delayed climatic effect.

In addition, consider also that the Earth’s magnetosphere intercepts the expanding solar corona by a fraction $\sim 0.45 \times 10^{-9}$ (see Gregori and Leybourne, 2026b). This is a very tiny fraction of open solar flux (see below for definition). That is, the Earth is a very tiny detector. Therefore, no reason can be suggestive of any periodical trend of solar activity that ought to be detected by the Earth. Differently stated, the Earth is a tiny “point-like” detector inside the huge physical system of the expanding solar corona. The solar corona can even display some approximately periodical features, although only when monitored on a large-scale size, while the scatter is very large on a “point-like” basis. Therefore, in general even in the case that the Sun displays some true and regular periodical trend, every cycle observed by the Earth can be quite different compared to every true solar cycle – because

the records are biased by the tiny detector represented by Earth's magnetosphere embedded in the expanding solar corona. In this respect, note that the solar irradiance displays a comparably much smaller variability, although a careful analysis envisages clear long-period trends (see e.g., the analysis by Velasco Herrera et al., 2015). In any case, all data confirm the very anomalous behavior of MiniMax.

Clette et al. (2014) specifically focus on the long-term solar activity. They claim that, during the last 250 years, in

general the GN and SN series agree after corrections. In addition, they compare - both the re-calibrated GN and the corrected SN series - with the base SN series and with the original GN series. They find that, after applying corrections, the secular trend in solar cycle amplitude is consistently reduced. This is shown in Fig. 8 (dashed line).

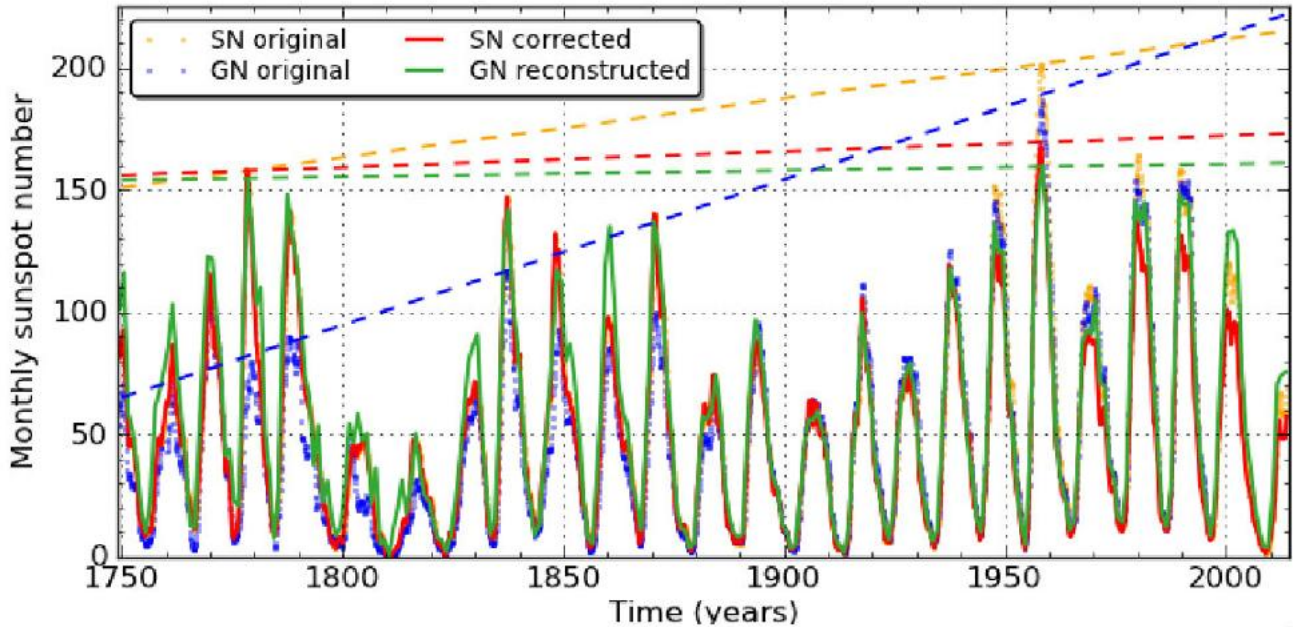


Fig. 8. “Comparison of the original and corrected SN and GN series over the entire interval 1749-2013, showing the limited difference in maximum cycle amplitudes between the 20th century and previous centuries after the new corrections. In order to better visualize the trends, dashed lines connect the highest maxima of the 18th and 20th century, for each series of the corresponding color.” Figure and captions after Clette et al. (2014). NASA copyright free policy.

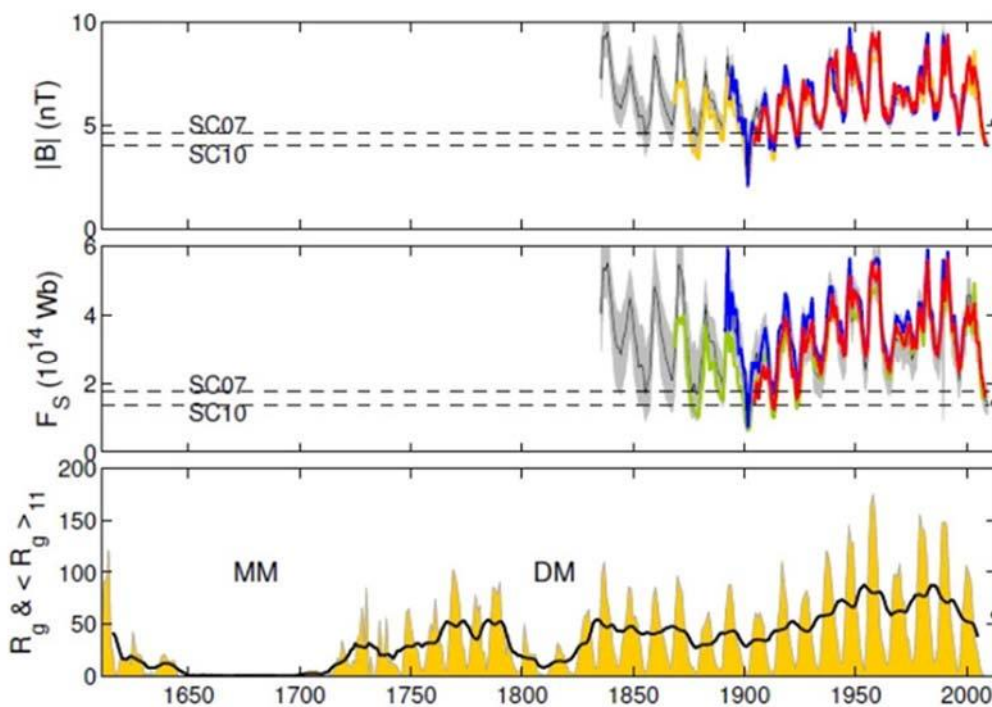


Fig. 9. “Long-term variations in (top) reconstructed IMF, B ; (middle) open solar flux, F_S , and (bottom) group sunspot number, R_g ... In the bottom panel the orange-shaded area gives annual means of the group sunspot number and the black line their 11 year running means. The black dot to the right of each panel is the maximum 12 month mean seen thus far in cycle 24 at the time of writing (31 March 2013).” Figure and captions after Lockwood (2013). With kind permission of Living Reviews in Solar Physics (“Platinum Open-Access”).

Clette et al. (2014) note that, except for cycle 19 that is the highest recorded (see Fig. 1), the maxima of highest cycles of the past centuries are basically identical to the recent maxima of the late 20th century. Clette et al. (2014) also stress that recent independent reconstructions of the Sun's open **B**, which relies only on geomagnetic records, display a limited difference compared to the highest peak of the 11 year amplitudes observed during the available 1840-2010 interval (see Fig. 9).

Therefore, Clette et al. (2014) envisage that the observed upward trend in solar activity levels between the 18th and 20th centuries is now questioned. Conversely, it was erroneously explained in several past interpretations and models, including the associated concept of an abnormally high "Grand Maximum" that was observed in the second half of the 20th century.

Fig. 9 requires some explanation. Lockwood (2013) is a learned and long review of geomagnetic indices and of the long-range variation of the 11 year solar cycle. Also, the "open solar flux" is defined. Unlike a formal non-dimensional index such as *SN* or *GN*, the open solar flux is a significant physical quantity that characterize the state of the Sun. It is defined by Lockwood (2013) as follows.

"The open solar flux, F_S , is the magnetic flux leaving the top of the solar atmosphere and entering the heliosphere. A notional surface, the 'coronal source surface' is envisaged at the top of the corona, which is everywhere perpendicular to the field, and F_S is the flux threading that surface and so is also called the 'coronal source flux'. This review (unless otherwise stated) considers the 'signed' open flux which means that only the flux of one polarity (inward or outward) is quantified. If we assume that Maxwell's equations hold such that there are not significant numbers of magnetic monopoles inside the coronal source surface, then the inward and outward fluxes are equal and the 'unsigned' open flux is simply twice the signed value. The source surface is usually taken to be a heliocentric sphere of radius $2.5 R_\odot$, where R_\odot is a mean solar radius (Arge and Pizzo, 2000)." Referring anew to Clette et al. (2014), they state that the amplitudes of recent cycles are not the repetition of five strong cycles observed during the last 60 years (cycles 17 to 22, with the exception of cycle 20). However, the recent cycles represent a unique episode during the whole 400 year record.

This unique feature is also observed when dealing with a sunspot byproduct, i.e., the number of spotless days during every minimum of the sunspot cycle. Clette et al. (2014) show a plot of the total number of spotless days from cycle 6 to 24, for which daily sunspot numbers is strongly anti-correlated with the amplitude of the adjoining cycles. Clette et al. (2014) note that the anomalous long-lasting 2008-2010 minimum is correlated with a particularly high count of spotless days (~ 800).

This high value was not attained since the early 20th century. However, this value was largely exceeded during the minimum between cycles 5-6 that belongs to the small Dalton minimum. Hence, in a long-term perspective this feature was not particularly exceptional, although it looks in contrast with recent minima. On the other hand, the full series of low spotless day counts during the last 6 cycles

looks to be a unique episode during the last 250 years and most probably during the last 400 years.

Then, Clette et al. (2014) carry out a detailed analysis of cycle 24, due to its anomalous MiniMax. The minimum between cycles 23-24 looks like a transition in the long-term solar activity. Therefore, Clette et al. (2014) consider in this context the subsequent evolution of cycle 24. Their purpose was to identify the range of possible scenarios that can be envisaged for the remaining part of this cycle. They stress the reliability of data derived from the *SN* series, compared to the current statistical or physics-based models of the solar cycle that refer only to global repetitive properties of the cycle – i.e., just on a mathematical assumption.

Clette et al. (2014) show a figure similar to Fig. 7, by aligning every cycle (1 to 24) at a common tie point (*SN* = 13) referred to the declining phase of the previous cycle. Thus, cycle 24 is among the late cycles preceded by a prolonged minimum. Owing to the argument specified in the following, this protracted minimum is (perhaps) the real primary cause of the consequent climate anomalies. They show that, even though cycles display a continuous range of amplitudes, two concentrations of cycle profiles can be recognized, as fast rising cycles reach high maxima (*SN* > 130) and slowly rising cycles reach moderate amplitude (*SN* ~ 60) and cycle 24 belongs to the second group.

In particular, in another figure (not here shown), Clette et al. (2014) compare cycle 24 with the weak cycles 5 and 6 that belonged to the Dalton minimum. The rise of cycle 24 is steeper, and the recent *SN* values clearly exceed the maxima of cycles 5 and 6. A striking difference is that cycle 4 preceded the onset of the Dalton minimum, while cycle 23 had a similar amplitude. Hence, they conclude that the peculiar evolution of cycle 24 does match the characteristics of the Dalton minimum.

Note the emphasis on the height of the maximum – and this is consistent with the well-known general intuitive feeling. Conversely, if the argument that is here proposed is correct, the concern ought to be, rather, about the long-period component of the e.m. induction by the solar wind into the mantle. This seems related also the observed duration of the minimum before the start of the increase of solar activity. That is, the height of the maximum seems to be a secondary, and maybe even an almost irrelevant, aspect. In fact, the physical mechanism should rely on the skin penetration depth of the e.m. signal, which is deeper for lower frequency. Thus, the efficiency changes of the *TD* dynamo, and the production of endogenous Joule heat. Note that the e.m. induction occurs through the natural "antennæ" represented by sea-urchin spikes, and is more or less effective depending on the resonance of deep Earth to the impinging signal (Gregori, 2002, Gregori and Leybourne, 2021).

Clette et al. (2014) also comment as follows. *"Actually, the only cycles that closely match cycle 24 are shown in a figure (not here shown, see Clette et al., 2014, Fig. 67), where we aligned cycles in a tie point (*SN* = 40) in the rise phase of the cycles. Those cycles (12, 14, 15 and 16) all belong to the late 19th and early 20th century. Cycle 24 thus seems to be a return to an average level of activity that*

prevailed during a 60 year period. Those moderate cycles are characterized by extended and rather flat maxima, lasting up to 4 years. The maximum phase is typically marked by a plateau, on which several peaks are superimposed. Consequently, the absolute maximum of the cycle can then occur quite late, like in cycles 12 and 16, when it occurred > 2 years after reaching the plateau phase and more than 5 years after the start of the cycle.” Note the repeated reference to the morphology of the maximum of the cycle, rather than to the duration of the minimum period that preceded the maximum.

In another figure (not here shown) Clette et al. (2014) plot of the monthly mean *SN* for cycles 14 and 24, aligned with reference to the *SN* = 40 crossing point of the 12 month smoothed *SN*. Both cycles 14 and 24 display a somewhat flat maximum formed by successive short peaks of activity. This flat maximum lasted only 2 – 4 months. That is, by this, they avoid the effect of smoothing, and they confirm the previous inference, although allowing for some disturbance by scatter. In any case, as shown by cycle 14, the culmination of moderate cycles is represented by a succession of multiple peaks or activity surges, up to 6. Hence, the exact determination of the maximum is somewhat elusive. In fact, either *SN* or *GN* is a simple 1D index, while the Sun is a physical system that can hardly be characterized by any 1D index. Therefore, the scatter must be expected.

Clette et al. (2014) note, however, that cycle 15 shares several features with cycle 24, i.e., a steep rise to a first peak is followed by an extended plateau close to $R_i = 60$, and it lasts for almost 2 years. However, cycle 15 had a second rise leading to a much higher peak, at twice the level of the initial plateau. Note that the focus, however, ought to be on the duration of the minimum that preceded cycles 15 and 24, rather than on the height of the cycle.

Summarizing, as expected, no “simple” correlation can be found between the solar cycle morphology and climate anomalies. The natural system is highly nonlinear with an intricate feedback, and the general scenario is therefore never repetitive.

Wezel (2018, p. 67) highlights as follows the climatic concern related to an anomalous solar cycle.⁶

“...during the Maunder Little Ice age (1645-1715) both strong earthquakes and volcanic eruptions were reported in different regions. During the subsequent Dalton Solar Minimum (1796-1830) seismic and volcanic events had a less global character. Starting from the decline of sunspots in 2008, we entered another solar minimum that includes the Solar Cycle 24. Thus, by around 2030, we have to expect a severe climate cooling of the same kind of the Dalton Minimum.

Solar cycles normally have a duration of 11 years, but they can vary between 7 – 15 years. The longer the duration, the colder the next cycle. [This is consistent with the aforementioned Feng and Tang (1997) analysis.] The Solar Cycle 23 had a duration of 13 years. Hence, a great subsequent cooling is expected. The Solar Cycle 23 was

similar to the long Solar Cycle 4 that lasted 13.6 years and preceded the Dalton Minimum, and a period of low temperature in Europe ... The rapid decline of solar activity started with the Solar Cycle 24.

In June 2011 the NSF National Solar Observatory announced that the Sun entered a dormant period with very low, or even absent, activity during the forthcoming solar Cycle 25 ...”

Wezel (2018, p. 68) supports therefore the Casey (2011) expectation of a possible hibernation period. Wezel (2018, p. 68) reminds about a classification of past climatic periods that was originally proposed⁷ by Eddy (1977) relying on ¹⁴C/¹²C in dendrochronological series. The original Eddy’s list was later updated, and the list is here shown, which is given by Wezel (2018, p. 68). This list gives a feeling of the kind of climate variability that can be eventually observed in the future, independent of the explanation and of the guessed drivers.

- 2720 BC-2610 BC-Sumerian maximum, copper age
- 2370 BC-2060 BC-Pyramid maximum, copper age
- 1870 BC-1760 BC-Stonhenge Maximum, ancient bronze age
- 1420 BC-1260 BC-Egyptian Minimum, recent Bronze Age
- 820 BC-640 BC-Homeric Minimum, iron age, climate deterioration
- 440 BC-360 BC-Greek Minimum, iron age, climate deterioration
- 20 BC-AD 80-Roman Maximum, warm Roman epoch, climatic optimum
- 640-710-High Medieval Minimum, climate deterioration
- 1120-1280-Medieval Maximum, climatic optimum, temperature peak +2°C
- 1400-1510-Spörer Minimum, extended Little Ice Age
- 1645-1715-Maunder minimum, extended Little Ice Age
- 1796-1820-Dalton Minimum, Little Ice Age, Cycles 5 and 6.
- 1850-1990-Modern Maximum, or climate optimum, minimum during 1940-1972, maximum in 1998
- 2011-2035 ?-future Minimum, or future Little Ice Age (Cycles 25 and 26).

In addition, Eddy (1977) lists also the following epochs:

- 5320 BC-5110 BC-Minimum
- 5070 BC-4510 BC-Maximum
- 4240 BC-3760 BC-Maximum
- 3690 BC-3470 BC-Minimum
- 3430 BC-3330 BC-Minimum
- 3220 BC-3110 BC-Minimum

⁶ Our English translation from the Italian original.

⁷ John Allen “Jack” Eddy (1931-2009) American astronomer, famous for his studies on historical climate.

As a general conclusion, the approach by means of the old-fashioned sunspot database looks somewhat intricate. No simple rule can be inferred on the long-range trend of solar activity. In fact, even the definition of active Sun is likely to be unrelated to the sunspot number, at least according to the standard old way of evaluation. Nobody can tell whether this depends on the arbitrariness of the definition of sunspot, or, rather on the response of the Sun encounters with interstellar matter.

Therefore, it is important to consider the analysis of solar activity, as inferred according to a formal analysis by means of *AI*.

The approach by machine learning (*ML*) and artificial intelligence (*AI*)

A recent outstanding investigation (Velasco Herrera et al., 2021) relies on machine learning (*ML*) and artificial

intelligence (*AI*) algorithms – basically advanced wavelet analysis and a probabilistic approach based on Bayesian statistics - applied to the *WDC* annual sunspot time-series (1700-2019; Version 2.0). The result is shown in Fig. 10. The authors briefly summarize and highlight as follows their most relevant results. The model “gives insights into the various patterns of the Sun’s magnetic dynamo that drives solar activity maxima and minima. We found that the variability in the ~ 11 year Sunspot Cycle is closely connected with 120 year oscillatory magnetic activity variations. We also identified a previously under-reported 5.5 year periodicity in the sunspot record. This 5.5 year pattern is comodulated by the 120 year oscillation and appears to influence the shape and energy/power content of individual 11 year cycles.

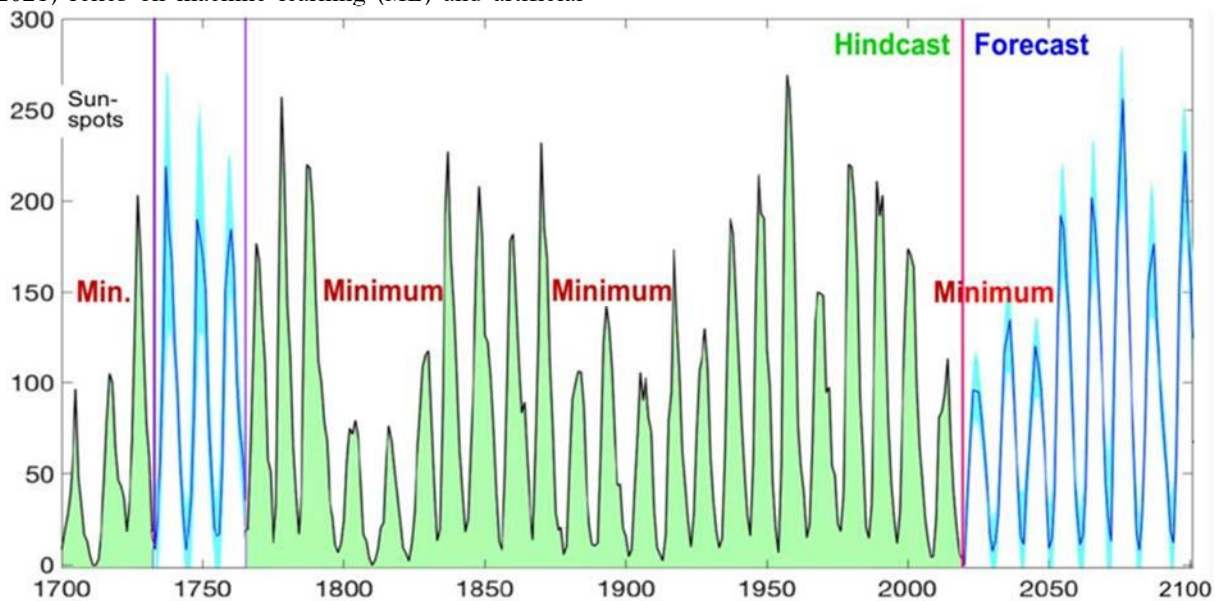


Fig. 10. Modified version of Fig. 5 of Velasco Herrera et al. (2021), according to information provided with permission by Victor M. Velasco Herrera, who illustrates it as follows. “Hindcasting and forecasting of Sunspot Cycles (blue line), 300 years backward (hindcast) and 100 years forward (forecast) based on the ML Bayesian inference of our LS-SVM (Least-Squares Support-Vector Machines) model (separated by the pink area back to 2019). Our model hindcasts relatively higher sunspot numbers for Cycles -1 to 1 (bounded by the yellow area) and extended low or weak future Cycles beginning from Cycle 24 and lasting until about 2050. The cyan shaded area represents the 95% confidence intervals of the Bayesian model” (private communication, 2021). The figure is borrowed after Rotter (2021).

Our ML algorithm was trained to recognize such underlying patterns and provides a convincing hindcast of the full sunspot record from 1700 to 2019. It also suggests the possibility of missing sunspots during Sunspot Cycles -1, 0, and 1 (~1730s-1760s). In addition, our ML model forecasts a new phase of extended solar minima that began prior to Sunspot Cycle 24 (~2008-2019) and will persist until Sunspot Cycle 27 (~2050 or so). Our ML Bayesian model forecasts a peak annual sunspot number (SSN) of 95 with a probable range of 80-115 for Cycle 25 between 2023-2025.”

Two comments are needed.

Compared to all models of the solar *MHD* dynamo, which are top-down and rely on a conspicuous amount of mathematical simplification and approximation, the

Velasco Herrera et al. (2021) analysis is bottom-up. That is, the focus is on objective observations, independent of any attempt to give a physical interpretation. Hence, the associated inferences must be taken into account like sound observational constraints. In addition, as shown below, this *ML/AI* approach gets rid of the several arbitrary choices of conversion factors aimed to reconstruct a reasonably – although arbitrarily presumed regular – data series.

With “quiet” Sun, sunspots coalesce into one or very few areas, while the Parker’s spiral-pattern shifts from 4 sectors to 2 sectors. Hence, the skin-depth of penetration of the e.m. induction by the solar wind into the Earth and planets gets much deeper - due to a doubled period of the inducing **B**. Thus, the *TD* dynamo, both in the Earth and in

every planetary object, is either less or more effective, originating a greater soil exhalation and tectonism.

The most updated analysis is reported by a long paper by Velasco Herrera et al. (2022), which gives a full report of the gigantic effort and data analysis, a real benchmark in this classical, old, and much debated, discussion that is paramount for the discussion of the solar influence on climate. Their main focus is on the definition of group sunspot numbers (*GSN*), original pioneered by D. Hoyt and colleagues. Then, they apply to *GSN* records some most modern algorithms of *AI* using *ML*. “*The goal is to offer a new vision in the reconstruction of sunspot activity variations, i.e. a Bayesian reconstruction, in order to obtain a complete probabilistic GSN record from 1610 to 2020. This new GSN reconstruction is consistent with the historical GSN records.*”

In addition, they carry out a comparison of their new probabilistic analysis of the most recent *GSN* reconstructions proposed by several authors, based on various assumptions and constraints. Thus, they evidence several unprecedented patterns and variations of the solar cycle. They afford to justify the complete *GSN* time variability, “*including intervals with extremely low or weak sunspot activity like the Maunder Minimum from 1645 – 1715*”.

They show that the observed *GSN* series are not simply related to the 11 year cycle alone. Rather, other cycles must be considered for a realistic reconstruction of *GSN* history, i.e. 5.5 year, 22 year, 30 year, 60 year, and 120 year oscillations. Therefore, the resulting comprehensive *GSN* reconstruction according to the *AI/ML* analysis gives an unprecedented insight “*on the nature and characteristics of not only the underlying 11 year-like sunspot cycles but also on the 22 year Hale’s polarity cycles during the Maunder Minimum, among other results previously hidden so far.*”

Velasco Herrera et al. (2022) also consider the canonical Wolf sunspot numbers (*WSN*) that, in the early 1850s, was defined by Wolf by multiplying by 1.25 the original sunspot number. If this multiplicative factor is removed, they show that during 1700-1879 the *GSN* and *WSN* series differ by only a few percent. They also compare their results with the aforementioned Clette et al. (2014) analysis of the international sunspot number (*ISN*), and find several differences. They conclude and stress the need for more sunspot observations including observers who are not yet included in the *GSN* database.

Velasco Herrera et al. (2022) begin and remind about the previous literature on sunspot number and analysis.⁸ They deal with the *WSN* or with the *ISN* (equivalently to the *SSN* or R_z), while Hoyt and Schatten (1998) introduced the *GSN* or R_g for better quantifying the role of solar magnetism (see Livingston et al., 2012; Nagovitsyn et al., 2012). The scope was also to reduce noise levels to smaller

and more sporadic individual spots (see, e.g., Hathaway, 2013; Carrasco et al., 2018b).

Velasco Herrera et al. (2022) address the original *GSN* series by Hoyt and Schatten (1998) and apply a set of powerful *AI* and *ML* algorithms.

Velasco Herrera et al. (2022) also warn about the need for additional research, and they compare their analysis with previous studies. In particular, they refer to the various arbitrary multiplicative correction factors, introduced by various authors – i.e. 1.25, or 1.55, or 1.208, and stress that “*if the adjustment factor of 1.25 had not been applied to the original pre-1849 Wolf series, then the original GSN record of Hoyt and Schatten (1998) would be in closer agreement with the original reconstruction by R. Wolf.*”

At last, Velasco Herrera et al. (2022) warn that “*it would also be good to compare our ML-based reconstruction with the recent attempt by Courtillot, et al. (2021) to reconstruct their sunspot activity record adopting a Sun-planet (i.e., using orbital ephemeris of four Jovian planets) interaction model. However, we strictly focus on a more immediate and direct comparison in this article. We provide our objective comparison as another independent scientific point of view rather than casting a strong judgement on which reconstruction should be the best.*”

Some brief mentions are here given of the “*powerful combination of algorithms involving AI and ML*”, while better details are given by Velasco Herrera et al. (2022).

The database relies on the yearly mean *GSN* or R_g based on reliable records of sunspots during 1610-1995, as used by Hoyt and Schatten (1998). The R_g values for 1996-2020 were computed by Velasco Herrera et al. (2015) and Soon et al. (2019), who also describe the methodology and calibration algorithm, relying on mean value and standard deviation of the R_g measurements. They compare the old data series with the new computed R_g based on *AI/ML* algorithms.

Velasco Herrera et al. (2022) used “*gapped wavelet*” algorithms (Frick et al., 1997; Frick et al., 1998; Soon et al., 2019). This is a variation of the best known classical wavelet technique (see, e.g., Torrence and Compo, 1998), which is used to analyze non-stationary time series. When the data series contains gaps, one must use gapped wavelet algorithms. Salcedo et al. (2012) proposed another variant for the analysis of irregularly spaced time series

Velasco Herrera et al. (2022) used also the cross-wavelet spectrum introduced by Hudgins et al. (1993) to study “*the co-varying nature and measures the synchronization in phase and/or frequency of two phenomena/variables X and Y (see, e.g., Soon et al., 2011).*”

Then, Velasco Herrera et al. (2022) analyze the power anomalies of the sunspot cycle. Every cycle is characterized, in the zeroth-order, by an amplitude (*A*) and by a duration or length (*L*). However, the comparison of different sunspot cycles must rely on a physically variable

⁸ Hoyt and Schatten (1998), Soon and Yaskell (2003), Arlt (2008, 2009a), Ogurtsov (2013), Clette et al. (2014), Arlt et al. (2016), Zito (2016), Tamazawa et al. (2017), Hayakawa et al. (2017a,b), Neuhäuser et al. (2018),

Muñoz-Jaramillo and Vaquero (2019), Arlt and Vaquero (2020), Carrasco et al. (2020a), Simpson (2020), Carrasco et al. (2021a,b), Hayakawa et al. (2021a,c), Vokhmyanin et al. (2021).

criterion that weighs all the characteristics of every cycle. Two important quantitative measures, which related to the intrinsic properties of the phenomenon, are power and energy (Landau and Lifshitz, 1988).

This information also reflects the changes of the cycles both in time and space. Feynman et al. (1963) define the power (P) as the energy transfer ratio per unit time. When dealing with a given physical variable, the power is identified to the integral of the squared amplitude (energy) during the time span of the event (Falkovich, 1978). In the case of sunspot cycle, the magnetic power of every cycle represents the amount of energy that is transmitted per sunspot cycle from the solar magnetic field. Hence, the magnetic power of every cycle is equal to the integral of the number squared of sunspots (A) divided by the length (L) of the sunspot cycle.

Owing to the discrete and non-continuous number of sunspots, the integral is a summation. Thus, the solar magnetic power of every sunspot cycle i is

$$P_i = \sum_{k=1}^n \frac{[A_i(k)]^2}{L_i} \quad (4)$$

“where $i = -12, -11, -10, \dots, 23, 24$ is the number of the individual sunspot cycle since 1610, and k is the year in the sunspot cycle i .” Therefore, $A_i(k)$ is the total number of sunspots in Cycle i , and L_i is the duration of Cycle i .

According to Velasco Herrera et al. (2015, 2021), and to Soon et al. (2019), a standardized power anomaly (\hat{P}) is defined for quantifying an either magnetically high (strong) or low (weak) sunspot cycle. That is, the standardized solar magnetic power anomalies is

$$\hat{P}_i = (P_i - \langle P_i \rangle) / \sigma_i, \quad (5)$$

where $\langle P_i \rangle$ denotes the mean value, and σ_i is the standard deviation of the magnetic power during sunspot cycle i .

Velasco Herrera et al. (2022) illustrate their *ML* algorithms and call them “*Bayesian inference for least-squares support-vector machine regression*”. Owing to brevity purpose we cannot give here details. They stress the need to use a reliable database. The Hoyt and Schatten (1998) series is reliable, although it has both quantifiable and unquantifiable uncertainties, such as missing data or observational gaps, or also yet reported data that are hidden in a library archive. Therefore Velasco Herrera et al. (2022) “*use the Bayesian inference ML model (see Suykens et al., 2005, for technical questions about the method) obtained from the R_g record from 1610 to 2020 to provide a probabilistic estimate of the variation in the sunspot activity cycles, including even during the Maunder minimum, and to reconstruct any missing data.*”

For such a purpose they rely on the Bayes’s theorem (Bayes, 1763). They compute the wavelet power spectral density (*PSD*) and its evolution vs. time. Refer to Velasco Herrera et al. (2022) for details of the entire computational procedure. Rather, the main focus is here, on the results.

The wavelet analysis of the yearly means *GSN* (i.e. R_g) series from 1610 to 2020 shows three periodicities with a confidence level $> 95\%$ (i.e., 5.5, 11, and 120 years and three periodicities with $< 95\%$ confidence level (i.e., 22, 30, and 60 years). These periodicities also display a time evolution. Velasco Herrera et al. (2022) warn that they do

not consider short periodicities, until higher monthly or even daily time resolutions *GSN* data are available.

They stress that the 5.5 year datum is a subharmonic of the 11 year periodicity (Polygiannakis et al., 2003; Velasco Herrera et al., 2021) and was reported in historical aurora records (Silverman, 1992), in the ^{10}Be cosmogenic isotope (Usoskin et al., 2006), in the *SSN* record (Kollath and Olah, 2009; Velasco Herrera et al., 2021), and in records of polar-facula activity (Le Mouél et al., 2019, 2020).

Velasco Herrera et al. (2021) reported that the 5.5 year datum is relevant for the energy characteristics of every sunspot cycle. Velasco Herrera et al. (2022) comment on the analogy to the Waldmeier effect (i.e., more active sunspot cycles are ore asymmetric). In fact, more active (less active) solar cycles display a very strong (weak) spectral power at the 5.5 year periodicity. Velasco Herrera et al. (2022) call this behavior the “Waldmeier spectral effect”.

The solar cycle length (*SCL*) varies between 9 years (e.g., Cycles 2, 3, 8, and 22) and 13 years (e.g., Cycle 4). This periodicity is a quantification of the global information, such as cycle amplitude and *SCL*. The 11 – year period is shared by different solar indices, from the photosphere, the chromosphere to the solar corona (i.e., sunspot, solar flare index, the 10.7 cm solar radio flux, the total solar irradiance, coronal hole area, etc; see, Hathaway, 2015 who gives a very comprehensive review).

Alterman et al. (2021) recently showed the dependence on the 11 year solar activity cycle of the helium-to-hydrogen abundance in the solar wind. This information ought to be correlated with the electrostatic model of the Sun, envisaged in Gregori et al. (2025s).

Velasco Herrera et al. (2022) review some historical information about the early inference of solar cycles, beginning from Schwabe (1844), Spörer (1887), and Maunder (1894). The telescopic study of historical sunspot activity is certainly qualitatively reliable. However, Hoyt et al. (1994) were concerned whether, about almost 100 years after Wolf’s death, the Wolf’s sunspot reconstruction is correct. According to Hoyt and Schatten (1998), or Clette et al. (2014), no full answer is still available to this question. Edward Walter Maunder’s death occurred in 1928, and Velasco Herrera et al. (2022) wonder if there is new evidence or methodology concerning the following questions:

1. Can we implement the correct reconstruction of maximum and minimum in sunspots during the Maunder minimum?
2. Is it correct to claim that the solar and sunspot activity really stopped?

In this respect, according to Gregori (2002), solar physics is affected by the encounters of the Solar System with clouds of interstellar matter. The encounter can even compress the heliosphere inside the Earth’ orbit. This should be the primary cause of geomagnetic field reversals (*FRs*), and of excursions. Therefore, the series of *FRs* ought to be the record of the time variation of the encounter of the Sun with clouds of interstellar matter. However, *FRs* refer

to the geological time scale, while the conventional sunspot cycle refers to a few centuries.

Hoyt and Schatten (1998) stress that - before 1893 - the evidence of *SSN* results from a mixture of direct observations and calculated values of sunspot number. For instance, Wolf filled gaps in R_z sometimes by interpolation, while other missing data were eventually filled by some authors (Wolf, 1859) by reference to magnetic needle observations according to a linear regression technique.

There is some concern about the implications of a false conclusion on the existence, or not, of the solar cycle during the Maunder minimum. Brehm et al. (2021) even claim that there is some difficulty to detect, consistently with the expectation, the 11 *year* cycle during the Maunder minimum by means of the tree-ring ^{14}C isotope proxy, beyond 1 *part per mille* level.

On the other hand, a relevant possible drawback biases different solar indices, because R_g was used as an indirect reference proxy, for reconstructing other solar indices, such as, e.g., the total solar irradiance (*TSI*) or galactic cosmic rays (*GCR*). Therefore, when using R_g it is found that the reconstructed *TSI* is almost constant during the Maunder minimum (see, e.g., Lean, 2000; Wang et al., 2005; Krivova et al., 2007; Vieira et al., 2011). Conversely, other reconstructions of *TSI* envisage that *TSI* might not be strictly constant during the Maunder minimum (e.g., Bard et al., 2000; Velasco Herrera et al., 2011; Shapiro et al., 2011; Velasco Herrera et al., 2015). Therefore, owing to missing or lost data from the R_g record, one can expect to observe an irregularity in the shape of sunspot cycles between 1610 and 1800, compared to cycles after 1800 (i.e., sunspot Cycles 6 – 24).

An answer to the first aforementioned question depends on a completion that is necessary of the R_g record. This can be accomplished in three different ways: (1) seeking new documents reporting direct observations of R_g , (2) filling the gaps by interpolations such as those carried out by R. Wolf, and (3) reconstructing probabilistically the missing data by means of *ML* algorithms.

The first way is certainly the most accurate and correct method. On the other hand, no time-plans can be made, and nobody can guarantee that the search will be successful (i.e., some most representative works are Hoyt and Schatten, 1998; Arlt, 2008, 2009a; Vaquero et al., 2016; Hayakawa et al., 2017a,b; Muñoz-Jaramillo and Vaquero, 2019; Arlt and Vaquero, 2020; Hayakawa et al., 2021a; Carrasco et al., 2021a,b; Vokhmyanin et al., 2021, ...).

The second way is mathematically possible, with no certainty however concerning the physical significance.

Velasco Herrera et al. (2022) apply the third way. They reanalyze the evolution of the periodicities of R_g , by applying different *ML* algorithms. Thus, they obtain the missing data, and fill the data gaps in R_g , although only probabilistically. They stress that, in any case no “exact data” can be reconstructed, while it is possible to evaluate probabilistic the missing data with suitable error bars. Hence, the R_g estimate has a high likelihood and can be associated to a quantifiable confidence level.

The *PSD* for the 11 *year* periodicity varies with time particularly during the Maunder, Dalton, and Modern minima. In addition, the 11 *year* intensity decreases, although it does not disappear during the Maunder minimum. In addition, the missing R_g data can be associated to the *PSD* irregularities referred to periodicities < 11 *years*. This occurs particularly during the Maunder minimum.

The 22 *year* periodicity is the Hale cycle of solar magnetic polarity cycle.

The *PSD* suggests that this periodicity is always observed, although with a relevant attenuation, particularly between solar minima. Sokoloff and NesmeRibes (1994) speculated that during the Maunder minimum the normal dipolar mode of magnetic polarity of sunspots might be overwhelmed by a dominant quadrupolar mode.

Also the *PSD* of the 30 *year* solar periodicity is very strongly attenuated. The same trend was reported in the cosmic ray records by Perez-Peraza et al. (2012).

The 60 *year* periodicity can be called Yoshimura–Gleissberg cycle (see Soon et al., 2014, for explanation and references): This is a well-known periodicity often reported in several proxies, although with the bias deriving from an insufficiently long data series. In fact, the 60 *year* cycle is considered an important modulator of the 11 *year* cycles. The *PSD* shows a very large attenuation during 1610-1700, particularly intense between 1700-1860, and substantially reduced until 2020. Recently, Velasco Herrera et al. (2021) envisaged a gravitational origin for this periodicity, and could derive this periodicity from the inertial motions of the Sun around the barycenter of the Solar System (Cionco and Pavlov, 2018). That is, as already mentioned with reference to Figs 2 and 3, gravitational effects can modulate the e.m. solar phenomena, hence also R_g . Stefani et al. (2020) envisage other physical mechanisms relying on Sun-planet interactions for this periodicity, as well as for the 11 *year* cycle. Just a remind deserves also the possibility that the aforementioned encounters of the Solar Wind with clouds of interstellar dust (Gregori, 2002) might module the intricate *MHD* machine of the Sun. The problem is open for discussion.

The *PSD* for the 120 *year* periodicity envisages its presence during the entire time interval of the R_g record. This signal is associated to the secular variation of solar maxima and minima (Velasco Herrera et al., 2008, 2015). Indeed, the 120 *year* periodicity was observed in the cosmogenic isotope records of ^{14}C and ^{10}Be (see Velasco Herrera et al., 2008; Usoskin et al., 2021b). This same cycle is observed throughout the Holocene (see Soon et al., 2014), and it also appears in the naked-eye observations of sunspots (Ma and Vaquero, 2019).

Then, Velasco Herrera et al. (2022) discuss the phase and amplitude of *GSN* oscillations. In fact, owing to the application of the gapped wavelet transform (see the original paper for details), they afford to reconstruct both amplitude and phase for every R_g periodicity. Thus, they give detailed plots (not here shown). We report only some relevant evidences.

The variation of the 5.5 *year* oscillation amplitude is observed during 1610 – 2020, although the amplitude is attenuated during solar minima. The attenuation is particularly relevant during the Maunder minimum. In fact, they comment that this result is surprising.

The R_g reanalysis, even with the few data during the Maunder minimum, shows that this periodicity is found according to the *ML* algorithm. In addition, Velasco Herrera et al. (2021) reported a modulation of the amplitude of the 5.5 *year* periodicity by the 120 *year* periodicity. This finding agrees with the aforementioned “Waldmeier spectral effect”, which means that the spectral power of the R_g of high or active cycles is maximum, while during the Maunder, Dalton, and Modern minima, the spectral power for the 5.5 *years* periodicity becomes minimum.

Velasco Herrera et al. (2022) stress that absence of sunspots during the Maunder minimum was a real fact, as reported by Maunder in 1894, although it was only apparent in terms of the cyclic trend of the Sun. According to Frick et al. (1997) one can enquire whether the solar dynamo was operative or not. The evidence provided by the analysis by Velasco Herrera et al. (2022) is that the 11 – *year* periodicity is always present, and the modulated amplitude is evident particularly during the Maunder, Dalton, and Modern solar minima. In any case, it is important to stress the continuity of the solar cycle during the Maunder minimum. That is, the lack of data - or a gapped time series - does not imply the interruption of the frequency or period. One can claim that the “apparent” missing data occurs in the “time” space, while in the “frequency” space the phenomenon maintain its characteristics, and the phenomenon is evident anew as soon as the information is restored.

In addition, a periodicity close to 11 *years* was found during the Maunder minimum in different cosmogenic isotopes, e.g. in ^{14}C (Stuiver and Braziunas, 1993; Miyahara et al., 2004; Muscheler et al., 2016; Beer et al., 2018; Brehm et al., 2021) and ^{10}Be (Beer et al., 1998; Velasco et al., 2008; Berggren et al., 2009; Beer et al., 2018) records. This is suggestive that the solar periodic dynamo is always operating (Frick et al., 1997). Rather, one should consider a special state of the solar dynamo that eventually works well below the normal operating power (Soon and Yaskell, 2003; Velasco Herrera et al., 2011; Poluianov et al., 2014; Usoskin et al., 2015). In particular, the analysis by Poluianov et al. (2014) shows that “*large 11 year solar cycles in cosmogenic data observed during the periods of suppressed sunspot activity do not necessarily imply strong heliospheric field.*”

Summarizing, Velasco Herrera et al. (2022) - on the basis of their reanalysis of the sunspot series - believe that no interruption occurred of the solar cycle during the Maunder minimum, or that the solar dynamo was operative during this minimum. This is consistent with the guess (Gregori, 2002) that the effectiveness of the solar dynamo can be modulated by the encounters of the Solar System with clouds of interstellar matter. On the geological time scale this phenomenon – at least concerning the most violent events - is recorded by the series of geomagnetic

FRs or by geomagnetic excursions, while, on the time scale of the last 4 *centuries* the records is represented by the mysterious solar minima.

Velasco Herrera et al. (2022) stress that, in any case, they were capable to reconstruct the R_g cycles on a probabilistic basis (see below). They also stress that the best known way to approach the Maunder minimum relies only on the number of observed sunspots. In contrast, there is very little concern about the solar magnetic cycle and the solar magnetic field reversal (i.e., the Hale cycle) during this minimum.

Miyahara et al. (2006) emphasized the relevant importance of the 22 *year* Hale cycles during the Maunder minimum, compared to 11 *year* Schwabe cycle. They also envisaged that, perhaps, the Hale cycle is prominent over the Schwabe cycle, as a common characteristic of solar activity during all cycle minima, including the Spörer and Dalton minima. The plots of Velasco Herrera et al. (2022) show a persistence of the 22 *year* oscillation, displaying a relatively high amplitude also during the Maunder minimum. In addition, the reversal of the solar magnetic field is always evident, envisaging that the solar dynamo is always quite effective.

In any case, it appears that by means of the *GSN* data series the solar magnetic cycle and the inversion of the solar magnetic field were effectively reconstructed for the first time by the astute algorithms used by Velasco Herrera et al. (2022). Combined with the 11 *year* solar cycle oscillation, this seems to be the most realistic reconstruction of the sunspot cycles during the Maunder minimum having a substantial improved likelihood.

Concerning other oscillations, the 30 *year* oscillation is always present in the Velasco Herrera et al. (2022) plots, although it is attenuated during the Maunder minimum. Conversely, the 60 *year* oscillation is almost always attenuated, except than during 1750–1850, while the 120 *year* oscillation displays practically constant amplitude and phase during the entire 1610–2020 time interval.

Summarizing, Velasco Herrera et al. (2022) show their reconstructed sunspot R_g cycles during 1610 to 2020, obtained by synthesizing the aforementioned trends into a Bayesian *ML* model (R_{B_g}), i.e., a probabilistic model of the R_g data series, according to the aforementioned algorithms. They comment that the trend displays some regularity, although the regularity cannot permit a representation by an analytic function (Gleissberg, 1939, 1942, 1945).

Differently stated, Velasco Herrera et al. (2022) warn that an “exact” reconstruction of the R_g data series is impossible, and any *AI/ML* model is limited by an intrinsic uncertainty principle (Velasco Herrera et al., 2015). Hence, the “exact number” of R_g and the “exact shape” of past solar cycles cannot be reconstructed. Only a retrograde probabilistic hindcasting is possible. Therefore, the challenge of solar activity research is to shift from the paradigms suited for an “exact” data series to a probabilistic approach with reliable uncertainties (Camporeale, 2019).

Several gaps still exist in historical sunspot observations before 1800. *AI* algorithms can fill the missing information

by means of a probabilistic approach, although depending on the physics of intrinsic sunspot activity patterns, and on a reliable historical data series. This warning particularly applies to the Maunder minimum interval.

In this same respect, according to solar magnetic patterns empirically obtained by the R_g - and by proxy records of solar activity in the cosmogenic isotopes - several authors (Steinhilber and Beer, 2013; Soon et al., 2014; Beer et al., 2018) showed the reasonably stable periodicities throughout the Holocene interval. Hence, the timing or phase morphology of solar magnetic cycles was reasonably the same also before 1800 and particularly during the Maunder minimum, even with a lack of direct historical observation.

A large number of non-linear physical factors of the solar magnetic field certainly affect the forms of R_g cycles, including the complex cycle morphologies, such as periods, variable amplitudes, and varying geometries. In any case, the change in time of morphology related to the conditions of the evolving solar magnetic field are such that similar conditions do not necessarily imply the same morphology or magnetic patterns, such as the Dalton and Modern secular sunspot minima.

Conversely, during a very different magnetic context - associated to a large decrease of observed sunspot activity during the Maunder minimum - the continuity of the solar cycle should display similar patterns, even though, topologically, with amplitudes comparatively weaker and lower than during the Dalton and Modern secular sunspot minima (see, e.g., Beer et al., 2018).

Velasco Herrera et al. (2022) stress that the aforementioned achievements of *AI/ML* algorithms agree with the evidence of the continuity of the solar cycle during the Maunder minimum, according to the previously reported evidence derived by cosmogenic isotopes ^{10}Be and ^{14}C (Beer et al., 1998; Berggren et al., 2009; Muscheler et al., 2016; Beer et al., 2018; Brehm et al., 2021) and also with the reconstruction of the *TSI* (Velasco Herrera et al., 2015).

Velasco Herrera et al. (2022) report an astute comment by E.W. Maunder who clearly stressed the approximate time frame concerning the sunspot minimum of 1645–1715 in his article Maunder (1894) with title “*A prolonged sunspot minimum*”:

“*With this great increase in activity, which gave rise to a yet more decided maximum in 1718, the long dearth came to an end. It would seem to have commenced when the maximum of 1639 - a low maximum itself - had fairly died down - that is to say, somewhere about 1645 ...*” (p. 143)

The Velasco Herrera et al. (2022) inference substantially agrees with Maunder, and also reasonably well with the estimates by Waldmeier (1961).

In contrast, the solar activity maxima of Beer et al. (1998) deduced by filtered ^{10}Be data, i.e. occurred in “1630, 1644, 1655, 1668, 1679, 1689, 1701, 1709, 1720” (p. 240 of that paper), show less agreement with the *ML* inference by Velasco Herrera et al. (2022) and with the original speculation and conclusion by Maunder (1922), Waldmeier (1961), and Schöve (1983). In addition, the

Velasco Herrera et al. (2022) analysis shows a relatively good agreement with Vaquero’s et al. (2015) estimates relying on sunspot active-day statistics.

Velasco Herrera et al. (2022) show the cross-wavelet transform applied to Bayesian $ML R_{Bg}$ and to two global ^{14}C production rates (being a direct proxy of *GCR*, hence an indirect proxy of solar activity) relying on tree-ring records studied by Brehm et al. (2021). Those authors cautioned about the low-amplitude variability in ^{14}C during the Maunder minimum, and warned about claiming any clear detection of the 11 *year*-like solar modulation. However, the results of the cross-wavelet seem consistent with an inverse relations between the R_{Bg} and the two records of ^{14}C production rates, particularly with reference to the 11 *year* and 60 *year* timescales. This general consistency supports the reliability of the *GSN* reconstruction implemented by Velasco Herrera et al. (2022).

Summarizing, Velasco Herrera et al. (2022) conclude that almost 100 *years* after Edward Walter Maunder’s death, some answers are now available to the two aforementioned key questions dealing with the nature of the Maunder minimum. Sunspot and solar activity cycles were clearly never interrupted, and a probabilistically correct reconstruction of the sequence of sunspot maxima can be exploited during this interval.

The advantages of the wavelet approach combined with Bayesian statistics are evident, compared to the simpler and more intuitive standard and old-fashioned approach. Therefore, Velasco Herrera et al. (2022) carry out a careful and thorough discussion of the comparison between their reconstruction based on *AI* and several other recent analyses.

The first *GSN* time series were by Hoyt and Schatten (1998). Others followed by Lockwood et al. (2014) and by Svalgaard and Schatten (2016). Velasco Herrera et al. (2022) shows the comparison of the Bayesian *ML* model R_{Bg} with other *GSN* series (figure not here shown).

Velasco Herrera et al. (2022) emphasize the different approach of the investigation that look for the best sunspot number, compared to the original effort by Hoyt and Schatten (1998) and who were only focused on the *GSN*. They also mention some criticism concerned with the so-called “backbone” approach, by which reference is made to the data series used by one arbitrarily chosen author, while other data are arbitrarily “corrected” by a suitable factor. For instance, the sunspot reconstructions for the late 1700s by Clette et al. (2014) and Svalgaard and Schatten (2016) relies on the chosen observer Staudacher, who - as reported by Wolf (1861b,c) and confirmed by Hoyt and Schatten (1998) - is the worst observer during that period. In fact, Staudacher missed about half of the sunspot groups. Wolf (1861b,c) and Hoyt and Schatten (1998) used a correction factor 2.0 for Staudacher, and Clette et al. (2014) used 3.0, thus increasing by 50% the solar activity in the late 1700s. In fact, the Staudacher’s data were used due to the paucity of observations. However, when more observations became available, Staudacher had been eliminated from any reconstruction.

Clette et al. (2014) also used Schwabe as a backbone with a correction factor of 1.55 compared to 1.208 in Hoyt and Schatten (1998). Thus, Clette et al. (2014) obtained in the 1800s a higher sunspot number by $\sim 30\%$. Most visual observers missed $\sim 10\text{--}20\%$ of the sunspot groups compared to the records by the *Royal Greenwich Observatory (RGO)*. The reliability of these records were confirmed by independent and quantitative analyses of the *Debrecen Heliophysical Observatory* (Baranyi et al., 2016; Györi et al., 2017). Hoyt and Schatten (1998) claimed that Schwabe missed $\sim 17\%$ of the sunspot groups. Clette et al. (2014) claim that Schwabe missed $\sim 35\%$ of the sunspot groups. Gustav Spörer and Heinrich Weber were the key observers used in the reconstruction by Hoyt and Schatten (1998), and this implied a correction factor 1.208 for Schwabe's data.

Concerning the 20th century, the backbone observers Wolf and Koyama were chosen by Clette et al. (2014) with an identical correction factors 1.0 . Conversely, Hoyt and Schatten (1998) used the factors 1.094 and 1.151 for Wolf and Koyama, respectively, implying a difference by $\sim 5\%$. Hence, the reconstruction by Clette et al. (2014) is not homogeneous. If the correction factors are kept identical, an incorrect downward trend is added. Another difference between Hoyt and Schatten (1998) and Clette et al. (2014) deals with the level of solar activity after 1947, i.e. concerning the treatment of the so-called Waldmeier Jump (see below).

R. Wolf, beginning around the early 1850s (see Hoyt, Schatten, and Nesme-Ribes, 1994; Clette et al., 2014; Friedli, 2016) used an upward correction of 1.25 (see p. 40 of Clette et al., 2014) concerning his original sunspot numbers before 1849. Thus, he obtained the presently known canonical Wolf sunspot numbers, R_z , and this explains the difference in the factors 1.55 and 1.208 applied to Schwabe's observations. If the factor 1.55 used by Clette et al. (2014) is divided by 1.25 , one gets a factor 1.24 for Schwabe's observations, which is close to 1.208 . Hoyt and Schatten (1998) gave no explanation for the reason why Wolf used 1.25 .

Indeed, R. Wolf and D. Hoyt reconstructed the *WSN* and the *GSN* - according to their feelings and purposes - while their reconstruction had no relationship with the behavior of the Sun's magnetic activity. In this sense, Clette et al. (2016) and Velasco Herrera et al. (2022) claim that the original *WSN* and *GSN* discrepancy is unacceptable. In any case, this differences must be fully explained.

Velasco Herrera et al. (2022) claim that the "inconsistencies" between the *GSN* and the *WSN* series are mainly caused by the arbitrary changes and adjustments applied to the *WSN* series, while neglecting every kind of physical argument from the point of view of solar physics. The simple principle was rather a matter of visual scalings. One should point out that since the *GSN* and the *WSN* are two complementary solar activity records, there will be always a differences between them. As stressed in Hoyt et al. (1994), the Wolf's reconstruction before applying the 1.25 factor is very similar to the *GSN* reconstruction (see also below).

Velasco Herrera et al. (2022) discuss agreement and disagreement between cycles in the different series. No details are here given. A special mention - as also stressed by Clette et al. (2014) - is devoted to sunspot Cycle -1 that, according to Hoyt and Schatten (1998), has three peaks (in 1736, 1739, and 1741). This peculiar shape, which is different than all other observed cycles, is denoted by Velasco Herrera et al. (2022) as the Ψ shape. Other authors suggested other interpretations of this peculiar cycle (i.e., Usoskin et al., 2003; Vaquero et al., 2007; Vaquero and Trigo, 2014), although the knowledge of the real shape of this cycle is not yet satisfactory, depending also on the need for new historical information (Clette et al., 2014).

Velasco Herrera et al. (2022) point out, however, that the Ψ shape is shared also by Cycles -2, -10, and -11, and guess that this can result from missing data, consistently with, e.g., Hoyt and Schatten (1998), Clette et al. (2014), Vaquero et al. (2016), Arlt and Vaquero (2020), who expect that it is still possible to find additional historical records of sunspot observations.

In this respect, Velasco Herrera et al. (2022) warn that, as a standard, polynomial interpolation (generally 3rd degree polynomials) are used to fill missing data in solar activity time series. This method, however, can be either overfitting or underfitting the sunspot series. In fact, such a procedure is equivalent to carry out an interpolation on the "noise" rather than to real information (Camporeale et al., 2018).

In contrast, a Bayesian *ML* method relies on no curve fitting method or interpolation. Concerning the Ψ shaped cycles and other unusual shapes, they disappear in the solar cycle series reconstructed with *ML*. All cycles behave topologically and morphologically according to the generally best known way.

In addition, Velasco Herrera et al. (2022) stress that, from the viewpoint of Bayesian *ML*, the Hoyt and Schatten (1998) *GSN* series is not incomplete, according to the solar magnetized photosphere. Rather, it is a relatively comprehensive sampling of the solar magnetic activity, and it is therefore possible to reconstruct probabilistically the "real" *GSN*. The advantage is therefore evident of *AI/ML* methods, compared to more standard and "intuitive" data handling.

Velasco Herrera et al. (2022) carry out a thorough discussion of the former R_z data series, of *WSN*, *ISN*, and *GSN* series, including all correction factors introduced by various authors. The interested reader ought to refer to the original paper. In any case, the Hoyt and Schatten (1998) *GSN* reconstruction agrees with the original *WSN* record, with no adjustment. Conversely, Wolf abandoned the unadjusted data series in the early 1850s relying on magnetic needle observations. In addition, it is not clear the weight of the bias by such a Wolf decisions to manage his data series. See Velasco Herrera et al. (2022) for details, who also stress the methodological differences between *WSN* and *GSN*, including the related arbitrariness. Owing to brevity purpose, we cannot report here the related critical analysis (and references). We just report the conclusion.

The canonical Wolf numbers, divided by 1.25 , is very close to the group numbers, except for 1870. During 1700-

1995 the mean Wolf numbers are only 4.3% lower than the group numbers. In any case, Velasco Herrera et al. (2022) stress that their analysis was carried out with no reference to the Wolf procedures. In addition, the computed group numbers for 1800–1882 rely on many observations that were unavailable to Wolf. All this supports the independence of the two reconstructions.

Several items are the object of Velasco Herrera et al. (2022), and are not here reported – such as the critical analysis of the evolution of the sunspot time series, of their reconstruction by means of improving telescopes, the controversies, and the *ad hoc* correction factors, etc., with the related conspicuous literature. This is basically a matter of reciprocal information. Clette et al. (2014) are the most updated and authoritative expression of the old-fashioned approach, relying on somewhat arbitrary choices of correction factors, aimed to infer a sunspot time series that is supposed to be seemingly uniform and regularly varying vs. time. The basic concern is therefore about the impact of the improvement of observational tool, quality of telescopes etc.

In contrast, Velasco Herrera et al. (2022) is the new frontier of the *ML/AI* methods, with a Bayesian probabilistic approach that gets rid of the need for every kind of arbitrary choice of correction factors. This is a fundamental quality for evaluating to correlation between sunspots and climate. In fact, some substantial disagreement exists between Clette et al. (2014) and Velasco Herrera et al. (2022). The key issue, however, is not the concern about the discrepancy dealing with every single given cycle. Rather, the focus is on the different methodological approach, and on the amount of “corrections” required aimed to get a supposedly uniform data series. This implies the implicit assumption that no relevant change should occur of Sun’s behavior. This assumption has no physical basis. The *ML/AI* methods, with a Bayesian probabilistic approach, imply a smaller amount of arbitrary decisions. Hence, no real comparison can be made between the two approaches. One can just take note of the differences.

We report here, rather, the discussion on the power anomalies of sunspot cycles according to the Bayesian *ML* reconstructed *GSN*.

The final analysis by Velasco Herrera et al. (2022) is a quantitative definition of sunspot activity and can distinguish different long-range trends of the dynamics of the solar magnetic field. Thus, it can understand the solar dynamo evolution. Conversely, the standard approach of sunspot activity by other studies addresses the shape of sunspot cycles, such as the asymmetry in rise and decay, etc.

Velasco Herrera et al. (2022) rely on a proxy, which is defined by the power of every sunspot cycle that is thus supposed to represent a physical index of the energy released by the solar dynamo and a quantification of the level of solar activity (Velasco Herrera, et al., 2021). By this, one can distinguish “high” or “low” sunspot cycles. That is, they refer to a standard of the power anomaly of the *GSN* of every solar cycle, rather than simply referring to the maximum amplitude of every *GSN* cycle (e.g., see Velasco

Herrera et al., 2015; Soon et al., 2019; Velasco Herrera et al, 2021, for detailed algorithm, explanation, and discussion).

Velasco Herrera et al. (2022) show a plot (not here shown) referred to Cycles -12 to 24. They define “high” or *strong* solar cycle when the anomaly is $> 0.5\sigma^+$ (i.e. over half a standard deviation above the mean value). In contrast, when it happens that $0 \leq anomaly < 0.5\sigma^+$ the cycle is named *neutral* or *near-normal*. The cycle is defined “low” when the *anomaly* < 0 as the cycle power is below the mean value. Whenever the *anomaly* $< 0.5\sigma^-$ (half a standard deviation below the mean value), the cycle displays a relatively large solar magnetic depression, and is defined “very low” or *weak*.

In addition, they define “*secular minimum*” a period of time with two or more consecutive negative power anomalies.

When the power anomaly is $< \sigma^-$ for a set of cycles, i.e. cycles are persistently weak, this is called “*grand minimum*” period (in this respect, they remind about Usoskin et al., 2016a, who studied a broader perspective spanning the Holocene giving an independent derivation and quantitative definition). A grand minimum applies to the Maunder minimum.

Concerning the observed features, the power anomalies are found negative and time persistent during secular minima, i.e., during the Maunder, Dalton, Modern minima, and during Cycles 23 and 24 (i.e., the Minimum of the 21st century).

In addition, these four secular minima occur at the time of the negative phases of the 120 year solar oscillation. This fact envisages a possible connection between the power anomalies and the magnetic activity state of the Sun. Owing to this evidence, Velasco Herrera et al. (2022) guess that in the 21st century a new solar secular minimum began (Velasco Herrera et al, 2015, 2021) and that it ought to last until sunspot Cycle 27 (Velasco Herrera et al., 2021).

They also propose to change the present names for these four secular minima and to call them, respectively, Maunder minimum, Dalton-Wolf minimum, Gleissberg-Waldmeier minimum, and 21st century minimum. The purpose is only to achieve better and full objectivity and accuracy, consistent with historical studies of sunspots.

As a final comment they note that the century-long total power anomalies from the 17th to the 20th century are characterized by an exceptionally high power observed during the 20th century compared to the 18th century. This holds even when individual *GSN* cycles display similar cycle amplitudes during both centuries. In addition, the lowest total power during the 410 *year* of *GSN* history occurred in 17th century, being suggestive of a probably very weak solar dynamo.

The paramount greater accuracy and objectivity of the *AI/ML* algorithms - compared to the old-fashioned approach - is therefore evident, and the *GSN* can be quantified within the framework of a probabilistic treatment, including confidence levels.

The role of single cycles (5.5 *year*, 11 *year*, 22 *year*, 30 *year*, 60 *year*, and 120 *year*) and their time variation is clearly evidenced. However, one should rebut the ancient

“dream” to find some “exact” periodicity in the solar activity, in order to be able to predict the future evolution of climate.

A reasonable guess is that the Earth’s magnetosphere captures a fraction $\sim 0.45 \times 10^{-9}$ of the expanding solar corona (Gregori et al., 2025s).

Similarly, the Solar System captures a comparably tiny (and unknown) amount of the clouds of interstellar dust. The size of the cloud of interstellar matter, and the time spent by the Sun to cross it, is perhaps crucial for the control of the solar dynamo. This control is monitored, on the geological time scale, by the sequence of *FRs* (Gregori, 2002, Gregori and Leybourne, 2026c).

Sunspots and climate are, rather, a record on the several centuries time scale. According to this rationale a correlation should therefore be found (perhaps) between sunspots and the guessed encounters with interstellar matter that are usually monitored by means of *VLBI* techniques (see Gregori, 2002 and references therein). To our knowledge, no investigation of this kind is reported as yet in the literature.

Velasco Herrera et al. (2022) envisage that their approach ought to improve the understanding of the time variation of solar activity and of climate (they mention, e.g., Hoyt and Schatten, 1997; Soon and Yaskell, 2003; Soon et al., 2014; Laurenz et al., 2019; Le Mouél et al., 2019, 2020; Connolly et al., 2021).

They also show how their inferred *GNS* agrees - or not - with previous standard series, which, on the other hand, are affected by arbitrary choices of compensation factor, aimed to get rid of the irregularity and heterogeneity of the available historical information. That is, the old-fashioned standard series are biased by the attempt of the researcher to reconstruct a reasonably uniform data sequence. However, are we sure that the data series must be homogeneous and fairly continuous?

In any case, they note that the results based on the *ML/AI* algorithms agree with the latest sunspot reconstruction by Usoskin et al. (2021b), envisaging the robustness of the new method. In addition, the new results agree with the old original series of Hoyt and Schatten (1998), being thus a clear support of the exceptionally low total power during the 17th century and the high total power during the 20th century.

In addition, the Velasco Herrera et al. (2022) analysis agrees with the information provided by cosmogenic isotope proxies, and gives a better insight on the nature of the operation of the solar dynamo during the known low sunspot activity intervals, such as the Maunder minimum of 1645–1715. They also claim that “importantly”, they outlined how to update indefinitely the original *GSN* record by Hoyt and Schatten (1998) with available sunspot observations, and also with the *Debrecen Photoheliographic Data*, the historical and ongoing sunspot observations from China (Lin et al., 2019) and also satellite records. Finally, they propose to rename the four solar secular minima as Maunder minimum, Dalton-Wolf minimum, Gleissberg-Waldmeier minimum, and 21st century minimum.

MiniMax and impact on climate

As far as the Earth is concerned - and the Earth is presently crossing through a heartbeat (determined by the timing of endogenous energy propagation, see Gregori, 2002, Gregori and Leybourne, 2021 and references therein) – climate change is particularly sensitive to the huge, delayed release of endogenous energy, i.e., to the “Earth’s battery” effect. The effect seems to be, perhaps, statistically more intense during active Sun years, while climate change reliefs a little bit with quiet Sun, while the opposite seems to occur in recent years. That is, it seems that the observed climate change is particularly intense due to the low solar activity, and that is going to get somewhat less violent during the subsequent period of increased solar activity. Maybe, the contradicting evidence derives from the time-delay, between endogenous heat production and release, of the “Earth’s battery”. Since, at present, we are through a heartbeat, the time-delay is almost null. Conversely, during non-heartbeat periods, the time delay can be even as long as 27.4 *Ma*. The challenge is represented by a phenomenon of an intensity that was never experienced by humankind.

In this same respect, Choi and Maslov (2010) investigated the relationship between earthquake frequency and solar activity by means of seismicity data during 1973–2010 archived by *USGS* at *NEIC*. Consider the drawback associated with (i) the uneven character of historical data series, (ii) the physically vague definition of sunspot number, (iii) the irregular time-delayed response of tectonic features to the time variation of endogenous heat production and release, and (iv) the aleatory character of a seismic event, which depends on the time-integrated accumulation of elastic energy (see Gregori et al., 2018). Even with the bias of all these limitations, Choi and Maslov (2010) can conclude that “*the number of earthquakes increases during the declining/trough periods. A small sharp spike occurs at the peak. On the other hand, earthquakes decrease during the rising period of the solar cycle ...*”

A related investigation was carried out by Choi and Tsunoda (2011) who investigated the increase of volcanic and seismic activities during periods of low solar activity – i.e., they state “*during the solar hibernation periods*”. No details are here needed. However, they state that “*a massive number of strong earthquakes and volcanic eruptions occurred during the Maunder Minimum or Little Ice Age (1645–1715) worldwide. Both magmatic and seismic activities dwindled dramatically after the end of the Maunder Minimum. The Dalton Minimum shows some regional variations; seismically still quiet in Japan and Turkey, whereas in some other regions including India, Indonesia, continental North America and northern South America very strong earthquakes occurred.* [That is, the regional dependence is related to the state of superswells at that time that determined the regions comparatively more prone to suffer by overthrust of lithospheric slabs into megasynclines.]

Indonesia’s Tambora volcano erupted in this solar low period. Magmatic and seismic events became active worldwide after the closure of the Dalton; this trend has continued until today with a conspicuous rise since 2000

when the 206 and 361 year solar cycles started to decline sharply. The recent spate of unusually strong natural disasters (earthquakes, volcanic eruptions, and extreme weather events) has occurred during the rapidly declining period of this longer solar cycle – probably comparable to the earliest stage of the Maunder Minimum. This paper confirms the remarkably heightened magmatic and seismic events during the major solar hibernation periods in the past ...” [Note the emphasis on the duration of the solar minimum activity, rather than on intensified activity.]

A MiniMax feature, which is relevant for the present discussion, is associated to an anomaly in the extension of sunspots. Fig. 11 shows the unusual largest active region seen on the Sun during the last 24 years that envisages an anomalous heterogenous spatial large-scale distribution of the solar wind at 1 AU. That is, the “open solar flux” F_S defined for Fig. 9, is characterized by a few anomalous and very large B flux-tubes that imply a consequent particular pattern of the expanding solar corona. See also the peculiar structure of Figs 12 and 13.

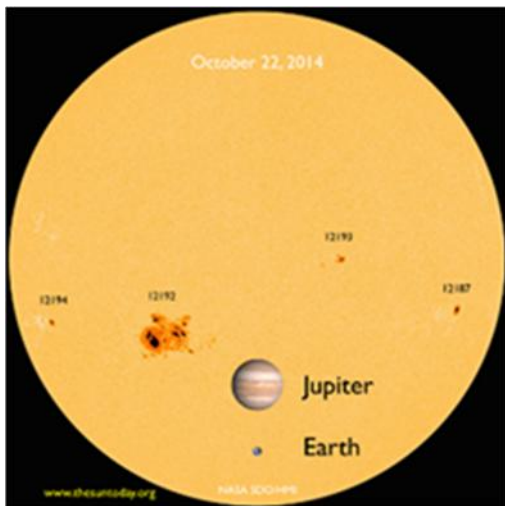


Fig. 11. “The Jupiter-sized sunspot AR 12192 is the largest active region seen on the Sun in 24 years. Credit: C. Alex Young/The Sun Today. The sunspot (called Active Region 12192 or AR 2192) shot off four powerful flares in four days recently, with many more smaller flares sprinkled in as well. The sunspot region was about the size of the planet Jupiter. AR 2192 was actually one of the biggest observed sunspots of all time, ranking 33rd largest of 32,908 active regions since 1874, according to NASA scientists C. Alex Young and Dean Pesnell.” Figure and captions after Kramer (2014c). NASA copyright free policy.

That is, on an indicative basis - and as far as solar physics can be treated like a precise cyclic phenomenon - let us refer to a mean rotation period of the Sun as it is detected by the Earth. Let us claim that this period is ~ 27 days. Much like one is concerned with the variation of the exact duration of the SCL on the scale length of a decade, let us consider the effects associated to the ~ 27 days period variation. According to the best known and approximately standard pattern of the interplanetary magnetic field (IMF), one envisages two “open solar flux” F_S tubes that are crossed by the ecliptic plane (such as e.g., in Fig. 3 of Gregori and Leybourne, 2026b). Hence, the

Earth experiences an e.m. induction by the solar wind with a period of, say, $\sim 27/2 = 13.5$ days.

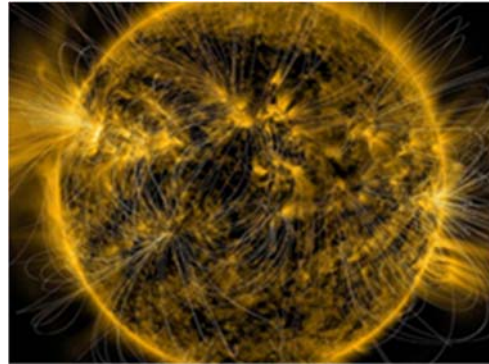


Fig. 12. “The Sun’s B field-lines, shown here using a model, can further twist and loop after they encounter near-Earth space. This leads to errors in space weather forecasts. But is there a way to monitor these late twists? Credit: NASA/SDO/AIA/LMSAL.” Figure and captions after Zastrow (2017a). AGU copyright free policy.

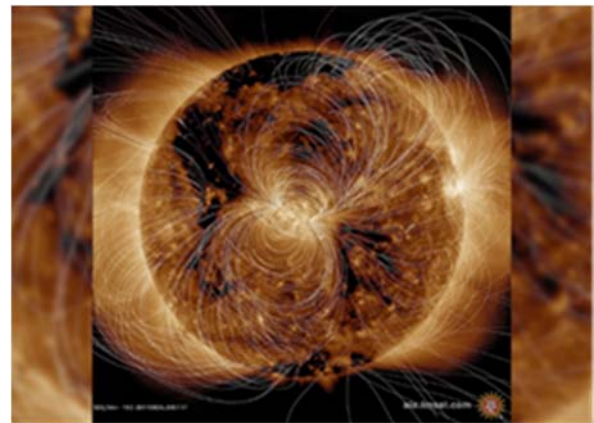


Fig. 13. Sun’s magnetic field-lines after the MiniMax. “The Sun is a ball of invisible, e.m. explosions. This stunning UV image taken by NASA’s SDO models what those swirling magnetic field-lines actually look like. Credit: SDO, NASA.” Figure and captions after Specktor (2018e). NASA copyright free policy. Compared to Fig. 12, note the much different pattern due to the abnormal behavior of the Sun during the MiniMax.

In contrast, the anomalous sunspot pattern of MiniMax envisages a unique large cluster of sunspots. The sunspot number, owing to the conventional rule chosen for its definition, is therefore low. However, it is likely that the cross-section with the Earth’s ecliptic plane is just with one “open solar flux” F_S tube alone. Hence, the Earth experiences an e.m. induction signal of period, say, ~ 27 days. This implies a deeper skin depth of penetration. Hence, deep induced currents are originated inside the mantle, and the TD dynamo changes performance. A different amount is produced of endogenous energy, and since we are during a time of maximum heartbeat, the time delay between endogenous heat production and release at Earth’s surface is almost null (Gregori, 2002; Gregori and Leybourne, 2021).

Differently stated, the amplitude of the sunspot cycle depends on the conventional definition of sunspot number. In contrast, the effect on the TD dynamo of the Earth (or of

any other planetary object) depends on the frequency of the e.m. induction signal that is characterized by the way the object detects the solar wind flow that crosses through its orbit.

Also, the “2016 geomagnetic pulse beneath South America” and the anomalous drift of the World Magnetic Pole (Witze, 2019), which is unexplained by the current models, are closely related to the substantial changes that in recent years ought to have occurred inside the Earth’s TD dynamo.

Wall (2015b) shows the “monster” flare of March 11, 2015 (Figs 14 and 15). “The Wednesday (March 11, 2015) flare registered as an X2.2 Sun storm on the scale used to measure solar tempests. Scientists classify strong solar flares into three categories: C, M and X, with C being the weakest, M being mid-level and X the strongest. X flares are 10 times more powerful than M flares. X2 and X3 flares are twice and three times as potent, respectively, as X1 flares ... Solar flares are often accompanied by CMEs ...”

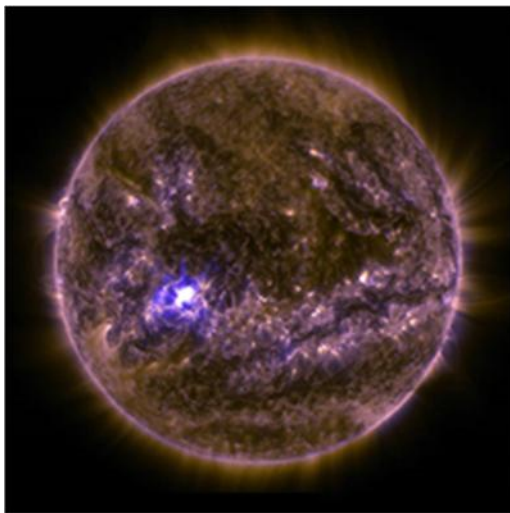


Fig. 14. “NASA’s SDO captured an image of an X2.2 solar flare on March 11, 2015, seen as a bright flash of light on the left side of the Sun ... Credit: NASA/SDO.” Figure and captions after Wall (2015b). NASA copyright free policy.

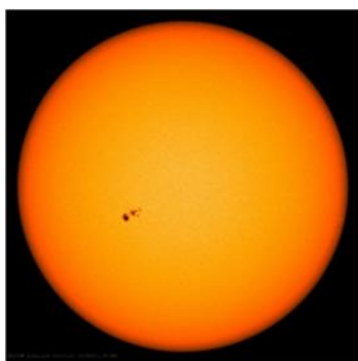


Fig. 15. “The sunspot AR12297 is visible in this image, taken by NASA’s SDO on March 11, 2015. Credit: NASA/SDO.” Figure and captions after Wall (2015b). NASA copyright free policy.

“In 2008 and 2009 an eerie quiet descended on the Sun. Sunspot counts dropped to historically-low levels and solar flares ceased altogether. As the longest and deepest solar

minimum in a century unfolded ... [Note the emphasis on solar minimum.] *Although textbooks call it the ‘11 year solar cycle’, the actual cycle can take anywhere from 9 to 14 years to complete. Some Solar Maxes are strong, others weak, [again, here the focus is on solar maxima] and, sometimes, as happened for nearly 70 years in the 17th century, the solar cycle can vanish altogether ... This solar cycle continues to rank among the weakest on record ... As a result, many researchers have started calling the ongoing peak a ‘MiniMax’ ... Solar cycle 24, such as it is, will probably start fading by 2015 ...*” Phillips (2014e).

In September 2017 the Sun continued to display a “monster” activity, in surprising contrast to the expected trend towards the next minimum (Lewin, 2017g; Salazar, 2017a). The extremely large anomalous scatter, both in space and time, is impressive of different solar emissions. The implication on “climate” is illustrated below.

Concerning the last solar minimum, Howell (2014d) claims that “the last minimum in 2009 was the weakest ever seen since the space age began in the 1950s ... [according to the argument here below, this anomalous solar minimum duration seems likely to be the primary responsible for the ongoing climate anomalies] *Some researchers believe the Sun’s next minimum of activity could be even lower than in 2009.*”

McCracken and Beer (2014) compare the extended solar minimum of 2006-2009 with the Spörer, Maunder, and Dalton Grand Minima and synthesize their findings as follows. “We use cosmic radiation records (neutron monitor and the cosmogenic radionuclides, ¹⁰Be and ¹⁴C) as a proxy to compare the solar activity during the extended solar minimum 2006-2009, with that during the Grand Solar Minima and Maxima that occurred between 1391 and 2010. The inferred cosmic ray intensities during the Spörer, Maunder, and Dalton Grand Minima were significantly greater than those during 2006-2009.

The onset phases of the three Grand Minima extended over between two and five Schwabe (sunspot) cycles, the cosmic ray intensity at the Schwabe minima increasing from a value approximating that of 2006-2009, to substantially higher values later in the Grand Minimum. The minimum estimated strengths of the heliospheric magnetic field (HMF) near Earth during the Grand Minima were 2.4 nT (Spörer), < 2.0 nT (Maunder), and 2.6 nT (Dalton), compared to 3.9 nT in 2009.

We conclude that the periods of highest solar activity during the Maunder Minimum approximated those near the sunspot minima between 1954-1996. The average ratio of the maximum to minimum estimated HMF in the six Schwabe cycles in the Maunder Minimum is 1.54 (range 1.30 – 1.85) compared to 1.52 (1.31 – 1.63) for the modern epoch suggesting similar operation of the solar dynamo in both intervals.

The onset phase of the Maunder Minimum extending over five Schwabe cycles, and the large increase in cosmic ray flux (and decrease in estimated HMF), leads us to speculate that the MHD amplification in the solar dynamo exhibits a relaxation time well in excess of the 11 year period of the Schwabe cycle.”

We note that the concern is only about solar activity, while a most critical control is represented by the time-delay between endogenous heat production and release. At present, the time delay is almost null, while during the entire human history it was substantially much longer.

The anomalous behavior of the Sun continued also in subsequent years. A total solar eclipse occurred on 21 August 2017, and Fig. 16 shows a photograph made from an aircraft that flew at altitudes $> 15 \text{ km}$ along the path of totality.



Fig. 16. Total solar eclipse of 21 August 2017 observed from the NASA's WB-57F high-altitude research aircraft, "using two 22 cm telescopes mounted aboard the craft that are tuned to see in green (approximately 530 nm), in the visible continuum (400 – 700 nm), and at medium-wave IR (3 – 5 μm) wavelengths. Imaging the Sun in green light helped the team focus on the light emitted by the corona itself rather than light produced by lower layers and scattered by the ultrahot, diffuse gas." Figure after Frazier (2017), and captions after Cartier (2018a). NASA copyright free policy.

Note the anomalous large "open solar flux" that characterizes huge **B** flux tubes inside the expanding solar corona. A few months later, in November 7-9, 2017, a broad hole in the corona was the Sun's dominant feature (Fig. 17). Also, in September 2018 the Sun seemed anomalous with a giant hole (Fig. 18).

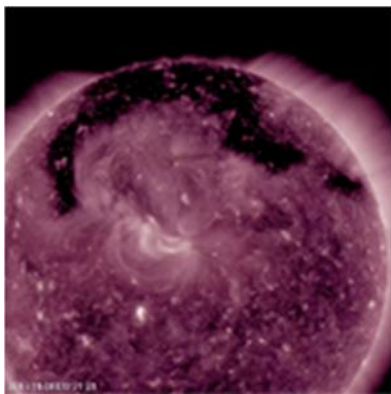


Fig. 17. "A broad hole in the corona was the Sun's dominant feature in November 7-9, 2017, as shown in this image from NASA's SDO. The hole is easily recognizable as the dark expanse across the top of the Sun and extending down in each side. Coronal holes are magnetically open areas on the Sun that allow high-speed solar wind to gush out into space. They always appear darker in extreme UV ... Image Credit: NASA/GSFC/SDO." Figure and captions after Smith (2017b). NASA copyright free policy.

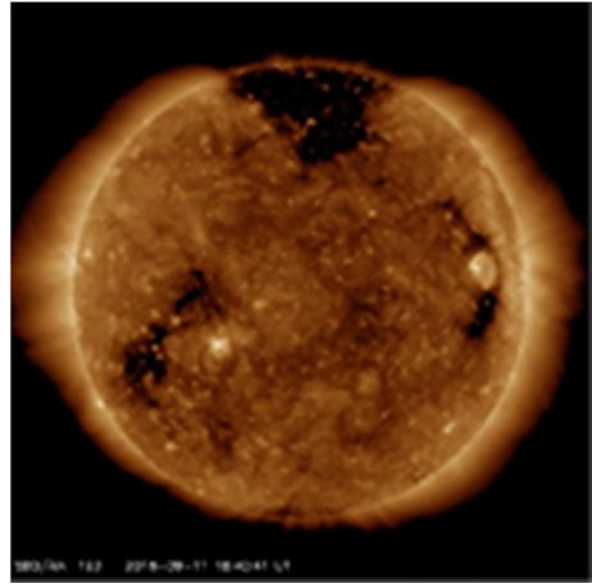


Fig. 18. "NASA's Solar Dynamics Observatory spacecraft captured this image of a giant hole (dark patch at top) in the Sun's outer atmosphere, or corona, on September 11, 2018. Credit: NASA/SDO." Figure and captions after Wall (2018k). NASA copyright free policy.

Also, the solar microwave spectrum was investigated, but it displayed no relevant variation. Shimojo et al. (2017) report as follows their analysis.

"The total solar fluxes at 1, 2, 3.75, and 9.4 GHz were observed continuously from 1957 to 1994 at Toyokawa, Japan, and from 1994 until now at Nobeyama, Japan, with the current Nobeyama Radio Polarimeters. We examined the multifrequency and long-term data sets, and found that not only the microwave solar flux but also its monthly standard deviation indicate the long-term variation of solar activity.

Furthermore, we found that the microwave spectra at the solar minima of cycles 20-24 agree with each other. These results show that the average atmospheric structure above the upper chromosphere in the quiet-Sun has not varied for half a century, and suggest that the energy input for atmospheric heating from the sub-photosphere to the corona have not changed in the quiet-Sun despite significantly differing strengths of magnetic activity in the last five solar cycles."

In any case, even independent of huge variations of long-period solar activity, also shorter, though extremely violent, short-duration events were reported. For instance, Mekhaldi et al. (2015) report about two events occurred in AD 774-775 and 993-994.

"The origin of two large peaks in the atmospheric radiocarbon (^{14}C) concentration at AD 774-775 and 993-994 is still debated. There is consensus, however, that these features can only be explained by an increase in the atmospheric ^{14}C production rate due to an extraterrestrial event. Here we provide evidence that these peaks were most likely produced by extreme solar events, based on several new annually resolved ^{10}Be measurements from both Arctic and Antarctic ice cores. Using ice core ^{36}Cl data in pair with ^{10}Be , we further show that these solar events

were characterized by a very hard energy spectrum with high fluxes of solar protons with energy above 100 MeV. These results imply that the larger of the two events (AD 774-775) was at least five times stronger than any instrumentally recorded solar event ...”

That is, either the previous solar minimum or the subsequent MiniMax denote a definitely unusual anomalous Sun’s behavior. Therefore, if the rationale is correct that is proposed in the present study, the relevant physical driver is expressed by formula (3) rather than by sunspot number or by any other index of solar activity. In addition, this parameter is substantially different during heartbeat, like at present, compared to all other periods.

In this respect, the empirical and approximate definition of the *SN* or *GN* series ought to be considered. In addition, according to Fig. 7, note that all cycles look almost the same after their respective first ~ 6 years. It seems that nobody has any explanation for this feature, even though a very detailed analysis was carried out as per Figs 65, 66, 67, 68, 69 of Clette et al. (2014) (not here reproduced).

In addition, the conclusion of this kind of analysis of the “cycle morphology” depends on the criterion chosen to superpose different cycles. No criterion is *per se* either wrong or correct. Every choice can lead to some indication. However, as already stressed above, no exact repetitiveness was ever observed of solar cycles.

According to the rationale that is here envisaged – in addition to the time delay between endogenous heat production and release at Earth’s surface - the control factor ought to be the spectral component of the e.m. interaction of the solar wind with the Earth’s mantle - which can occur through the “antennae” represented by the sea-urchin spikes. In fact, an e.m. resonance affects the production of endogenous heat that - with a suitable time delay - can be different in both space and/or time while dealing with every different case history, and thus finally affect climate. That is, the system is highly non-linear, and mostly the time delay is enormously different at different times.

In any case, consider the electrostatic explanation of the solar cycle (see Gregori and Leybourne, 2026b). Fig. 7 - if it is correct - is suggestive that the first ~ 6 years of every cycle are characterized by a different amount of total starting negative electric charge stored by the Sun. Hence, the set of huge van de Graaff generators, which are to be detected like sunspots, is triggered every time with a different spacetime distribution, as every sunspot cycle it is well-known to display a different distribution (both in size and in relative timing) of sunspots.

Note also that the spatial distribution of sunspots is a morphological feature that is other than the aforementioned “open solar flux” F_S . In addition, consider that every planetary object is an almost “point-like” detector of the expanding solar corona. Hence, a “point-like” detector is sensitive to the geometry of the solar corona expansion - i.e., to a local almost “point-like” flux of solar wind flow. In contrast, it is not sensitive to the integral of the large-scale features of the solar wind. That is, compared to the overall integrated “open solar flux” F_S , the morphology is much more important of the geometry and size of sunspots, as this morphology directly affects the local “point-like”

features of the solar wind that are detected by a planetary object.

In fact, consider the great variability displayed by the expanding solar corona. It is nonsensical to suppose that e.m. induction can be comparable at different epochs. The induction originated by the solar wind inside every given planetary object can be quite different in every case history.

In general, as already mentioned, according to observational evidence, the solar **B** pattern looks comparably much more regular and better organized during quiet Sun periods, and more scattered and erratic during active Sun (Fig. 19).

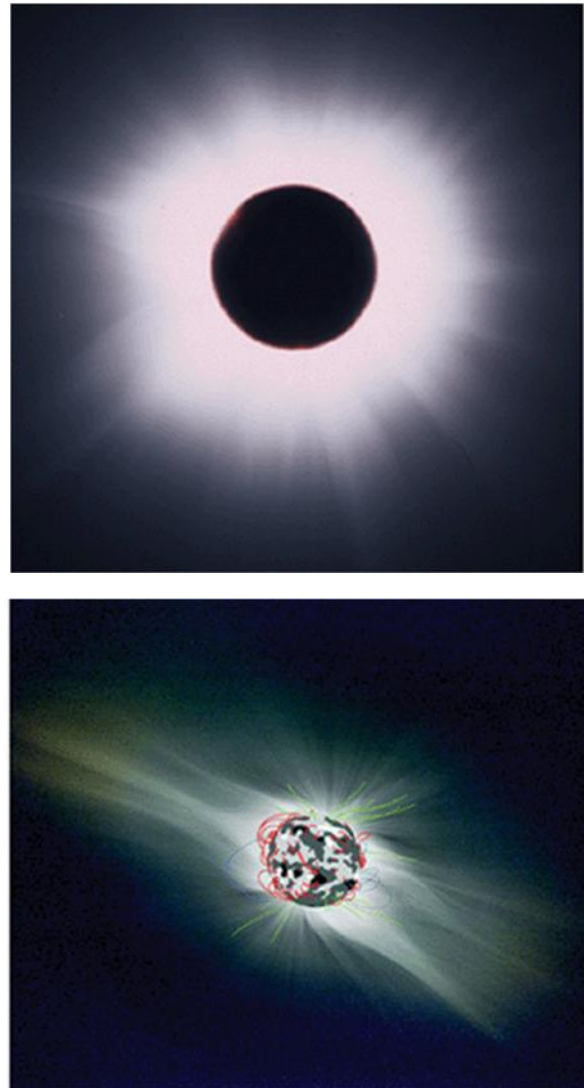


Fig. 19 - “Eclipse images of the corona in white light on 11 August 1999 during solar maximum (a) and on 26 February 1998 during solar minimum (b). The thin colored lines overlaid on the 1998 eclipse image are the results of source-surface **B** calculations, and trace the **B** lines resulting from these calculations. (Eclipse image courtesy Christian Viladrich, **B** line calculations courtesy Y.-M. Wang.)” Figure and captions after Habbal and Woo (2004).

Fig. 20 is the picture of a solar eclipse observed at ground by a telescope Takahashi FSQ106 f/5 and a digital camera Nikon D2x. A rapid sequence of 18 pictures were

taken, every one with a different exposure time (1/8000 sec, 1/4000, 1/2000, ... , 2 sec). This series of pictures was then assembled by computer, upon selecting the details provided by every image. The series of 15-18 pictures was completed by ~ 10 sec.



Fig. 20. (a) Total solar eclipse observed from the Libyan desert on 29 March, 2006. Computer composition of 18 camera pictures by different exposure times. See text. Credit: Gianni Fardelli, gianni@widepicture.com, www.widepicture.com, from the cover of *Astronomia, La rivista dell'Unione Astrofili Italiani*, with kind permission of Gianni Fardelli. May-June 2006.

Fig. 21 shows an annular eclipse. Note that sunspots are located where **B** field-lines are more radial, i.e. where the “van de Graaff generator” ejects electrons that break through the photosphere. Also other stars (not here shown) display similar features.

Figs 19 through 27 recall several representation of the Sun (the God “Ra”), as a winged figure - the so-called “winged Sun” - which is found on several classical ancient Egyptian low reliefs (Saito, 1992). If this is correct, either the ancient Egyptians exploited a great skill in the observation of solar corona (e.g. during total eclipses, by some device suited to eclipse the solar disk, etc.), or the Sun was through some period of extremely low activity, and such a “winged” pattern looked visually much better evident than at present.

A short historical account of the representation of the solar corona during total eclipse is given by *Anonymous* (2017k).

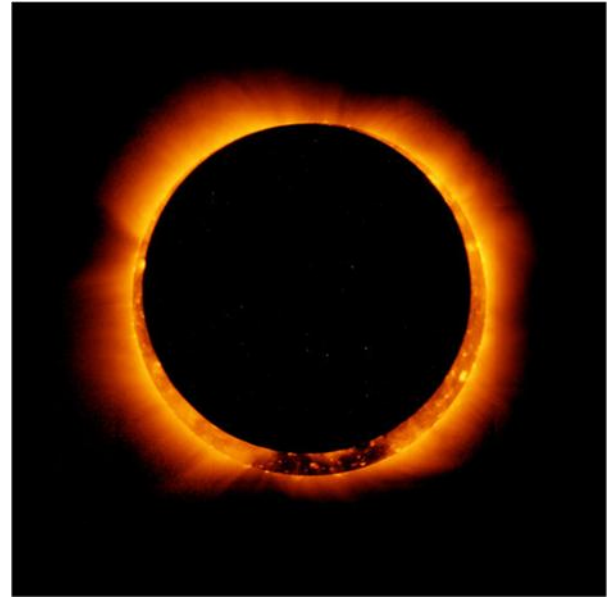


Fig. 21 - “Sunspots can be seen in this image that captures the Moon moving across the face of the Sun during an annular eclipse on May 20, 2012. The eclipse was visible in Tokyo; the shadow then traveled across the Pacific Ocean and all the way to Texas.” Figure and captions after Cofield (2017a). NASA copyright free policy.

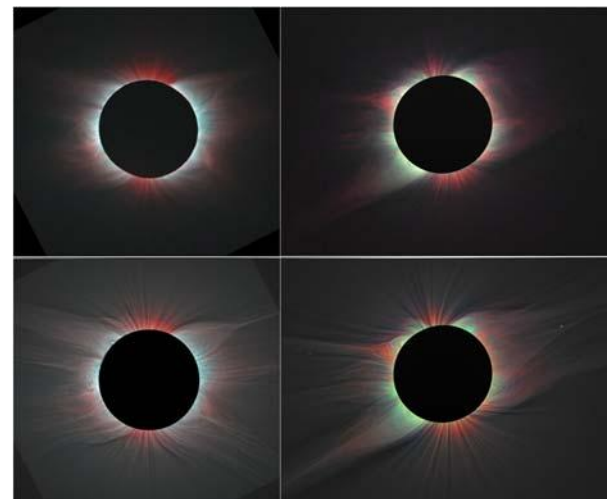


Fig. 22 - Images of the solar corona, shown as color overlays of the emission from highly ionized iron lines for the 2006 eclipse (left column) and 2008 eclipse (right column), with white-light images added in the bottom row. Red indicates the line Fe XI 789.2 nm, blue represents the line Fe XIII 1074.7 nm, and green shows the line Fe XIV 530.3 nm. These are the first maps that show the 2D distribution of coronal electron temperature and ion charge state. Credit: Habbal *et al.*, after Layton (2010). NASA copyright free policy.

“We don’t really know how long humans have noticed the spectacular corona of our Sun, but it seems likely we have admired it for as long as humans have existed. The first western description of the corona during a total solar eclipse was probably that of Lucien in 932 BC ’ ... a kind of light is visible about the rim which keeps the shadow [of the Moon] from being profound and absolute.’ Some ancient petroglyphs and other primitive art seem to suggest a Sun disk with ‘protrusions’ of one kind or another, but we can’t

be certain of this interpretation. Amazingly, we have no accurate sketches of the corona until perhaps as recently the May 25, 1751 eclipse, drawn by Cambridge Professor Roger Cotes from England ... “

Anonymous (2017k) shows a few historical figures. Only Figs 23 and 25 are here reported. No steady regularity seems to occur. Rather, a somewhat erratic behavior of the magnetic pattern of the expanding solar corona.

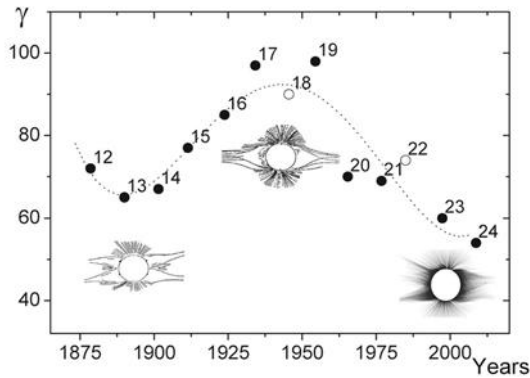


Fig. 23 - “Coronal shape changes 1870 to 2004. (Credit Tlatov: Astronomy and Astrophysics, 2010).” The number are Cycle number. The index γ “characterizes the angle between high-latitude boundaries of the large coronal streamers at a distance of $2R_{\odot}$. The γ index is the sum of the angles at the eastern and western limbs: $\gamma = \gamma_W + \gamma_E$. Fig. 24 gives the scheme showing how parameter γ is determined. In fact, the γ index is a simpler version of the corona flattening indices (Ludendorff, 1928; Nikolskiy, 1955).” Figure and captions after Anonymous (2017k) and <https://arxiv.org/ftp/arxiv/papers/0804/0804.1989.pdf>. NASA copyright free policy.

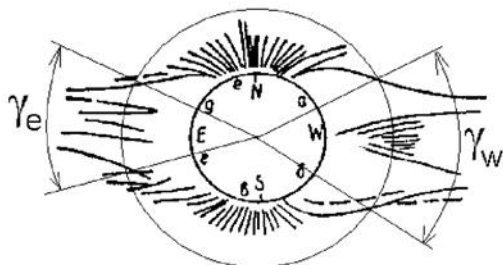


Fig. 24 - “Scheme showing how the angles defining parameter $\gamma = \gamma_W + \gamma_E$ are found for the eclipse of 1923.”

In particular, concerning MiniMax, consider the very anomalous pattern shown during the August 2017 total solar eclipse (Figs 26 and 27). Therefore, some anomalous time-delayed response has also to be expected, displayed by the outer planets (see Gregori et al., 2025u).

However, always relying on Fig. 7, after ~ 6 years the former cycle-to-cycle difference is no more crucial, of the original total stored negative charge. Hence, the behavior becomes standard and approximately almost the same of the whole huge MHD machine represented by the Sun.

In any case, upon comparing the first half of different solar cycles, the long-period spectral composition seems to be dramatically different of every given solar cycle. This applies also to the minimum stage of every solar cycle - when the Sun, after reaching its maximum negative electric charge, prepares the forthcoming huge van de Graaff

generators that are shortly going to become operative and generate sunspots.

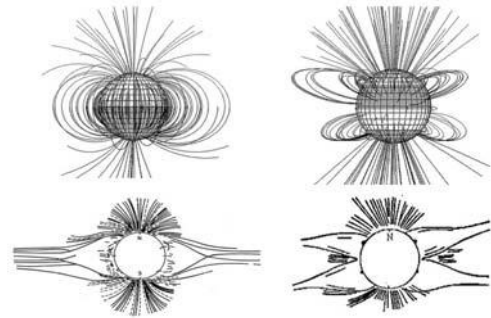


Fig. 25 - “Coronal changes (Credit Tlatov: Astronomy and Astrophysics, 2010). This figure shows the predicted magnetic field in the corona for Cycle 13 in 1889 (left) and Cycle 19 in 1954 (right) ...” Figure and captions after Anonymous (2017k). NASA copyright free policy.

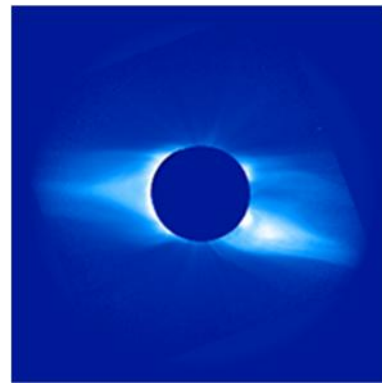


Fig. 26. “Total solar eclipses allow researchers a unique opportunity to study the Sun’s corona, which in turn informs what we know about space weather. Credit: NCAR High Altitude Observatory/NSF.” Figure and captions after Anonymous (2017l). With kind UCAR permission (“Fair Use”).

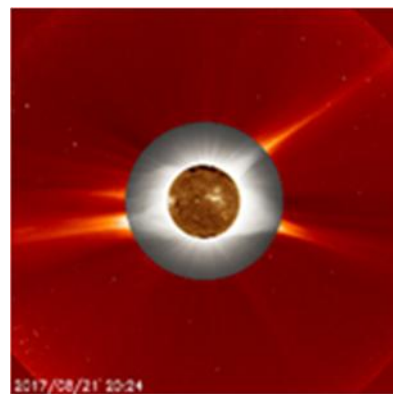


Fig. 27. “A ground-based image of the total solar eclipse on August 21, 2017 (gray, middle ring), is superimposed over an image of the Sun’s atmosphere, called the corona (red, outermost ring), as seen by ESA and NASA’s Solar and Heliospheric Observatory (SOHO), which watches the Sun from space. At center is an image of the Sun’s surface as seen by NASA’s SDO in extreme UV wavelengths of light ... Credits: innermost image: NASA/SDO; ground-based eclipse image: Jay Pasachoff, Ron Dantowitz, Christian Lockwood and the Williams College Eclipse Expedition/NSF/National Geographic; Outer image: ESA/NASA/SOHO.” Figure and captions after Garner (2017). NASA copyright free policy.

That is, a short-lived anomalous solar particle ejection is responsible for anomalous auroral displays, for the hazard of space probes instruments, or for blackouts either of power lines and/or communication networks.

In contrast, paradoxically it is found that anomalous long solar minimum periods are responsible for anomalous operation of planetary *TD* dynamos, for endogenous energy generation, for ocean/atmosphere dynamics, for violent convective patterns, for meteorological hazards and climate instability, for ionospheric charging processes, for *TGF* generation and air-crash probability, and also for anomalous crustal stress, telluric currents, air-earth currents, *l.o.d.* variation and pole movement, earthquake trigger, etc., consistently with the aforementioned analysis by Choi and Maslov (2010) and Choi and Tsunoda (2011).

Differently stated, the comparatively short-lived period of time of maximum solar activity ought to be responsible for comparatively shorter period e.m. variations that influence phenomena occurring through the “external” way. That is, these e.m. signals do not seem to resonate inside the mantle. Hence, they are not effective for the control of the “internal” way.

In contrast, a prolonged period of solar minimum ought to characterize the long-period component of solar activity and of its associated e.m. signal. This long-period component resonates with the Earth’s mantle. Thus, it strongly affects the production of endogenous energy and all phenomena controlled through the “internal” way.

By the way, upon a qualitative and intuitive feeling, when the Earth approaches the top of a heartbeat of the Earth electrocardiogram, no relevant time-delay ought to exist between the observed prolonged solar minimum duration and the impact on climate. That is, the existing sear-urchin spikes are efficient “channels” to convey rapidly to the Earth’s surface a large fraction of the changes of endogenous heat production by the *TD* dynamo (Gregori, 2002, Gregori and Leybourne, 2021, and references therein).

That is, in any case as far as the climate impact is concerned, the difference is determined by the duration of the solar minimum that precedes a maximum, rather than by the intensity of the maximum.

Differently stated, whenever the Sun affords to break the magnetic bottle that - through Biermann’s blocking - confines its total negative electric charge, the Sun releases its excess Coulomb charge during a comparably short time. This is the duration of the solar maximum. The intensity of the maximum depends both on the total amount of negative charge to be released by the Sun, and by the number of “van de Graaff generators”. In any case, the discharge phenomenon occurs as rapidly as possible almost independent of the total charge to be released. Duration and intensity of the discharge are independent features.

This holds independent of the correct explanation of the observed inter-cycle comparative difference of sunspots. Note that, if this is correct, the largest comparative anomalies between different cycles ought to occur during the first ~ 6 years of every respective cycle, although the manifestation of these anomalies perhaps can require some time-delay before being detectable by climate.

Hence, a reasonable attempt could be to carry out a spectral analysis of the first half of every cycle. This could be done e.g., by a truncated Fourier series of periods equal to 11 years plus a discrete set of its higher harmonics.

The parameter of formula (3) ought to be larger for some frequency, which is in resonance with some internal structure of the Earth, so that it can more effectively influence the generation of endogenous energy by means of the *TD* dynamo, and of the impact on “climate” and geodynamics, although with a varying time delay.

At present, *a priori* we cannot know what is this resonance frequency (or frequencies). Suppose as a working hypothesis to choose one frequency f_0 for which a relative maximum is observed during different solar cycles. It is thus possible to define a hierarchy of the different cycles, depending on the amplitude of the spectral component of frequency f_0 . Define one different hierarchy by means of a set of suitable different trial frequencies f_j ($j = 0, 1, 2 \dots$). Finally, one can try to envisage what members of the hierarchy appear to be better correlated with the observed (time-delayed?) “climate anomalies”.

Increased endogenous heat flow vs. climate control

The key factor for “climate” control is therefore the space- and time-variation of the release of endogenous energy.

Note, however, that the definition of “climate anomaly” is *per se* very vague and not clearly defined. It is an *ad hoc* term that ought to indicate whether “climate” is more or less “comfortable” or “harmful” for the humans. However, also the sunspot number is vaguely defined. Hence, it is very difficult to make any precise and quantitative science by means of vaguely defined quantities. In any case, if the aforementioned attempt is successful, a resonance frequency ought to be found (or a set of a few resonance-frequencies), which is typical of the Earth’s *TD* dynamo. All this, however, as yet has never been carried out.

On the other hand, the physics is other than a mere mathematical search for some trial frequencies f_j ($j = 0, 1, 2 \dots$). Indeed, no full exploitation is possible of one complete wave at these very low frequencies, as their wavelength in general is much larger than the size of the whole Solar System. These frequencies are to be considered as the mathematical Fourier description of some more or less large, and almost step-like, non-cyclic changes of the solar wind flow. That is, the frequency concept is related to time variation, hence to time gradient, while a more realistic physical description ought to consider rather the space gradient of the solar wind flow. The connection between the two viewpoints is through the orbital motion of every planetary object. In general, therefore, a solar wind flow with a comparatively smaller (larger) space gradient is associated with comparatively higher (lower) frequencies. The time variation is more familiar and easier to understand only when dealing with phenomena that last for time lags equal to several full periods of the observed phenomena. In contrast, the space variation viewpoint is more akin to natural reality, when phenomena last less than the time lag

of one full periodical variation. The phenomenon is the same, but the viewpoint different.

Differently stated, concerning the solar-terrestrial climate control, in terms of physics, one should refer to space gradient, and in terms of mathematics one should refer to time gradient. Therefore, when sunspots have some anomalous size, such as in Fig. 11, the time variation of the e.m. induction by the solar wind into the Earth is characterized by anomalously low frequencies and by few and very large *IMF* flux tubes.

In any case, whatever is the mechanism that controls the time varying release of endogenous heat, the greater release must be associated with a tetrahedron pattern (Gregori and Leybourne, 2021). The tetrahedron is “exact” in a strict sense, and the Earth’s surface morphology is perturbed by the drift of the lithosphere over the *ALB*. A vertex of the tetrahedron is located exactly beneath the North Pole (geographic), which, therefore, must be expected to be a large region of relatively larger release of endogenous heat. This explains the present intense climate change ongoing in the Arctic Polar Cap.

The concern is how such a feature involves also the lower latitudes. The key is the location of the jet stream.

The jet stream is typically ~8 – 15 km high in the troposphere, while two vortices are located above the North and South polar region, at much greater heights in the stratosphere (16 – 48 km). In the Southern Hemisphere even a comparatively stronger polar vortex stratosphere occurs in the local winter. The dynamics of the ocean/atmosphere system is quite intricate. We cannot enter into details, as they ought to require an extensive discussion of the presently largely understood hemispherical or planetary oscillations of the whole natural system.

Let us refer only to descriptive features and consider how observations fit with the mechanism of the modulation of the *TD* dynamo, and of the time-varying release of endogenous energy, mainly beneath the North Pole and the large surrounding cap.

According to *NOAA*’s description of the vortex phenomenon (Fig. 28), the polar vortex typically does not interact with the jet stream. When the polar vortex is strong and stable, the jet stream stay farther north with fewer “kinks”. This configuration keeps cold air confined over the Arctic cap and mid-latitudes experience a warmer and milder climate.

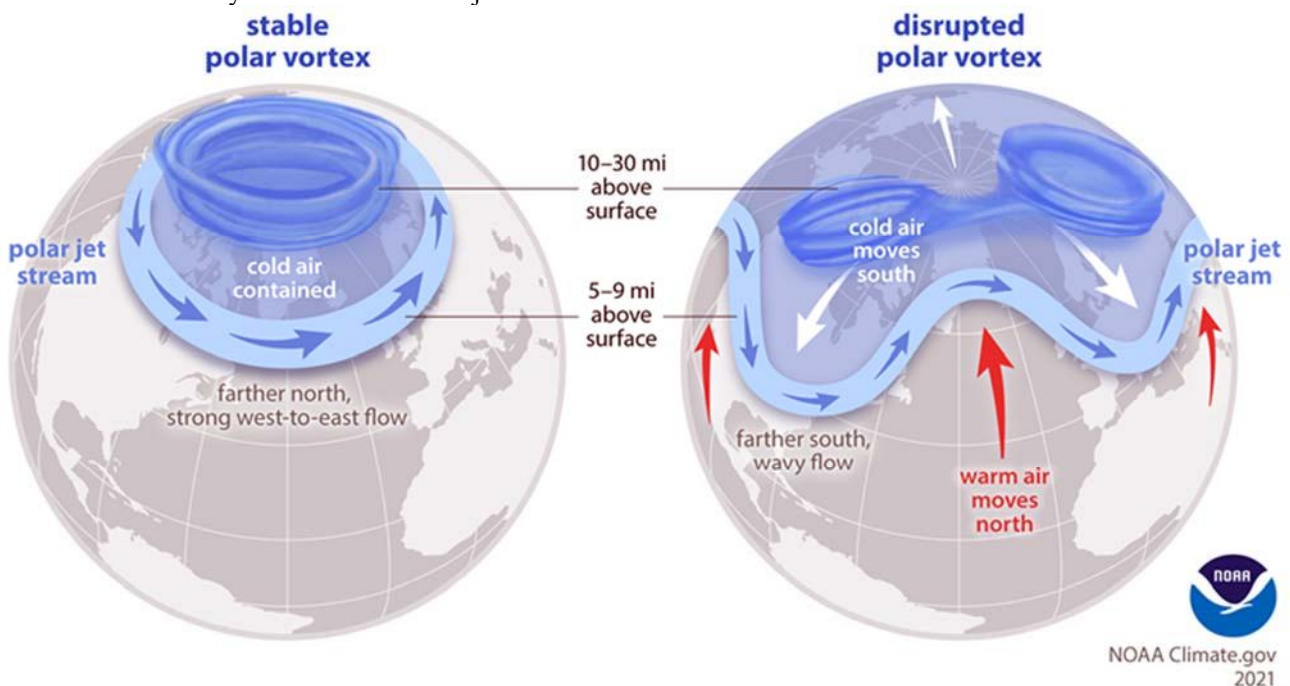


Fig. 28 – Polar vortex and jet stream with “kinks”, and related climate anomalies at different longitudes. See text. Reproduced with kind permission of *NOAA* (fee copyright policy).

However, when a burst occurs of the release of endogenous energy – i.e. when an increase occurs of air-earth currents – the polar vortex is eventually abruptly intensified, and it can even break into two vortices. The jet stream becomes weaker and wavy, i.e. it displays “kinks”. Somewhere the stratosphere experiences the phenomenon known as sudden stratospheric warming. At Earth’s surface, cold air moves to mid-latitudes and warm air to polar latitudes. The phenomenon is not fully understood. However, in general according to the rationale here proposed, the greater the endogenous energy release, the wider the amplitude of the “kinks”.

Thus, it happens that, in general, a greater release of endogenous energy occurs everywhere on the Earth, and all atmospheric precipitations are enhanced. Depending on the relative position of a site with respect to the “kink” and of its longitude, the local climate can be characterized by drought or by flashfloods, by anomalous hot or cold temperature etc.

A cold extreme occurred in February 2021 in the south-central United States, as discussed in Lindsey (2021). Another example occurred in the winter 2022-2023 in the European sector. Mediterranean countries experienced an extremely severe, maybe unprecedented drought. A

latitudinal band roughly along southern France and northern Italy experienced comparatively frequent hailstorms, with hail grains typically even as large as a tennis ball. At other low latitudes, whenever it rained, frequent devastating flashfloods occurred, while in central and northern Europe a “record” snow cover was reported.

That is, a larger amount is available everywhere of released endogenous heat flow – hence, of local air-earth currents. Unfortunately no array is available to monitor this phenomenon according to the rationale explained in Gregori et al. (2025c). The larger available energy increased the strength of the Cowling dynamo at different scale-sizes (as per Gregori et al., 2026d). Hence, whenever the conditions occurred suited for a given phenomenon, i.e. either snow, or rain, or hail precipitation, the phenomenon displayed an anomalous extreme violence.

This is “climate change” that, however, is manifested in a different way depending on the location relative to the “kinks” of the jet stream.

In any case, the phenomenon is not an occasional, short-lived and sporadic anomaly. Rather, it implies an eventually prolonged anomaly and it can even change the local interaction with the biosphere. For instance, one of the authors (JRW) in January 2023, while driving, noticed a bit of paler green that he guessed was vegetation near the edge of the driveway. That is, the phenomenon was reasonably diffuse as to be visible while driving car. He made a photo (Fig. 29), which appeared to show a lichen, one that may have spawned some of itself onto the dead leaves. Lichens are actually symbiotic associations between fungi and algæ or photosynthetic bacteria. They grow on tree trunks and rocks, and dog lichen is known for ruining lawns. Lichens survive on exposed rocks very near glaciers. They thrive in the Arctic north.



Fig. 29 – Lichens beside a driveway in Cotter, Arkansas, in January 2023. See text. Unpublished figure.

At present, a substantial controversy exists concerning the explanation of these phenomena. A key issue deals with the distinction between the “external” and “internal” way in solar-terrestrial relations (Gregori et al., 2026a). The most fashionable approach is in terms of the “external” way, i.e.

a variation of the solar wind flow (or of solar radiation), or the “space weather”, affects progressively lower atmospheric layers, until controlling climate change at Earth’s surface.

JRW lived in Oklahoma for 31 years, and remembers a very hot summer of drought, followed a few years later by an especially cold winter. Oklahoma’s very hot, driest July of the century was in 1980, and the average statewide precipitation was only 1.04 cm. That was near the peak of solar Cycle 21. The temperature measured in the shade on one of those July 1980 days was 47.6 °C. The cold record was in December of 1983 (near 1984), most of the way down to the minimum that followed solar Cycle 21. The average state temperature during that December 1983 was -3°C, and Oklahoma City stayed below freezing from December 17th to the 31st (not the usual situation).

It should be stressed, however, that the natural system is a unique entity (Gregori et al., 2022, 2022a, 2025w). Concerning solar-terrestrial relations, one must consider the unique system composed of Sun, Earth’s atmosphere, ocean, and solid Earth. The e.m. induction by the solar wind controls the efficiency of the TD dynamo – which is supplied mainly by the lunar tide (Gregori, 2002, Gregori and Leybourne, 2021). Hence, the control is extended to the time-delayed of endogenous energy released by the “Earth’s battery”. Therefore, an “internal” way for the control of climate is operative, through the control by the solar wind of the release of endogenous heat – hence of air-earth currents. Or the control is of “internal” origin, although the generation of endogenous energy is controlled by the Sun.

Several unexplained phenomena seem to support the “internal” way, including e.g. the correlation of climate change with the expected increase of seismic and volcanic activity. However, no account can be here given of the long discussion carried out in Gregori (2002).

Also palæoclimatology and ice ages should require a very long discussion that cannot be here illustrated by a few statements. An extensive discussion ought to be required, and cannot be here even briefly mentioned.

We stress, rather, that MiniMax and climate anomalies seem to be reasonably associated each other. The treatment of sunspot cycle is not, however, sufficiently clear. It seems likely that, perhaps - much like the Earth’s magnetosphere captures a tiny fraction of the expanding solar corona - the heliosphere captures a maybe even smaller fraction of clouds of interstellar wind and dust. The whims of the Sun seem therefore to be controlled by the encounters of interstellar clouds, in a perspective of Galaxy-Sun-Earth relations (Gregori, 2002).

The same rationale applies to anomalous storms eventually observed on the large gaseous outer planets. The possible association with the MiniMax are discussed in Gregori et al. (2025u).

In any case, a long way, hard thinking, and unprecedented data records are needed - mainly concerned with a suitable monitoring of air-earth currents - before achieving a reasonable understanding.

"There are more things in heaven and earth, Horatio,
Than are dreamt of in your philosophy" (Hamlet, Act I,
Scene, IV, 166-167).

Conclusions

Sound physical reasons, related to solar processes, very likely seem consistent with a positive charge of the solar wind. The electrical unbalance of the Sun is cyclically reset through the ejection of huge amounts of electrons, inside huge van de Graaff accelerators, and this is the most straightforward explanation of the sunspot cycle.

Concerning the impact of the solar cycle on climate, on a statistical basis - and allowing for all uncertainties related to sunspot cycle definition - a low solar activity is correlated with a comparatively milder climate. This conclusion seems, however, contradicted by the recent MiniMax cycle. This inference is suggestive of an agreement with the expected dominant dependence on the time-delay between endogenous heat production by the *TD* dynamo, and energy release at Earth's surface through air-earth currents. In fact, the recent MiniMax occurred while the Earth is going through a heartbeat of the Earth's electrocardiogram, when the time delay is basically null. In contrast, during the entire time span of human history - and also during the time interval spanned by several proxies - the time-delay has been varying, being eventually as long as $\sim 27.4 Ma$. That is, the seemingly higher impact on climate during active Sun derives from the time-delay of the release of endogenous energy produced during a much longer previous time interval. Therefore, no direct correlation must be expected between a single solar cycle and climate, unless observations are carried out during a maximum of an Earth's heartbeat.

If this interpretation is correct, a leading factor is therefore the encounters of the Solar System with clouds of interstellar matter, which control the Sun's dynamo, solar activity, hence the morphology of every cycle through a modulation of solar radiation, and mostly of the solar wind, in a perspective of Galaxy-Sun-Earth relations.

An accompanying paper (Gregori et al., 2025u) highlights several morphological features of different planetary objects. In addition, the Pluto/Charon binary system is found to be a natural laboratory suited to check this whole proposed interpretation.

Acknowledgement

We acknowledge all co-workers that, during decades, and in different ways contributed to the exploitation of the analyses mentioned in the present study.

Mostly, we thank Willie Soon and Victor Manuel Velasco Herrera for some relevant information, and in particular concerning their fundamental papers Velasco Herrera et al. (2021, 2022), with high-quality figures and permission to use figures.

We also warmly thank Dong WenJie and Gao Xiaoqing for providing valuable information on some investigations

of the school of the late Professor Tang MaoCang. We like also to thank for the warm encouragement we had from several outstanding scientists.

Funding Information

G.P. Gregori is retired since 2005. B.A. Leybourne is a semi-retired self-funded independent researcher.

Author's Contributions

This study derived from a long-lasting cooperation by both authors. The backbone draft was prepared by the first author, although a large number of ideas resulted from the emergence of long lasting discussions with all coauthors and friends.

Ethics

This article is original and contains unpublished material. Authors declare that there are no ethical issues and no conflict of interest that may arise after the publication of this manuscript.

References

- Alessandrini, B., G.F. Papi, G. de Franceschi, and G.P. Gregori, 1987. The secular variation of the geomagnetic field and the shape of the Earth. *Physics of the Earth and Planetary Interiors*, 48: 84-114; DOI:10.1016/0031-9201(87)90114-2
- Alterman, B.L., J.C. Kasper, R.J. Leamon, and S.W. McIntosh, 2021. Solar wind helium abundance heralds solar cycle onset. *Solar Physics*, 296: 67
- Anonymous, 2012l. Cassini: 15 years of exploration, JPL/Caltech/Cassini/Resources, issued October 30, 2012.
- Anonymous, 2017k. The solar corona, *NASA, ECLIPSE 101*, retrieved December 22, 2017
- Arge, C.N., and V.J. Pizzo, 2000. Improvement in the prediction of solar wind conditions using near-real time solar magnetic field updates, *Journal of Geophysical Research, Space Physics*, 105 (A5): 10,465-10,479; DOI:10.1029/1999JA000262
- Arlt, R., 2008. Digitization of sunspot drawings by Staudacher in 1749 - 1796. *Solar Physics*, 247: 399
- Arlt, R., 2009a. The butterfly diagram in the eighteenth century. *Solar Physics*, 255: 143
- Arlt, R., and J.M. Vaquero, 2020. Historical sunspot records. *Living Reviews of Solar Physics*, 17: 1
- Arlt, R., V.S. Pavai, C. Schmiel, and F. Spada, 2016. Sunspot positions, areas, and group tilt angles for 1611 - 1631 from observations by Christoph Scheiner. *Astronomy and Astrophysics*, 595: A104
- Baranyi, T., L. Györi, and A. Ludmány, 2016. On-line tools for solar data compiled at the Debrecen Observatory and their extensions with the Greenwich sunspot data. *Solar Physics*, 291: 3081

- Bard, E., G. Raisbeck, F. Yiou, and J. Jouzel, 2000, Solar irradiance during the last 1200 years based on cosmogenic nuclides, *Tellus B*, 52: 985
- Bayes, T., 1763. An essay towards solving a problem in the doctrine of chances. *Philosophical Transactions of the Royal Society of London*, 53: 370
- Beer, J., S. Tobias, and N. Weiss, 1998. An active sun throughout the Maunder Minimum. *Solar Physics*, 181: 237
- Beer, J., S.M. Tobias, and N.O. Weiss, 2018. On long-term modulation of the Sun's magnetic cycle. *Monthly Notices of the Royal Astronomical Society*, 473: 1596
- Berggren, A.-M., J. Beer, G. Possnert, A. Aldahan, P. Kubik, M. Christl, S.J. Johnsen, J. Abreu, and B.M. Vinther, 2009. A 600-year annual ¹⁰Be record from the NGRIP ice core, Greenland. *Geophysical Research Letters*, 36: L11801
- Brehm, N., A. Bayliss, M. Christl, H. Synal, F. Adolphi, J. Beer, B. Kromer, R. Muscheler, S.K. Solanki, I. Usoskin, N. Bleicher, S. Bollhalder, C. Tyers, and L. Wacker, 2021. Eleven-year solar cycles over the last millennium revealed by radiocarbon in tree rings. *Nature Geosciences*, 4: 10
- Camporeale, E., 2019. The challenge of machine learning in space weather: nowcasting and forecasting. *Space Weather*, 17: 1166
- Camporeale, E., J. Johnson, and S. Wing, 2018. *Machine learning techniques for space weather*, Elsevier, Amsterdam
- Carrasco, V.M.S., H. Hayakawa, C. Kuroyanagi, M.C. Gallego, and J.M. Vaquero, 2021b, Strong evidence of low levels of solar activity during the Maunder Minimum. *Monthly Notices of the Royal Astronomical Society*, 504: 5199
- Carrasco, V.M.S., J.M. Vaquero, R.M. Trigo, and M.C. Gallego, 2018b. A curious history of sunspot penumbrae: an update. *Solar Physics*, 293: 104
- Carrasco, V.M.S., M.C. Gallego, and J.M. Vaquero, 2020a. Number of sunspot groups from the Galileo-Scheiner controversy revisited. *Monthly Notices of the Royal Astronomical Society*, 496: 2482
- Carrasco, V.M.S., M.C. Gallego, J. Villalba Álvarez, and J.M. Vaquero, 2021a. A reanalysis of the number of sunspot groups recorded by Pierre Gassendi in the cycle before the Maunder Minimum. *Solar Physics*, 296: 59
- Cartier, K.M.S., 2018a. Seeing green: a stratospheric view of the 2017 total eclipse, *EOS, Transactions of the American Geophysical Union*, 99; DOI:10.1029/2018EO099915
- Casey, J., 2011. *Cold Sun*, Trafford Publishing Bloomington, IN, pp: 1-184
- Choi, D.R., and F. Tsunoda, 2011. Volcanic and seismic activities during the solar hibernation periods, *New Concepts in Global Tectonics, Newsletters*, (61): 78-87
- Choi, D.R., and L. Maslov, 2010. Earthquakes and solar activity cycles, *New Concepts in Global Tectonics, Newsletters*, (57): 85-97
- Cionco, R.G., and D.A. Pavlov, 2018. Solar barycentric dynamics from a new solar-planetary ephemeris. *Astronomy and Astrophysics*, 615: A153
- Clette, F., E.W. Cliver, L. Lefèvre, L. Svalgaard, J.M. Vaquero, and J.W. Leibacher, 2016. Preface to topical Issue: recalibration of the sunspot number, *Solar Physics*, 291 (9/10), 2479–2486; DOI:10.1007/s11207-016-1017-8
- Clette, F., L. Svalgaard, J.M. Vaquero, and E.W. Cliver, 2014. Revisiting the sunspot number. A 400-year perspective on the Solar Cycle, *Space Science Review*, 186, (1/4): 35–103; DOI:10.1007/s11214-014-0074-2
- Cliver, E.W., F. Clette, L. Svalgaard, and J.M. Vaquero, 2015. Recalibrating the Sunspot Number (SN): The 3rd and 4th SN Workshops, *Central European Astrophysical Bulletin*, 39: 1-19
- Cofield, C., 2017a. Amazing solar eclipse pictures from around the world, *Space.com*, issued May 29, 2017
- Connolly, R., W. Soon, M. Connolly, S. Baliunas, J. Berglund, C.J. Butler, R.G. Cionco, A.G. Elias, V.M. Federov, H. Harde, G.W. Henry, D.V. Hoyt, O. Humlum, D.R. Legates, S. Lüning, N. Scafetta, J.-E. Solheim, L. Szarka, H. van Loon, V.M. Velasco Herrera, R.C. Willson, H. Yan, and W. Zhang, 2021. How much has the Sun influenced northern hemisphere temperature trends? An ongoing debate. *Research in Astronomy and Astrophysics*, 21: 131
- Courtilot, V., F. Lopes, and J.L. Le Mouél, 2021. On the prediction of solar cycles. *Solar Physics*, 296: 21
- Eddy, J.A., 1977. Climate and the changing sun, *Climatic Change*, 1, 173-190; DOI:10.1007/BF01884410
- Falkovich, S.E.V., 1978, *Estimation of signal parameters*, Sovetskoye Radio, Moscow [in Russian]
- Feng, S., and Tang Maocang, 1997. The solar activity and air temperature fluctuation in recent 2500 years, *Quaternary Science*, (01); DOI:cnki:ISSN:1001-7410.0.1997-01-003
- Feynman, R.P., R.B. Leighton, and M. Sands, 1963. *The Feynman Lectures on Physics, Mainly Mechanics, Radiation, and Heat*, I.
- Frazier, S., 2017. Eclipse 2017: Science from the moon's shadow (*NASA's GSFC*), *Phys.org*, issued 11 December 2017
- Frick, P., A. Grossman, and P. Tchamitchian, 1998. Wavelet analysis of signals with gaps. *Journal of Mathematical Physics*, 39: 4091
- Frick, P., S.L. Baliunas, D. Galyagin, D. Sokoloff, and W. Soon, 1997. Wavelet analysis of stellar chromospheric activity variations. *Astrophysical Journal*, 483: 426
- Friedli, T.K., 2016. Sunspot observations of Rudolf Wolf from 1849 – 1893. *Solar Physics*, 291: 2505
- Friis-Christensen, E., and K. Lassen, 1991. Length of the Solar Cycle: an indicator of solar activity closely associated with climate, *Science*, 254: 698-700; DOI:10.1126/science.254.5032.698
- Garner, R., 2017. Aug. 21 solar eclipse, from ground and space, *NASA, Eclipses and Transits*, Last updated: August 22, 2017
- Gleissberg, W., 1939, A long-periodic fluctuation of the Sun-spot numbers. *Observatory*, 62: 158
- Gleissberg, W., 1942. Probability laws of sunspot variations. *Astrophysical Journal*, 96: 234

- Gleissberg, W., 1945. A forecast of solar activity. *Nature*, 156: 539
- Gregori, G. P., and B. A. Leybourne, 2026d. Measuring the electric field at ground. *New Concepts in Global Tectonics, Journal*, 14, (2): 120-128
- Gregori, G. P., and B. A. Leybourne, 2026e. The physics of electrical discharges – I. Small-scale phenomena - Fog - atmospheric precipitation – BLs. *New Concepts in Global Tectonics, Journal*, 14, (2): 129-152
- Gregori, G. P., and B. A. Leybourne, 2026f. The physics of electrical discharges – II. RB & TGFs - Runaway breakdown – terrestrial gamma flashes – GK effect. *New Concepts in Global Tectonics, Journal*, 14, (2): 153-170
- Gregori, G. P., and B. A. Leybourne, 2026g. The physics of electrical discharges – III. Sparks and lightning - electrostatics of the ionosphere – TLEs - plasma jets collimation – Birkeland currents & sea-urchin spikes - stellar and galactic alignments. *New Concepts in Global Tectonics, Journal*, 14, (2): 171-207
- Gregori, G. P., M. T. Hovland, B. A. Leybourne, S. Pellis, V. Straser, B. G. Gregori, G. M. Gregori, and A. R. Simonelli, 2025w. Air-earth currents and a universal “law”: filamentary and spiral structures - Repetitiveness, fractality, golden ratio, fine-structure constant, antifragility and “statistics” - The origin of life, *New Concepts in Global Tectonics, Journal*, 3, (1): 106-225
- Gregori, G.P., 1997. Historical data and global change. Case studies. In W. Schröder (ed.), *Physics and Geophysics with Special Historical Case Studies (A Festschrift in Honour of Karl-Heinrich Wiederkehr). Mitteilungen des Arbeitskreises Geschichte der Geophysik der DDG*, 16, Jahrgang (1997): (2/5): and Newsletter of IDCH-IAGA, (25), Science Edition / IDCH-IAGA / AKGGKP (Arbeitskreis Geschichte der Geophysik und Kosmischen Physik der DDG): Science Edition, Bremen Roennebeck and Potsdam, pp: 183-210
- Gregori, G.P., 2002. Galaxy – Sun – Earth relations. The Origin of the Magnetic Field and of the Endogenous Energy of the Earth, with Implications for Volcanism, Geodynamics and Climate Control, and Related Items of Concern for Stars, Planets, Satellites, and Other Planetary Objects. A Discussion in a Prologue and Two Parts. *Beiträge zur Geschichte der Geophysik und Kosmischen Physik*, Band 3, Heft 3: pp. 1-471 [Available at <http://ncgtjournal.com/additional-resources.html>]
- Gregori, G.P., and B.A. Leybourne, 2021. An unprecedented challenge for humankind survival. Energy exploitation from the atmospheric electrical circuit, *American Journal of Engineering and Applied Science*, 14 (2): 258-291; DOI:10.3844/ajeassp.2021.258.291
- Gregori, G.P., and B.A. Leybourne, 2025i. Wildfires from the Banda Sea through Beijing and through Karakoram. *New Concepts in Global Tectonics, Journal*, 13, (6): 854-887
- Gregori, G.P., and B.A. Leybourne, 2026b. The electrostatic Sun. *New Concepts in Global Tectonics, Journal*, present issue
- Gregori, G.P., and B.A. Leybourne, 2026c. The solar cycle and MiniMax - Effects on other planets. *New Concepts in Global Tectonics, Journal*, present issue
- Gregori, G.P., B.A. Leybourne, and J.R. Wright, 2026d. Generalized Cowling theorem and the Cowling dynamo. *New Concepts in Global Tectonics, Journal*, 14, (1): 90-112
- Gregori, G.P., B.A. Leybourne, and L.A.G. Hissink, 2018. Natural “catastrophes”: “forecast” and management deontological obligation and common sense, *New Concepts in Global Tectonics, Journal*, 6 (3): 327-346
- Gregori, G.P., B.A. Leybourne, G. Paparo†, and M. Poscolieri, 2026a. The global Sun-Earth circuit. *New Concepts in Global Tectonics, Journal*, present issue
- Gregori, G.P., C.W. Monckton of Brechley, W. Soon, R. Tattersall, A. D'Amico†, G. Zimatore, V.M. Velasco Herrera, B.A. Leybourne, and Z.A. Oziewicz†, 2022. The Golden Ratio, variational principles, cyclic and wave phenomena, and quanta. In H.M. Colin Garcia, J-de-J. Cruz Guzman, L.H. Kauffman, and H. Makaruk, (eds), *Scientific Legacy of Professor Oziewicz, selected papers from the International Conference “Applied Category Theory Graph-Operated-Logic”* held in honor of Professor Zbigniew Oziewicz in Memoriam (August 25th to 27th, 2021), World Scientific, Series on Knots and Everything; DOI:10.1142/9789811271151.0018: 363-389; <http://ncgtjournal.com/additional-resources.html>
- Gregori, G.P., W. Soon, V. Straser, and B.A. Leybourne, 2022a. Golden ratio, fractals, and the arrow of time. Irreversibility vs. reversibility - Space, time, antitime - The foundations of physics. *New Concepts in Global Tectonics, Journal*, 10, (3): 158-201
- Gross, R.S., 2007. Earth rotation variations-long period. Section 3.09. In T.A. Herring (ed), *Physical geodesy. Treatise on geophysics*, vol. 11, Elsevier, Amsterdam, pp: 239-294
- Györi, L., A. Ludmány, and T. Baranyi, 2017. Comparative analysis of Debrecen sunspot catalogues. *Monthly Notices of the Royal Astronomical Society*, 465: 1259
- Habbal, S.R., and R. Woo, 2004. The solar wind and the Sun–Earth link, *Astron. Geophys.*, 45, (4): 4.38-4.43, DOI:10.1046/j.1468-4004.2003.45438.x
- Hathaway, D.H. 2015. The solar cycle. *Living Reviews of Solar Physics*, 12: 4
- Hathaway, D.H., 2013. A curious history of sunspot penumbrae. *Solar Physics*, 286: 347
- Hayakawa, H., C. Kuroyanagi, V.M. Carrasco, S. Uneme, B.P. Besser, M. Soma, and S. Imada, 2021c. Sunspot observations at the Eimmart Observatory and in its neighborhood during the late Maunder Minimum (1681 – 1718). *Astrophysical Journal*, 909: 166
- Hayakawa, H., H. Tamazawa, Y. Ebihara, H. Miyahara, A.D. Kawamura, T. Aoyama, and H. Isobe, 2017a. Records of sunspots and aurora candidates in the Chinese official histories of the Yuan and Ming dynasties during 1261 – 1644. *Publications of the Astronomical Society of Japan*, 69: 65
- Hayakawa, H., K. Iwahashi, H. Tamazawa, Y. Ebihara, A.D. Kawamura, H. Isobe, K. Namiki, and K. Shibata,

- 2017b. Records of auroral candidates and sunspots in Rikkokushi, chronicles of ancient Japan from early 7th century to 887. *Publications of the Astronomical Society of Japan*, 69: 86
- Hayakawa, H., T. Iju, S. Uneme, B.P. Besser, S. Kosaka, and S. Imada, 2021a, Reanalyses of the sunspot observations of Fogelius and Siverus: two “long-term” observers during the Maunder Minimum. *Monthly Notices of the Royal Astronomical Society*, 505: 650
- Herrera, A., C.S. Cockell, S. Self, M. Blaxter, J. Reitner, T. Thorsteinsson, G. Arp, W. Drose, and A.A. Tindle, 2009. A cryptoendolithic community in volcanic glass. *Astrobiology*, 9: 369-381
- Howell, E., 2014d. Weak Sun poses radiation risk for Mars-bound astronauts, *Space.com*, issued November 08, 2014
- Hoyt, D., and K.H. Schatten, 1997, The Role of the Sun in climate change, Oxford University Press, London
- Hoyt, D., and K.H.: Schatten, 1998. Group sunspot numbers: a new solar activity reconstruction. *Solar Physics*, 181: 491
- Hoyt, D.V., and K.H. Schatten, 1998a. Group sunspot numbers: a new solar activity reconstruction, *Solar Physics*, 179: 189-219
- Hoyt, D.V., and K.H. Schatten, 1998b. Group sunspot numbers: a new solar activity reconstruction, *Solar Physics*, 181: 491-512
- Hoyt, D.V., K.H. Schatten, and E. Nesme-Ribes, 1994: The one hundredth year of Rudolf Wolf's death: Do we have the correct reconstruction of solar activity? *Geophysical Research Letters*, 21: 2067-2070
- Hudgins, L., C.A. Friehe, and M.E. Mayer, 1993, Wavelet transforms and atmospheric turbulence. *Physical Review Letters*, 71: 3279
- Knorr, G., M. Butzin, A. Micheels, and G. Lohmann, 2011. A warm Miocene climate at low atmospheric CO₂ levels, *Geophysical Research Letters*, 38: L20701 [5 pp.]; DOI:10.1029/2011GL048873
- Kollath, Z., and K. Olah, 2009. Multiple and changing cycles of active stars: I. Methods of analysis and application to the solar cycles. *Astronomy and Astrophysics*, 501: 695
- Kramer, M., 2014c. Largest sunspot in 24 years wows scientists, but also mystifies, *Space.com*, issued November 03, 2014
- Krivova, N.A., L. Balmaceda, and S.K. Solanki, 2007. Reconstruction of solar total irradiance since 1700 from the surface magnetic flux. *Astronomy and Astrophysics*, 467: 335
- Landau, L.D., and E.M. Lifshitz, 1988. *The classical theory of fields 2*, Nauka, Moskow [in Russian]
- Larmor, Sir J., 1919. How could a rotating body such as the Sun become a magnet? *British Association Report*: 159-160, Bournemouth
- Larmor, Sir J., 1919a. Possible rotational origin of magnetic fields of Sun and Earth. *Electrical Review*, 85: 412 (or 512?)
- Larmor, Sir J., 1920. How could a rotating body such as the Sun become a magnet? *Report of the British Association for the Advancement of Science, Bournemouth Meeting*, 1919: 159-160, also in *Mathematical and physical papers*, Vol. II, Cambridge University Press, 1929: 611-612
- Lassen, K., and E. Friis-Christensen, 1995. Variability of the solar cycle length during the past five centuries and the apparent association with terrestrial climate, *Journal of Atmospheric and Terrestrial Physics*, 57: 835-845
- Laurenz, L., H.J. Lüdecke, and S. Lüning, 2019, Influence of solar activity changes on European rainfall. *Journal of Atmospheric and Solar-Terrestrial Physics*, 185: 29
- Layton, L., 2010. Eclipses yield first images of elusive iron line in solar corona, *NASA news, Release No.:* 10-01 (01/05/10)
- Le Mouél, J.L., F. Lopes, and V. Courtillot, 2019. A solar signature in many climate indices. *Journal of Geophysical Research*, 124: 2600
- Le Mouél, J.L., F. Lopes, and V. Courtillot, 2020, Characteristic time scales of decadal to centennial changes in global surface temperatures over the past 150 years. *Earth and Space Science*, 7: e2019EA000671
- Lean, J., 2000. Evolution of the Sun's spectral irradiance since the Maunder Minimum. *Geophysical Research Letters*, 27: 2425
- Lewin, S., 2017g. Sun unleashes monster solar flare, strongest in a decade, *Space.com*, issued Sep 6, 2017
- Leybourne, B.A., and M.B. Adams, 2020. El Niño tectonic modulation in the Pacific basin (revisited), *Systemics, Cybernetics and Informatics*, 18, (4); 107-112. 1st published in *Marine Technology Society Oceans '01 Conference Proceedings*, Honolulu, Hawai'i, November 2001, <https://www.iiisci.org/journal/sci/FullText.asp?var=&iid=IP094LL20>
- Lin, G.H., X.F. Wang, S. Liu, X. Yang, G.F. Zhu, Y.Y. Deng, H.S. Ji, T.H. Zhou, L.N. Sun, Y.L. Feng, Z.Z. Liu, J.P. Tao, M.X. Ben, J. Lin, M.D. Ding, Z. Li, S. Zheng, S.G. Zeng, H.L. He, X.Y. Zeng, Y. Shu, and X.B. Sun, 2019. Chinese sunspot drawings and their digitization (I) Parameter Archives. *Solar Physics*, 294: 79
- Lindsey, R., 2021. Understanding the Arctic polar vortex, *NOAA release*, issued March 5, 2021
- Livingston, W., M.J. Penn, and L.:Svalgaard, 2012, Decreasing sunspot magnetic fields explain unique 10.7 cm radio flux. *Astrophysical Journal*, 757: L8
- Lockwood, M., 2013. Reconstruction and prediction of variations in the open solar magnetic flux and interplanetary conditions, *Living Reviews in Solar Physics*, 10: 4-88; DOI:10.12942/lrsp-2013-4
- Lockwood, M., and C. Fröhlich, 2007. Recent oppositely directed trends in solar climate forcings and the global mean surface air temperature. *Proceedings of the Royal Society of London. Series A, Mathematical and Physical and Engineering Science*, 463, (2086): 2447-2460; DOI:10.1098/rspa.2007.1880
- Lockwood, M., and C. Fröhlich, 2007a. Recent oppositely directed trends in solar climate forcings and the global mean surface air temperature, *Proceedings of the Royal Society of London A*: 1-14; DOI:10.1098/rspa.2007.1880

- Lockwood, M., M.J. Owens, and L. Barnard, 2014. Centennial variations in sunspot number, open solar flux, and streamer belt width: 2. Comparison with the geomagnetic data. *Journal of Geophysical Research*, 119: 5183
- Ludendorff, H., 1928. Die Veranderlichen Sterne, *Sitzungsberichte der Königlich Preussischen Akademie der Wissenschaften zu Berlin*, 16: 185
- Ma, L., and J.M. Vaquero, 2019. New evidence of the Suess/de Vries cycle existing in historical naked-eye observations of sunspots. *Open Astronomy Journal*, 28: 28
- Maunder, E.W., 1894. A prolonged sunspot minimum. *Knowledge*, 17: 173
- Maunder, E.W., 1922. The prolonged sunspot minimum, 1645–1715. *Journal of the British Astronomical Association*, 32: 140
- McCracken, K.G., and J. Beer, 2014. Comparison of the extended solar minimum of 2006–2009 with the Spörer, Maunder, and Dalton Grand Minima in solar activity in the past, *Journal of Geophysical Research, Space Physics*, 119 (4): 2379–2387; DOI:10.1002/2013JA019504
- Mekhaldi, F., R. Muscheler, F. Adolphi, A. Aldahan, J. Beer, J.R. McConnell, G. Possnert, M. Sigl, A. Svensson, H.-A. Synal, K.C. Welten, and T.E. Woodruff, 2015. Multiradionuclide evidence for the solar origin of the cosmic-ray events of AD 774/5 and 993/4, *Nature, Communications*, 6: 8611; DOI:10.1038/ncomms9611
- Miyahara, H., D. Sokoloff, and I.G. Usoskin, 2006. The solar cycle at the Maunder Minimum epoch. In: W.-H. Ip, and M. Duldig, M. (eds.), *Advances in Geosciences: Volume 2: Solar Terrestrial (ST)*. World Scientific, Singapore
- Miyahara, H., K. Masuda, Y. Muraki, H. Furuzawa, H. Menjo, and T. Nakamura, 2004. Cyclicity of solar activity during the Maunder Minimum deduced from radiocarbon content. *Solar Physics*, 224: 317
- Muñoz-Jaramillo, A., and J.M. Vaquero, 2019. Visualization of the challenges and limitations of the long-term sunspot number record. *Nature Astronomy*, 3: 205
- Muscheler, R., F. Adolphi, K. Herbst, and A. Nilsson, 2016. The revised sunspot record in comparison to cosmogenic radionuclide-based solar activity reconstruction. *Solar Physics*, 291: 3025
- Nagovitsyn, Y.A., A. Pevtsov, and W. Livingston, 2012. On a possible explanation of the long-term decrease in sunspot field strength. *Astrophysical Journal*, 758: L20
- Neuhäuser, R., R. Arlt, and S. Richter, 2018. Reconstructed sunspot positions in the Maunder Minimum based on the correspondence of Gottfried Kirch. *Astronomische Nachrichten*, 339: 219
- Nikolskiy, G.M., 1955. Prediction of the solar corona shape for 20 June 1955, *PIS'MA v Astronomicheskii Zhurnal (Astronomy Letters)* (in Russian), 160: 11
- Ogurtsov, M.G., 2013. Instrumental data on the sunspot formation in the 17th–18th centuries: correct information or approximations. *Geomagnetism and Aeronomy*, 53: 663
- Perez-Peraza, J., V. Velasco, I.Ya. Libin, and K. Yudakhin, 2012. Thirty-year periodicity of cosmic rays. *Advances in Astronomy*, 691408: 11
- Phillips, T., 2014e. Solar Mini-Max, *Science@NASA*, issued June 10, 2014
- Poluianov, S.V., I.G. Usoskin, and G.A. Kovaltsov, 2014. Cosmogenic isotope variability during the Maunder Minimum: normal 11-year cycles are expected. *Solar Physics*, 289: 4701
- Polygiannakis, J., P. Preka-Papadema, and X. Moussas, 2003. On signal-noise decomposition of time-series using the continuous wavelet transform: application to sunspot index. *Monthly Notices of the Royal Astronomical Society*, 343: 725
- Rotter, C., 2021. Scientists use AI to predict sunspot cycles, *Press release, Watts Up With That?* Issued 23 April 2021, retrieved 20/04/2023
- Saito, T., 1992. Winged Sun and the coronal sheet model. In W. Schröder and J.-P. Legrand, (eds), *Solar terrestrial variability and global change*, Interdivisional Commission on History of IAGA, Bremen-Roennebeck: 127-140
- Salazar, D.-E., 2017a. Monster solar flare marks 7th powerful Sun storm in 7 days, *Space.com*, issued September 11, 2017
- Salcedo, G.E., R.F. Porto, and P.A. Morettin, 2012. Comparing non-stationary and irregularly spaced time series. *Computational Statistics and Data Analysis*, 56: 3921
- Scafetta, N., 2010. Empirical evidence for a celestial origin of the climate oscillations and its implications, *Journal of Atmospheric Terrestrial Physics*, 72, (13): 951-970; DOI:10.1016/j.jastp.2010.04.015
- Schaefer, B., 1993. Visibility of sunspot, *Astrophysical Journal*, 411: 909–919
- Schove, D.J., 1983. *Sunspot cycles*, Hutchinson Ross, Stroudsburg
- Schröder, W., and H.-J. Treder, 1996. A note on the suggested variability of the length of the solar cycle during recent centuries and some consequences, *Acta Geodica et Geophysica Hungarica*, 31, (1/2): 271-273
- Schwabe, H., 1844. Sonnen-Beobachtungen im Jahre 1843. *Astronomische Nachrichten*, 21: 233
- Shimojo, M., K. Iwai, A. Asai, S. Nozawa, T. Minamidani, and M. Saito, 2017. Variation of the solar microwave spectrum in the last half century, *Astrophysical Journal*, 848 (3): 62-.; DOI:10.3847/1538-4357/aa8c75
- Silverman, S.M., 1992. Secular variation of the aurora for the past 500 years. *Reviews of Geophysics*, 30: 333
- Simpson, J., 2020. Naked-eye sunspot observations: a critical review of pre-telescopic western reports. *Journal of the British Astronomical Association*, 130: 5
- Smith, Y., 2017b. Behold! Observing the Sun, *NASA – SDO Solar Mission*, issued November 20, 2017
- Sokoloff, D., and E. Nesme-Ribes, 1994. The Maunder Minimum: a mixed parity dynamo mode? *Astronomy and Astrophysics*, 288: 293

- Soon, W., and S.H. Yaskell, 2003. *The Maunder Minimum and the variable Sun-Earth connection*, World Scientific, Singapore
- Soon, W., K. Dutta, D.R. Legates, V. Velasco, and W. Zhang, 2011. Variation in surface air temperature of China during the 20th century. *Journal of Atmospheric and Solar-Terrestrial Physics*, 73: 2331
- Soon, W., V. Velasco Herrera, K. Selvaraj, R. Traversi, I. Usoskin, C.-T.A. Chen, J.-Y. Lou, S.-J. Kao, R.M. Carter, V. Pipin, M. Severi, and S. Becagli, 2014. A review of Holocene solar-linked climatic variation on centennial to millennial timescales: physical processes, interpretative frameworks and a new multiple cross-wavelet transform algorithm. *Earth Sciences Reviews*, 134: 1
- Soon, W., V.M. Velasco Herrera, R.G. Cionco, S. Qiu, S. Baliunas, and R. Egeland, 2019. Covariations of chromospheric and photometric variability of the young Sun analogue HD 30495: evidence for and interpretation of mid-term periodicities. *Monthly Notices of the Royal Astronomical Society*, 483: 2748
- Specktor, B., 2018e. Stunning NASA image lets you watch the Sun explode in real time, *Live Science*, issued August 17, 2018
- Spörer, G., 1887. Ueber die Periodicität der Sonnenflecken seit dem Jahre 1618, vornehmlich in Bezug auf die heliographische Breite derselben, und Hinweis auf eine erhebliche Störung dieser Periodicität während eines langen Zeitraumes. *Vierteljahrsschrift der Astronomische Gesellschaft*, 22: 323
- Stefani, F., J. Beer, A. Giesecke, T. Gloaguen, M. Seilmayer, and R. Stepanov, 2020. Phase coherence and phase jumps in the Schwabe cycle. *Astronomische Nachrichten*, 341: 600
- Steinhilber, F., and J. Beer, 2013. Prediction of solar activity for the next 500 years. *Journal of Geophysical Research*, 118: 1861
- Stuiver, M., and T.F. Braziunas, 1993. Modeling atmospheric ¹⁴C influences and ¹⁴C ages of marine samples to 10,000 BC. *Radiocarbon*, 35: 137
- Suykens, J., T. Gestel, J. De Brabanter, B. De Moor, and J. Vandewalle, 2005. *Least squares support vector machines*, World Scientific, Singapore.
- Svalgaard, L., and K.H. Schatten, 2016. Reconstruction of the sunspot group number: the backbone method. *Solar Physics*, 291: 2653
- Tamazawa, H., A.D. Kawamura, H. Hayakawa, A. Tsukamoto, H. Isobe, and Y. Ebihara, 2017. Records of sunspot and aurora activity during 581–959 CE in Chinese official histories concerning the periods of Sui, Tang, and the Five Dynasties and Ten Kingdoms. *Publications of the Astronomical Society of Japan*, 69: 22
- Tang, Maocang, and Tang Chi, 2002. Climatic condition and Chinese history (II): "good (bad) climatic condition" and "peaceful (trouble) times" in Chinese history, *Plateau Meteorology*, (01); DOI:CNKI:SUN:GYQX.0.2002-01-002
- Tang, Maocang, Gao Xiaoqing, and Zhu Deqin, 2003. The evidences and the causes for the shift of climate pattern in northwest China during this century, *Journal of Glaciology and Geocryology*, (02); DOI:cnki:ISSN:1000-0240.0.2003-02-008
- Tang, Maocang, Liu Yanxiang, and Feng Song, 2002. A new millenary warm period may be emerged, *Plateau Meteorology*, (02); DOI:cnki:ISSN:1000-0534.0.2002-02-002
- Tang, Maocang, Liu Yanxiang, and Guo Weidong, 2001. Climatic condition and Chinese history (I): SCL and Chinese climate, *Plateau Meteorology*, (04); DOI:CNKI:SUN:GYQX.0.2001-04-003
- Tattersall, R., 2013. The hum: log-normal distribution and planetary–solar resonance, *Pattern Recognition in Physics*, 1: 185–198; DOI:10.5194/prp-1-185-2013
- Tattersall, R., 2013a. Apparent relations between planetary spin, orbit, and solar differential rotation, *Pattern Recognition in Physics*, 1: 199-202; DOI:10.5194/prp-1-199-2013
- Tattersall, R., 2013b. A remarkable discovery: all Solar System periods fit the Fibonacci series and the Golden Ratio. Why Phi? *Tallbloke's Talkshop*, issued February 20, 2013
- Torrence, C., and G. Compo, 1998. A practical guide to wavelet analysis. *Bulletin of the American Meteorological Society*, 79: 61
- Usoskin, I.G., K. Mursula, and G.A. Kovaltsov, 2003. Reconstruction of monthly and yearly group sunspot numbers from sparse daily observations. *Solar Physics*, 218: 295
- Usoskin, I.G., R. Arlt, E. Asvestari, E. Hawkins, M. Kapyla, G.A. Kovaltsov, N. Krivova, M. Lockwood, K. Mursula, J.O. O'Reilly, M. Owens, C.J. Scott, D.D. Sokoloff, S. Solanki, W. Soon, and J.M. Vaquero, 2015. The Maunder Minimum (1645–1715) was indeed a grand minimum: a reassessment of multiple datasets. *Astronomy and Astrophysics*, 581: A95
- Usoskin, I.G., S.K. Solanki, N. Krivova, B. Hofer, G.A. Kovaltsov, L. Wacker, N. Brehm, and B. Kromer, 2021b. Solar cyclic activity over the last millennium reconstructed from annual ¹⁴C data. *Astronomy and Astrophysics*, 649: A141
- Usoskin, I.G., Y. Gallet, G.A. Kovaltsov, and G.: Hulot, 2016a. Solar activity during the Holocene: the Hallstatt cycle and its consequence for grand minima and maxima. *Astronomy and Astrophysics*, 587: A150
- Vaquero, J.M., and R.M. Trigo, 2014. Revised group sunspot number values for 1640, 1652, and 1741. *Solar Physics*, 289: 803
- Vaquero, J.M., G.A. Kovaltsov, I.G. Usoskin, V.M.S. Carrasco, and M.C. Gallego. 2015. Level and length of cyclic solar activity during the Maunder Minimum as deduced from the active-day statistics. *Astronomy and Astrophysics*, 577: A71
- Vaquero, J.M., L. Svalgaard, V.M.S. Carrasco, F. Clette, L. Lefèvre, M.C. Gallego, R. Arlt, A.J.P. Aparicio, J.-G. Richard, and R. Howe, 2016. A revised collection of sunspot group numbers, *Solar Physics*, 291 (9/10): 3061–3074

- Vaquero, J.M., M.C. Gallego, and R.M. Trigo, 2007. Sunspot numbers during 1736–1739 revisited. *Advances in Space Research*, 40: 1895
- Velasco Herrera, V., B. Mendoza, and G. Velasco Herrera, 2011. Estimating total solar irradiance during the 21st century. *arXiv [astro-ph.SR]*
- Velasco Herrera, V.M., B. Mendoza, and G. Velasco Herrera, 2015. Reconstruction and prediction of the total solar irradiance: the Medieval Warm Period to the 21st century, *New Astronomy*, 34: 221–233; DOI: 10.1016/j.newast.2014.07.009
- Velasco Herrera, V.M., W. Soon, and D.R. Legates, 2021. Does machine learning reconstruct missing sunspots and forecast a new solar minimum? *Advances in Space Research*, 68: 1485–150; DOI:10.1016/j.asr.2021.03.023
- Velasco Herrera, V.M., W. Soon, D.V. Hoyt, and J. Muraközy, 2022. Group sunspot numbers: a new reconstruction of sunspot activity variations from historical sunspot records using algorithms from machine learning, *Solar Physics*, 297: 8, DOI:10.1007/s11207-021-01926-x
- Velasco, V., B. Mendoza, and J. Valdés-Galicia, 2008. The 120-yr solar cycle of the cosmogenic isotopes. In: *Proceedings of the 30th International Cosmic Ray Conference*, 1, 553
- Vieira, L.E.A., S.K. Solanki, N.A. Krivova, and I. Usoskin, 2011. Evolution of the solar irradiance during the Holocene. *Astronomy and Astrophysics*, 531: A6
- Vokhmyanin, M., R. Arlt, and N. Zolotova, 2021. Sunspot positions and areas from observations by Cigoli, Galilei, Colonna, Scheiner, and Colonna in 1612–1614. *Solar Physics*, 296: 4
- Waldmeier, M., 1961. *The Sunspot activity in the years 1610–1960*, Schulthess & Company AG, Zürich
- Wall, M., 2015b. Sun unleashes 1st monster solar flare of 2015, *Space.com*, issued March 11, 2015
- Wall, M., 2018k. Hole in Sun's atmosphere amps up northern lights, *Space.com*, issued September 11, 2018
- Wang, Y.M., J.L. Lean, and N.R.Jr. Sheeley, 2005. Modeling the Sun's magnetic field and irradiance since 1713. *Astrophysical Journal*, 625: 522
- Wang, Zhongrui, Gao Xiaoqing, and Tang Maocang, 2002. The air temperature change in the past 2000 years simulated using solar activity indices, *Plateau Meteorology*, (06); DOI:cnki:ISSN:1000-0534.0.2002-06-003
- Wang, Zhongrui, Song Feng, and Tang Maocang, 2003. A relationship between solar activity and frequency of natural disasters in China, *Advances in Atmospheric Sciences*, 20 (6): 934-939; DOI:10.1007/BF02915516
- Weiss, N.O., 1988. Is the solar cycle an example of deterministic chaos? In F.R. Stephenson, and Sir A.W. Wolfendale, (eds), *Secular solar and geomagnetic variations in the last 10,000 years*, Kluwer Acad. Publ., Dordrecht, etc.; DOI:10.1007/978-94-009-3011-7_41988, pp: 69-78
- Wezel, F.C., 2018. *Terra, pianeti e spirito. Il fenomeno geologico come simbolo di un fondamento immateriale*, Carabba, Roma, pp: 1-210
- Willis, D.M., H.E. Coffey, R. Henwood, E.H. Erwin, D.V. Hoyt, M.N. Wild, and W.F. Denig, 2013. The Greenwich photo-heliographic results (1874 - 1976): summary of the observations, applications, datasets, definitions and errors, *Solar Physics*, 288: 117-139
- Witze, A., 2019. Earth's magnetic field is acting up and geologists don't know why, *Nature, News*, 565: 143-144; 10.1038/d41586-019-00007-1
- Wolf, R., 1851. Sonnenflecken Beobachtungen in der zweiten Hälfte des Jahres 1850 [Universal sunspot numbers: sunspot observations in the second part of the year 1850], *Mitteilungen der Naturforschenden Gesellschaft in Bern*, 207: 89-95; or *Naturf. Gesell. Bern. Mitt.*, 1: 89-95
- Wolf, R., 1856. Mitteilungen über die Sonnenflecken, I, *Astron. Mitteil. Eidgn. Sternw. Zürich*, 1: 3-13
- Wolf, R., 1859. Mittheilungen über die Sonnenflecken. *Vierteljahrsschrift der Naturforschenden Gesellschaft in Zürich*, 9 . 207
- Wolf, R., 1861b. Abstract of his latest results. *Monthly Notices of the Royal Astronomical Society*, 21: 77
- Wolf, R., 1861c. Mitteilungen über die Sonnenflecken. *Astronomische Mitteilungen der Eidgenössischen Sternwarte Zürich*, 2: 41
- Wu, Hong-chun, 2025. Jet stream's disturbances as possible precursors of earthquakes, *preprint*
- Wu, Hong-chun, and B.A. Leybourne, 2020. Using jet stream's precursors to make earthquake forecast, *Systemics, Cybernetics and Informatics*, 18 (4): 62-65; <https://www.iiisci.org/journal/sci/FullText.asp?var=&id=ZA646AQ20>
- Zastrow, M., 2017a. Explaining unexpected twists in the Sun's magnetic field, *EOS, Transactions of the American Geophysical Union*, 98; DOI:10.1029/2017EO071007
- Zito, R.R., 2016. Possible Mesoamerican naked-eye observation of sunspots – V: evidence from Río azul Tomb I Murals and related artifacts. *Social Anthropology*, 4: 953

Acronyms

- AGU – American Geophysical Union
AIA/LMSAL - Atmospheric Imaging Assembly/ Lockheed Martin Solar and Astrophysics Laboratory
BCC - bad climatic condition
CAAT - Chinese annual air temperature
CMB - core mantle boundary
CME – coronal mass ejection
CMSS - center of mass of the Solar System
e.m. - electromagnetic
ESA – European Space Agency
GCC - good climatic condition
GCR - galactic cosmic rays
GN – improved sunspot number series
GSFC – Goddard Space Flight Center
HMF - heliospheric magnetic field
IMF- interplanetary magnetic field
l.o.d. – length of the day
LS-SVM - Least-Squares Support-Vector Machines

MHD - magneto-hydro-dynamics
ML - machine learning
NASA –National Atmospheric and Space Administration
NCAR –National Center for Atmospheric Research
NGDC –National Geophysical Data Center
NH – northern hemisphere
NSF – National Science Foundation
SCL – solar cycle length
SCMSS – speed of the center of mass of the Solar System
SDO - Solar Dynamics Observatory
SN – sunspot number series

SOHO - Solar and Heliospheric Observatory
SSN – sunspot number series
TD - tide-driven (dynamo)
TGF – terrestrial gamma flashes
UCAR - University Corporation for Atmospheric Research
USAF/SOON - Solar Observing Optical Network (SOON)
 composed of three U.S. Air Force solar observatories
WDC – World Data Center
WS - weakening solar activity stage

The solar cycle and MiniMax - Effects on other planets

Giovanni Pietro Gregori^{1,2}, Bruce Allen Leybourne²

¹IDASC-Istituto di Acustica e Sensoristica O. M. Corbino (CNR), Roma, now merged into IMM-Istituto per la Microelettronica e Microsistemi (CNR) and ISSO-International Seismic Safety Organization, Italy

²GeoPlasma Research Institute-(GeoPlasmaResearchInstitute.org), Aurora, CO 80014, USA

Corresponding Author: G. P. Gregori, IDASC-Istituto di Acustica e Sensoristica O. M. Corbino (CNR), Roma, now merged into IMM-Istituto per la Microelettronica e Microsistemi (CNR);
Email: giovannipgregori38@gmail.com
leybourneb@iascc.org

Abstract: In general, a solar minimum is characterized by a clustering of sunspots inside small patches. Consequently, the interplanetary magnetic field shifts from the best known four-sector pattern to a two-sector pattern. This implies a change of the e.m. induction inside planetary objects, thus affecting their respective internal dynamo. In addition, the large-scale scatter of the solar wind flow is changed. This anomaly was particularly intense during the so-called MiniMax, i.e., when the sunspot cycle displayed a particularly low maximum. This phenomenon was seemingly associated with peculiar climate events on the Earth. On other planets, mostly on the large gaseous external planets, the phenomenon is likely to be associated with anomalous large atmospheric storms. That is, the observations of giant cyclones on the outer gaseous planets are a way to monitor the large-scale propagation of the solar wind, associated with an anomalous and less usual state of the solar corona.

Keywords: MiniMax – anomalous solar wind – cyclones on outer planets – monitoring solar wind propagation at large distances

Introduction

If the argument is correct concerning the impact of MiniMax on the Earth (see Gregori et al., 2026c), one must detect equivalent effects of the solar wind on other planets, which can be considered like probes aimed to monitor the space gradient of the solar wind flow at their respective orbit.

In addition, consider that the amplitude of the relative space variation of the solar wind flow - with respect to its scatter from some smooth mean trend - is more amplified the larger the distance from the Sun. That is, this implies a progressively lower frequency (i.e., in time) detected by a planetary object located at a larger heliocentric distance.

The structure of the Parker spiral is being investigated “very close” to the Sun. Badman et al. (2023), and Bale et al. (2023) illustrated by University of California – Berkeley (2023), report about the NASA’s Parker Solar Probe (PSP) observations of the origin and structure of the solar wind as close as 13.3 R_{\odot} (Sun’s radii), based on records of high-energy particles aligned with flows in coronal holes. The focus of the present paper is, rather, at very large heliospheric distances.

As mentioned in Gregori et al. (2026c), an anomalous intense auroral display on a planet is indicative of a short-lived - almost “instant” - anomalous particle precipitation on the planet’s atmosphere. This is the “external” way (see Gregori et al., 2026c). In contrast, a large-scale geometrical pattern of the solar wind flow is a long-lasting space-gradient phenomenon, which implies an anomalous operation of the endogenous TD (tide driven) dynamo of the planetary object (whenever present; see Tables 2 and 3 of Gregori et al., 2026a). The mechanism is intuitively illustrated in Fig. 1.

This implies an eventual time delayed release of endogenous heat to the planet’s surface. This release affects

the atmospheric dynamics that can sometimes be observed like enormous storms and giant temporary spots in the planet’s atmosphere. This is the “internal” way (see Gregori et al., 2026c).

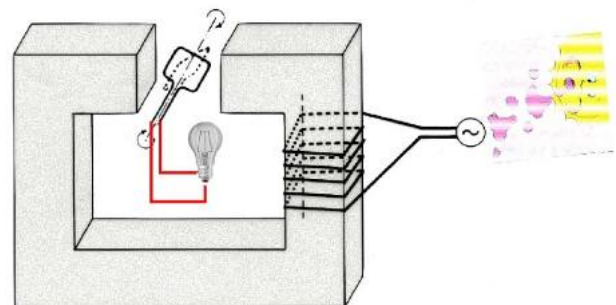


Fig. 1. The Sun modulates the solar wind flow that affects the e.m. induced currents inside the mantle of the planetary object. These currents influence the efficiency of the TD dynamo (here shown by the supply to a lamp). According to this principle, the solar wind modulates the release of endogenous energy (“internal” way) which affects the dynamics of the outer gaseous layers of the giant external planets. See text. Unpublished figure.

For instance, polar auroræ observed on some planetary objects refer to the “external” way (see, e.g., Zhang et al., 2024, illustrated by Lea, 2024). In this respect, we point out that polar auroræ are observed to occur near the poles when the main magnetic field of the planetary object is largely dipolar. In contrast, in the case of an erratic magnetic field (such as, e.g., on Mars), auroræ occur at low latitudes, consistently with the local spatial pattern of the magnetic field.

Comets are other natural probes for the solar wind that monitor the expansion of the solar corona through the entire Solar System. In fact, when a comet evaporates, it is

surrounded by a cloud of plasma and develops a miniature magnetosphere (“cometosphere”) that, however, must be suitably calibrated. Also, comets are a case of an “external” way interaction.

Conversely, the present paper addresses phenomena that occur through the “internal” way.

Several anomalous large storms have often been observed on the outer planets – either by ground-based telescopes or by space probes - although their eventual correlation must be investigated with peculiar features of sunspots and other solar morphological features. In this paper we discuss a few case histories of this kind.

The giant outer planets, i.e., Jupiter, Saturn, Uranus and Neptune, often display phenomena that clearly remind one about Earth’s hurricanes. Wall (2011) pinpoints the key item that represents the seemingly crucial issue for present modelers. He stresses that these huge planetary storms “are not fed by warm ocean water the way terrestrial hurricanes are”. In addition, he also reports a statement by Andrew Ingersoll of *Caltech (California Institute of Technology)*, a researcher with *Cassini* mission: “there certainly are storms that have thunder and lightning and rain that are bigger than terrestrial hurricanes, and the more violent winds on those planets, [the storms] are stronger, too.”

Let us first consider the way these impressive phenomena can be explained according to the general rationale of the present study. Then, consider other presently envisaged explanations, which are reported in the literature. Then, we focus on how observations can confirm either one possibility or another.

These huge outer planets are well-known to be characterized by very strong magnetic fields B , extensively mapped by space probes, with huge magnetospheres etc. The origin of their B fits very well with the TD dynamo mechanism, as extensively discussed with reference to Tables 2 and 3 of Gregori et al. (2026a).

In addition, a concrete possibility also exists that a few, or all, of these planets contain an internal nuclear reactor. This important – and often insufficiently emphasized - item ought to require, however, a long discussion. Only a few mentions can be given here concerning a georeactor inside the Earth. Refer to Herndon (2014) (see also Herndon, 2010), who relies on a discussion of the composition of meteorites with the purpose of envisioning a reasonable composition of the Earth’s interior.

According to Herndon’s scheme, the composition of the upper layers of the Earth’s mantle is unknown. These layers can include components from ordinary and carbonaceous chondrite matter. This chemical composition of deep-Earth arises upon assuming that the endo-Earth was separated from solar matter under conditions that severely limited oxygen availability. Compared to the Earth conceived like an ordinary chondrite, this fact determined some profound differences.

Therefore, in addition to a different geochemical perspective and to its consequent implications, the possible temporary existence of a nuclear reactor inside deep Earth is one relevant item. This speculation seems to be almost unavoidable. It is basically shared by every attempt to model the deep Earth’s interior. This warning applies

therefore to every model for deep Earth - which has been implemented by different authors, and that can be tracked through the whole history of Earth’s sciences.

For instance, the criticism by some authors of the nuclear reactor hypothesis is that the deep Earth’s environment can be simulated in no laboratory. On the other hand, this applies, e.g., also to the naïve argument that the inner core (IC) is “solid” because it transmits S-waves, hence it is “cooling” etc. (see Gregori et al., 2026a).

In addition, while implementing an energy balance of deep Earth’s phenomena, reference is made to the best of our knowledge available in physics and chemistry. Herndon’s argument stresses some important aspects of our actual knowledge of nuclear engineering. Science is made of ideas, to be eventually discussed and/or contended with, but new ideas are always needed. Herndon proposes new ideas. That is, the Ockham’s razor must always apply, while every *a priori* and conservative criticism does not partake of true science.

The Herndon model therefore deserves a specific illustration, due to its several relevant implications that appear to be far beyond any confirmation based on seismological evidence alone. In particular, the Herndon model can explain some observational features that can hardly be justified by any conventional approach. Therefore, the Herndon perspective seems provocative and innovative, but is worthy of discussion and consideration in order to focus on future possible evidence either pro or con.

In particular, we recall the mystery of the $^3\text{He}/^4\text{He}$ ratio in basalt. In fact, the classical radioactive families inside the Earth produce only ^4He , and no ^3He . Hence, the amount of ^3He observed inside basalt - which cannot be explained by the ^3He concentration in the atmosphere – is a great mystery. To our knowledge, the former presence of an active georeactor seems to be the unique realistic hypothesis suited to explain this mystery.

The following statements are borrowed after Herndon (2010). “Herndon (1993, 1994) applied the nuclear reactor theory of Fermi (1947) to demonstrate the feasibility of a naturally occurring nuclear fission at the center of the Earth, now called the georeactor, as the energy source for the geomagnetic field... Herndon (1996) disclosed the sub-structure of the Earth’s IC , describing the two-component structure of the georeactor as consisting of an actinide sub-core, surrounded by a sub-shell composed of the products of nuclear fission and radioactive decay, all surrounded by the IC , as illustrated in Fig. 2. He also noted the possibility that the sub-shell might be a liquid or slurry.

Hollenbach and Herndon (2001) published the first georeactor numerical simulation conducted using Oak Ridge National Laboratory’s SCALE software, which had been validated with nuclear reactor operating data combined with analyses of spent fuel rods (SCALE, 1995). The numerical simulations showed that the georeactor could function over the entire time since Earth’s formation, about 4.5 Ga, as a fast neutron breeder reactor. Moreover, the calculations showed that georeactor-produced ^3He and ^4He would have the same range of compositions as He measured in oceanic basalts (Hilton and Porcelli, 2003).

Subsequently, Herndon (2003) published more precise numerical simulation data, examples of which are shown in Fig. 3 and provide strong evidence for the existence of Earth's georeactor. The marked, progressive increase in $^3\text{He}/^4\text{He}$ ratios over time occurs primarily as a consequence of diminished ^4He production from radioactive decay as U is consumed. Herndon (2003) suggested that the high $^3\text{He}/^4\text{He}$ ratios observed in Hawai'ian and Icelandic lavas (Hilton et al., 1999) portend the demise of the georeactor, although the time scale is uncertain."¹

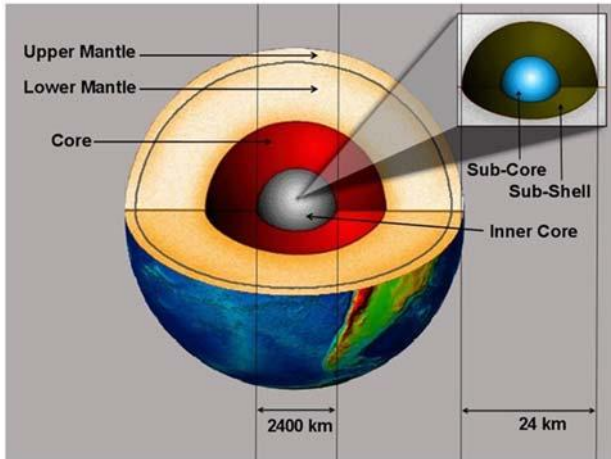


Fig. 2. "Schematic representation of the major parts of the Earth showing the georeactor at the center in expanded view. From (Herndon, 2008)." Figure and captions after Herndon (2010). *History of Geo- and Space Sciences* is an "Open Access" journal. With kind EGU permission by CC BY 3.0 license.

Another support for this entire guess is that the trace element, U, occurs almost exclusively in the alloy portion of the Abee meteorite – which is a peculiar observed meteorite (details are here omitted) - and, hence, it should occur also inside the Earth's core. Therefore, owing to physical-chemical arguments, a process of anoxic fall-in precipitation of heavy elements led to the formation of the enstatite meteorites composition of the Earth's core. In reality, its exact composition is unknown. It is rather only guessed by an analogy with some very seldom occurring meteorites. Maybe, these meteorites are rare because, owing to the abrupt fall in their environmental pressure, they change their state at the time of fracturing of their parent body. On the other hand, another possibility is that they might also change due to some "slow" transformation by weathering after their precipitation.

From the viewpoint of an Earth's physicist whose concern is physics and does not mind about the chemistry of the IC, this entire item can appear just a matter of curiosity, but this reductive feeling is wrong in two respects as follows.

First, the previous model for the formation of the IC relied on the physically perplexing hypothesis of a cooling Earth's core, which began to cool from its innermost

volume, due to some unknown process of change-of-state-of-matter - in such a way as to justify in some way the transformation from a seemingly "fluid" state to a seemingly "solid" state in the IC. A physicist may feel unhappy with this *ad hoc* assumption – recall the Buffon cooling cannon balls aimed only to justify in some physically unrealistic way the S-wave propagation (see Gregori et al., 2026a).

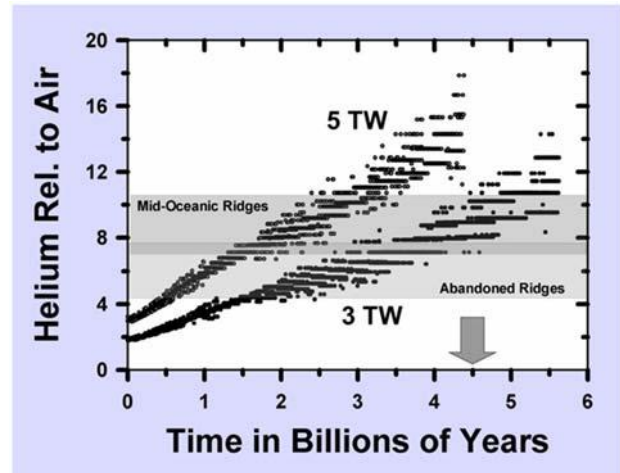


Fig. 3. "Fission product ratio of $^3\text{He}/^4\text{He}$, relative to air, from nuclear georeactor numerical simulations at 5 TW (upper) and 3 TW (lower) power levels, from (Herndon, 2003). The bands comprising the 95% confidence level for measured values from MORB are indicated by the solid lines and shading. The age of the Earth is marked by the arrow. Note the distribution of values at 4.5 Ga, the approximate age of the Earth. The increasing values are the consequence of U fuel burn-up. Icelandic "plume" basalts present values ranging as high as 37 (Hilton et al., 1999). Adapted from (Herndon, 2008)." Figure and captions after Herndon (2010a). *History of Geo- and Space Sciences* is an "Open Access" journal. With kind EGU permission by CC BY 3.0 license.

The aforementioned Herndon model has substituted this starting hypothesis by the assumption that the process began at the time of the early planetesimal accretion of the Earth - and claims that, rather, the process relies on the present observational evidence given by enstatite chondrites. That is, this second hypothesis seemingly is better supported by observations, although the final problem always remains a difficult challenge, as it deals with the mechanism that ought to explain the formation of the IC.

Second, a difference in the chemical composition of the Earth's core may be crucial in determining – or not – the ignition of nuclear reactions, and this is a fundamental item for the overall energy balance, as shown below.

Therefore, according to Herndon's guess, upon assuming a reasonable composition – and upon relying on the present knowledge about the operative performance of nuclear reactors – it seems reasonable to infer a concrete possibility that a georeactor has been (or maybe is still partly) active inside the IC of the Earth. The uncertainties

due either to chemical reactions or to the penetration of sea-urchin spikes.

¹ Reminder: the trapping of He in stable compounds at high ambient pressure depends on the volumetric changes

and arbitrariness about the composition of the system are certainly relevant, and their conspicuous consequences emerge also from the scatter of points in Fig. 3. Nevertheless, it appears that this working hypothesis cannot be ruled out. Hence, it must be taken into account as a realistic possibility. Indeed, to our knowledge, this seems to be the unique viable explanation of the mystery of the $^3\text{He}/^4\text{He}$ ratio in basalt.

This mechanism, however, – according to Herndon's (2010a) estimates – relies on processes that occurred only once, during the entire Earth's history. That is, this is strictly connected with the planetary evolution of the Earth on the *Ga* time scale. It is therefore possible and reasonable that the georeactor was active in the past, while at present it is exhausted, as it seems to be envisaged by Fig. 3. This is also consistent with the fact that at present no sign is found of a present georeactor, such as, e.g., some specific radiation (neutrinos or other; see below).

Another key point of concern is the total available energy from such a speculated georeactor – that seemingly lasted only for a limited time lag during the history of the planet Earth. Conversely, when dealing with large exoplanets, the entire scenario gets much different (see below).

Summarizing, according to our rationale, the present primary endogenous energy source of the Earth is Joule heat originated by the decay of the currents j of the *TD* dynamo that is powered by the tidal interaction. Additional – and optional – fossil energy sources are possible, such as radioactivity or some surviving thermal energy, both originating from the heat caused by the former planetesimal implosion. In addition, the energy released by a georeactor – active in the past, or maybe only partly even at present – can be included as an optional energy source in the general energy balance of the Earth.

In this respect, the total mass of the planet Earth can be crucial to support a nuclear reactor, depending either (i) on the aforementioned speculated fall-in proto planetesimal process, or (ii) on the present lithostatic pressure at Earth's center.

All this is evidently speculative, similarly to every hypothesis, which is the object of exploratory analysis. A numerical simulation – such as the aforementioned *Oak Ridge National Laboratory's SCALE* software model – is a part of confirmatory analysis. Only some observational evidence – that can be explained only by some process and not by others – can determine a choice. Every credible model can be accepted only if it can justify observations, otherwise it must be rejected in favor of other models that seemingly can better explain data.

In this respect, some additional observational evidence deals with the Oklo nuclear reactor. Only very few mentions are here given. Herndon (2010) recalls several related items, i.e., “*the prediction by Kuroda (1956) of the possibility of nuclear fission chain reactions in ancient uranium-ore veins, the discovery of the fossil natural nuclear reactors at Oklo (Bodu et al., 1972), the existence of U in the alloy portion of the Abee meteorite (Murrell and Burnett, 1982), the Earth's interior being like an enstatite chondrite (Herndon, 1980), and more. Herndon (1992)*

applied the nuclear reactor theory of Fermi (1947) to demonstrate the feasibility of planetocentric natural nuclear fission reactors as energy sources for the giant planets.”

The Oklo (Gabon) case history looks very intriguing (Lamoreaux and Torgerson, 2004; Meshik et al., 2004), and it proves the former guess of the possible existence of a natural nuclear reactor during past Earth's history (its geographic location is shown in a figure by Herndon, 2014, which is not here shown).

In this same respect, an additional argument is related to the comparison between Mars, Venus, and Earth, i.e., three terrestrial planets listed in order of increasing mass. Only a very brief reminder is given here. These planets are three models of analogous physical systems that display, however, great differences in their respective B , and also in their respective surface morphology and environmental temperature. The georeactor hypothesis – possibly depending on the total mass, or composition, or density of the planet – can explain, perhaps, the very anomalous case history of Venus.

That is, in the case of Mars a reactor could never have existed, or it never played even a secondary and temporary role. In contrast, it played a role during an early fraction of the planetary evolution of the Earth. Moreover, it appears to be still active inside the comparatively larger planet Venus, thus justifying the great temperature in the present atmosphere and the peculiar topographic features of Venus. In fact, recent evidence envisages that volcanism is still in progress on Venus. No additional details can be here given for brevity purpose.

Conversely, according to such a speculation on the dependence on the total mass of the planet, the large planets can still have an active endogenous reactor.

In any case, concerning the effects of MiniMax on large planets, their respective *TD* dynamo is certainly controlled through the “*internal*” way by the long period e.m. induction of the solar wind, much like the Earth's *TD* dynamo is controlled by induced currents in the mantle. Hence, whenever the solar corona is characterized by large clusters of sunspots, such as, e.g., during MiniMax (see Gregori et al., 2026c, and Figs 7 and 18 of Gregori et al., 2026c), it is reasonable to expect that anomalous long-period inducing e.m. fields are transported by the solar wind (as per Fig. 1). Hence, an anomalous intensification occurs within every respective outer planet's *TD* dynamo. This originates some anomalous release of endogenous heat through some regions that are located over some bunch composed of many sea-urchin spikes. This heat release causes a burst of endogenous energy into the planet's atmosphere, and may power a very large hurricane, according to the same mechanism that supplies an Earth's hurricane (see Gregori and Leybourne, 2025j).

This is an indirect – though effective – way to monitor the state of the solar wind at some distance $\gg 1 AU$ by using every outer planet like a natural probe, much like cometary morphology can also be used (perhaps) as a tool in order to treat comets like natural “sensors” of the spacetime changes of the solar wind, inside its whole wide domain (see Gregori and Leybourne, 2021).

Three issues, however, of this whole mechanism are to be emphasized, which are unlike what occurs on the Earth:

- there is no need for the existence of any “ocean” on the planet, either of water or of any other substance, as the released heat crosses through any medium inside the planetary body – due to Hamilton’s principle and by the sea-urchin spike (or *ESI*) mechanism (see Gregori et al., 2026a and Gregori and Leybourne, 2021) - until hot fluids exhale into its outer atmosphere (see Gregori et al., 2026d);
- the role of solar e.m. radiation is completely irrelevant, as – indeed - at this large heliocentric distance the solar radiation is almost negligible;
- the role of the so-called “*Space Weather*”, associated to the “*external*” way, is likely to be much less relevant at the larger the heliocentric distance of the planetary object.

Let us first refer to the phenomenon that has been more extensively investigated. It is interesting to report the following statements reported by Wall (2011).

“On Earth, hurricanes gain their power from warm ocean water ... Jupiter and Saturn don’t have oceans, so their spinning storms aren’t ‘hurricanes’ in the strict, terrestrial sense. But similar processes spawn them, according to Ingersoll.

‘Heat makes buoyancy; hot air rises’ Ingersoll said. ‘Heat also causes evaporation of moisture, and when the moisture condenses and forms rain, that [phenomenon] releases the energy.’

‘Most of the energy driving Earth’s hurricanes ultimately comes from the Sun. But that may not be the case on Jupiter and Saturn, which orbit our star from much farther away than Earth does.’ They are so giant that they have still retained some of their heat of formation’ Ingersoll said. ‘So, they have their own internal heat that can generate these giant storms.’

[This explanation² disagrees with the mechanism which is here envisaged. A time-varying source inside the planet’s interior - and its “battery” behavior much like it occurs on the Earth - ensures a time varying availability of endogenous heat that can be released with conspicuous spatial gradient, due to the mechanism of Hamilton’s principle and of sea-urchin spikes. Hence, there is no need to appeal either to primordial heat retained since their original formation, and/or to the possible existence of an internal nuclear reactor (see Tables 2 and 3 of Gregori et al., 2026a). That is, the timing of seasons is not controlled by the spin-axis orientation with respect to the ecliptic, as it occurs on the Earth where, owing to the shorter heliocentric distance, solar radiation is a leading energy source. The seasonal timing on the large outer planets is, rather, mostly controlled by endogenous energy release that depends on the e.m. induction by the solar wind through the *TD* dynamo. This is shown in an impressive way by the Pluto/Charon binary system (see below).]

The moisture requirement explains why gigantic, hurricane-like storms don’t seem to occur on Venus or

Mars, he added. ‘The giant planets have moisture down below the clouds’ Ingersoll said. ‘But Venus doesn’t. Venus is dry as a bone, hot and dry. It’s not comparable. And Mars is cold and dry.’”

[Note that, as mentioned above, Venus is very anomalous, with its thick atmosphere, and this paradox seems to be explained (maybe) only by the presence of an internal nuclear reactor. In contrast, the extremely tiny atmosphere of Mars can justify, at most, the occurrence of the well-known “dust devils” or low latitude aurora.]

We report in the following some evidence concerning large storms on other planets. The list, however, is incomplete, as additional similar evidence is steadily reported as soon as they are observed either by space probes or by powerful astronomical observatories either orbiting, or ground-based.

Jupiter

The well-known Jupiter’s Great Red Spot (Figs 4 and 5) is likely to be a permanent dynamic feature of the atmosphere, maybe associated to some anomalous pattern on the deep Jovian body that determines a steady anomalous local energy balance. The time variation of the Great Red Spot ought to be associated with time changes of endogenous heat generated by the Jovian *TD* dynamo.



Fig. 4. “Close-up of Jupiter’s Great Red Spot as seen by a Voyager spacecraft. Credit: NASA/JPL-Caltech.” Figure and captions after Wall (2011). NASA copyright free policy.

Just as a curiosity, analogous phenomena are also to be expected on dwarf stars, where, however, only storms are observed that last at most up to 2 *Earth’s years* (e.g., Clavin and Johnson, 2015).

Dunn et al. (2016) reported the first clear evidence of a direct “instant” connection between impinging solar

² A text inside square brackets deals with comments added by the authors, like inserts inside some quotation verbatim loaned from some other paper.

radiation and polar aurora on Jupiter. That is, their explanation is correct only as an “external” way, invoking a “Space Weather”, process. They summarize their records as follows.



Fig. 5. “Trapped between two jet streams, the Great Red Spot is an anticyclone swirling around a center of high atmospheric pressure that makes it rotate in the opposite sense of hurricanes on Earth. Credits: NASA/JPL/SSI.” Figure and captions after Molar Candanosa (2015). NASA copyright free policy.

“We report the first Jupiter X-ray observations planned to coincide with an interplanetary Coronal Mass Ejection (ICME). At the predicted ICME arrival time, we observed a factor of ~ 8 enhancement in Jupiter’s X-ray aurora. Within 1.5 hours of this enhancement, intense bursts of non-10 decametric radio emission occurred. Spatial, spectral, and temporal characteristics also varied between ICME arrival and another X-ray observation two days later.

Gladstone et al. (2002) discovered the polar X-ray hotspot and found it pulsed with 45 min quasiperiodicity. During the ICME arrival, the hotspot expanded and exhibited two periods: 26 min periodicity from sulfur ions and 12 min periodicity from a mixture of carbon/sulfur and oxygen ions. [Hence, the atmospheric dynamics was profoundly affected.]

After the ICME, the dominant period became 42 min. By comparing Vogt et al. (2011) Jovian mapping models with spectral analysis, we found that during ICME arrival at least two distinct ion populations, from Jupiter’s dayside, produced the X-ray aurora. Aurora mapping to magnetospheric field-lines between $50 - 70 R_J$ were dominated by emission from precipitating sulfur ions ($S^{7+, \dots, 14+}$). Emissions mapping to closed field-lines between $70 - 120 R_J$ and to open field-lines were generated by a mixture of precipitating oxygen ($O^{7+, 8+}$) and sulfur/carbon ions, possibly implying some solar wind precipitation ...”

This phenomenon is illustrated by a false color brightness figure (not here reported) shown by Gladstone et al. (2002); also see Fig. 6.

The Jupiter’s Great Red Spot has been observed continuously for at least 180 years. A century ago, its size was $\sim 40,000$ km across (i.e., over 3 times the diameter of the Earth). Now, it measures about half that, while it appears to be getting smaller and more circular. This should envisage a secular variation of the e.m. induction by the solar wind inside the Jovian TD dynamo.

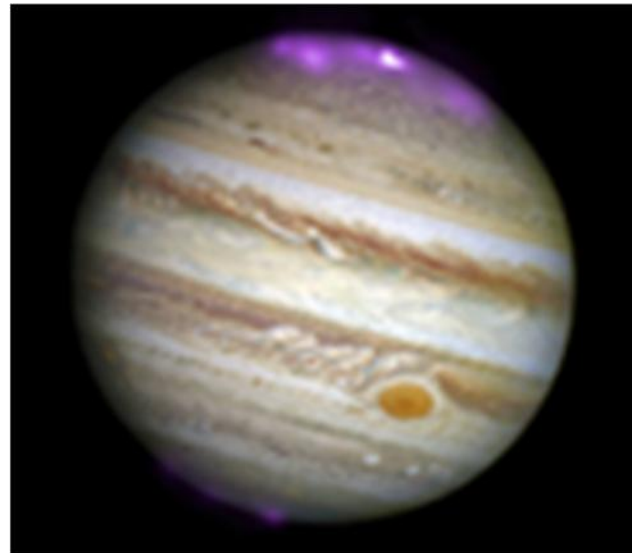


Fig. 6. “This is a Hubble Space Telescope (HST) image of Jupiter. The strength of X-ray auroras on October 2, 2011 are superimposed to create this composite image. The Chandra X-ray observatory found the auroras on this day to be about 8 times brighter than normal over a large area of the planet. Image credit: X-ray-NASA / CXC / UCL / W. Dunn et al.; Optical-NASA / STScI.” Figure and captions after Imster (2016f). NASA copyright free policy.

Also, the chemistry and color of these pictures are still poorly understood (Molar Candanosa, 2015). Recently (Zubritsky, 2015) Kelvin waves have been detected near Jupiter’s equator in images obtained by the NASA’s New Horizons spacecraft that flew by the planet in 2007. They are fluid dynamical effects and move at $164 - 176 \text{ m sec}^{-1}$.

“When the New Horizons images were first studied, scientists had classified the feature as a gravity-inertia wave, but the newer analysis indicates that a Kelvin wave is more likely. The wavelength in this case is ~ 300 km, which is short compared to Kelvin waves in Earth’s atmosphere ...

The structure of a Kelvin wave is determined by a balance between the Coriolis force generated by the planet’s rotation and a boundary of some kind. In Earth’s oceans, that boundary could be the coastline. In a planet’s atmosphere, the zone near the equator serves as a boundary.

In Earth’s atmosphere, Kelvin waves contribute to the quasi-biennial oscillation (QBO), a pattern of tropical winds in the stratosphere. Every 2 – 3 years, the wind shifts from easterly to westerly - accompanied by changes in temperature – and back again. The influence of this pattern sometimes can be felt as far away as the northern or southern polar vortex.

An analogous pattern of global winds and temperatures has been found in Jupiter’s stratosphere. This pattern, the QBO, repeats every 4 – 5 Earth years. A similar pattern on Saturn repeats roughly every 15 Earth years ... “

A huge storm was also observed on Jupiter in April 2018. Videos are reported by Wall (2018e), Pappas (2018) and Mathewson (2018b).

Saturn

Concerning Saturn, Li and Ingersoll (2015; see also Choi, 2015c) report a huge anomalous storm (Fig. 7). “A giant storm erupted on Saturn in December 2010. It produced intense lightning and cloud disturbances and encircled the planet in six months. Six giant storms-also called Great White Spots-have been observed on Saturn since 1876, recurring every 20 – 30 years and alternating between mid-latitudes and the equator ...” Also, videos are given by Anonymous (2012k, 2012l).

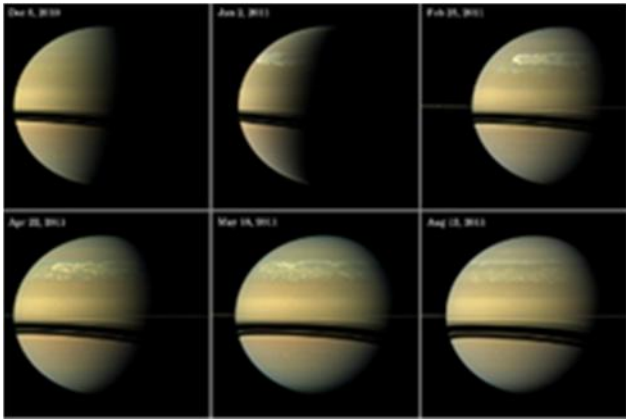


Fig. 7. “This series of images from NASA’s Cassini spacecraft orbiting Saturn chronicles the evolution of a truly titanic storm system on the planet between December 2010 and August 2011. Such a planet-encircling storm occurs every 30 years on Saturn. Credit: NASA/JPL-Caltech/SSI.” Figure and captions after Choi (2015c). NASA copyright free policy.

In addition, Lewin (2017f) briefly reports about the Cassini observations of Saturn during one full season. “...During the Solstice Mission, researchers watched a huge storm encircle the planet and disperse over the course of seven months. They watched the hexagonal jet stream surrounding Saturn’s North Pole change from blue to yellow (except for the very center) over the course of the Northern Hemisphere’s (NH) spring.

Cassini data suggests that the increased sunlight interacts with compounds in the upper atmosphere to form particles called photochemical aerosols, which accumulate into a yellowish haze. The very center may stay blue for one of two reasons it hasn’t been exposed to sunlight as long as the areas around it because it’s at the very top of the planet, or the circulation in the whirling vortex pulls the compounds downward. [In fact, an increase of endogenous energy release intensifies the atmospheric dynamics and storminess, and gas mixing of gas exhalation from the lower layers, hence a change of color.]

Cassini saw the seasonal changes come over the planet suddenly based on latitude, rather than gradually ...”

A detailed meteorological investigation was carried out by Fletcher et al. (2017).

“...The equatorial middle atmospheres of the Earth, Jupiter and Saturn all exhibit a remarkably similar phenomenon - a vertical, cyclic pattern of alternating temperatures and zonal (east-west) wind regimes that propagate slowly downwards with a well-defined multi-Earth-year period. Earth’s QBO (observed in the lower

stratospheres with an average period of 28 months) is one of the most regular, repeatable cycles exhibited by our climate system (Baldwin et al., 2001), and yet recent work has shown that this regularity can be disrupted by events occurring far away from the equatorial region (Osprey et al., 2016; Newman et al., 2016), an example of a phenomenon known as atmospheric teleconnection.

Here we reveal that Saturn’s equatorial Quasi-Periodic Oscillation (QPO, with a ~ 15 year period) can also be dramatically perturbed. An intense springtime storm erupted at Saturn’s northern mid-latitudes in December 2010 (Fletcher et al., 2011; Sánchez-Lavega et al., 2011; Fischer et al., 2011), spawning a gigantic hot vortex in the stratosphere at 40°N that persisted for 3 years (Fletcher et al., 2012).

Far from the storm, the Cassini temperature measurements showed a dramatic ~ 10 K cooling in the 0.5 – 5 mbar range across the entire equatorial region, disrupting the regular QPO pattern and significantly altering the middle-atmospheric wind structure, suggesting an injection of westward momentum into the equatorial wind system from waves generated by the northern storm.

Hence, as on Earth, meteorological activity at mid-latitudes can have a profound effect on the regular atmospheric cycles in the tropics, demonstrating that waves can provide horizontal teleconnections between the phenomena shaping the middle atmospheres of giant planets.”

The same storm is addressed by Wall (2011). The thunderstorm ~ 10,000 km wide, i.e., almost as large as to contain the Earth inside it, that in December 2010 erupted on Saturn (Fig. 8). It is known as the Great White Spot. It appears to persist, “and some of its clouds have wrapped all the way around the ringed planet.” It “also generates lots of lightning, just like thunderstorms here on Earth. ‘We can see the lightning flashes on the night side, and we can hear the radio static from the lightning,’ Ingersoll told ... ‘The energy in the lightning flashes is a lot stronger than terrestrial lightning.’”

Wall (2011) also emphasizes what he calls the “Saturn storm mysteries”.

“Saturn’s Great White Spot tends to erupt every few decades, shattering long periods of calm and quiescence. Scientists still aren’t sure why some storms on the giant planets should be so big, and so infrequent. ‘For some reason, they store up that energy for a long time, then let it loose in a violent, huge storm’ Ingersoll said. ‘It didn’t have to work out that way; they could let off a little popcorn now and then. But they don’t do that.’ “

[According to the mechanism, which is here envisaged, this timing is essentially related to the timing of the expansion of the solar corona, as an outer planet is a probe that monitors the state of the solar wind. The confirmation of this interpretation can very easily derive from monitoring the expansion of the solar corona, and how it originates anomalous “hurricanes” on either one of the four outer planets, when they are likened to four probes for the instant monitoring of the state of the solar corona.]

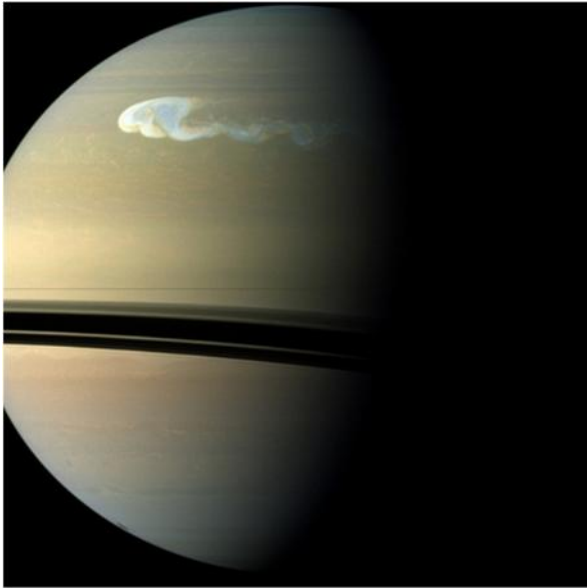


Fig. 8. “An image of Saturn taken in December 2010 by the Cassini spacecraft shows a storm with a latitudinal and longitudinal extent of 10,000 km and 17,000 km, respectively. The latitudinal extent of the storm’s head is approximately the distance from London to Cape Town. A ‘tail’ emerging from its southern edge extends further eastward. Credit: Carolyn Porco and CICLOPS; NASA/JPL-Caltech/SSI.” Figure and captions after Wall (2011). NASA copyright free policy.

Li et al. (2023) is illustrated by University of California – Berkeley (2023a), and reports about a more detailed analysis of this giant storm. The focus is on “long-lasting megastorms on Saturn, similar to Jupiter’s Great Red Spot, through the study of radio emissions and ammonia gas disruptions. The research uncovers significant atmospheric differences between the two gas giants and challenges the current understanding of megastorms ...

... Saturn, although more unassuming in appearance compared to Jupiter’s colorful visage, also has long-lasting megastorms. These storms have impacts deep in the atmosphere that persist for centuries...

... The research ... examined radio emissions from the planet, originating from beneath the surface, and discovered long-term disruptions in the distribution of ammonia gas. [See Fig. 9]

Megastorms occur approximately every 20 to 30 years on Saturn and are similar to hurricanes on Earth, although significantly larger. But unlike Earth’s hurricanes, no one knows what causes megastorms in Saturn’s atmosphere, which is composed mainly of hydrogen and helium with traces of methane, water, and ammonia [According to the explanation here envisaged, these phenomena can result from a secular variation of the solar wind flow.]

Imke de Pater, a UC Berkeley professor emerita of astronomy and of Earth and planetary sciences, has been studying gas giants for over four decades to better understand their composition and what makes them unique, employing the Karl G. Jansky Very Large Array (VLA) in New Mexico to probe the radio emissions from deep inside the planet.

‘At radio wavelengths, we probe below the visible cloud layers on giant planets. Since chemical reactions and

dynamics will alter the composition of a planet’s atmosphere, observations below these cloud layers are required to constrain the planet’s true atmospheric composition, a key parameter for planet formation models,’ she said. ‘Radio observations help characterize dynamical, physical and chemical processes including heat transport, cloud formation and convection in the atmospheres of giant planets on both global and local scales.’

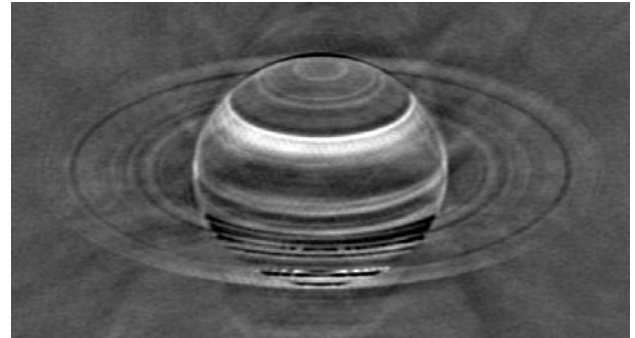


Fig. 9. “Radio image of Saturn taken with the VLA in May 2015, with the brighter radio emissions from Saturn and its rings subtracted to enhance the contrast in the fainter radio emissions between the various latitudinal bands in the atmosphere. Since ammonia blocks radio waves, the bright features indicate areas where ammonia is depleted and the VLA could see deeper in the atmosphere. The broad bright band at northern latitudes is the aftermath of the 2010 storm on Saturn, which apparently depleted ammonia gas just below the ammonia-ice cloud, which is what we see with the naked eye. Credit: R. J. Sault and I. de Pater.” Figure and captions after University of California – Berkeley, (2023a). Reproduced with AAAS’s gold open-access permission.

According to the team, the concentration of ammonia is lower at midaltitudes, just below the uppermost ammonia-ice cloud layer, but has become enriched at lower altitudes, 100 to 200 km deeper in the atmosphere. They believe that the ammonia is being transported from the upper to the lower atmosphere via the processes of precipitation and reevaporation. What’s more, that effect can last for hundreds of years ...

The study further revealed that although both Saturn and Jupiter are made of hydrogen gas, the two gas giants are remarkably different. While Jupiter does have tropospheric anomalies, they have been tied to its zones (whitish bands) and belts (darkish bands) and are not caused by storms like they are on Saturn ...”

Therefore, Jupiter and Saturn monitor the state of the impinging solar wind, although the interpretation of Jupiter and Saturn storms requires some care and harder thinking.

Fletcher et al. (2017) shows several quantitative plots, not here reported, drawn according to the standards of the meteorology of Earth’s stratosphere. They also show several figures, but a composite figure (not here shown) is particularly expressive for the present discussion. It shows several images of Saturn compared to one another. The images were collected by VLT/VISIR 7.9µm records ranging in time from 2009 to 2016. VLT/VISIR is ESO’s VLT spectrometer and imager for the mid-IR. A bright equatorial band is visible in 2009-2010 - and only faintly at

the start of 2011. However, the growing intensity of the northern stratospheric vortex in March-May 2011 caused difficulty to detect contrasts in the equatorial region. *VISIR* was not available during 2012-2014. However, they relied on annual observations since 2015, using a much-improved sensitivity and detector plate scale. Thus, they found the absence of the warm equatorial band, because at that time the *QPO* (quasi-periodic oscillation) was in its westward phase.

In any case, as illustrated by Fletcher et al. (2009), data were reduced, remapped, and calibrated. As far as the present discussion is concerned, the figure shows a storm in Saturn's north polar stratosphere as the planet approaches summer solstice in May 2017. The storm is displayed as a growing brightness, together with continued presence of a warm homogeneous band at Saturn's northern mid-latitudes, being a remnant of the storm.

The Earth's *QBO* is a classical topic in the literature and is not here illustrated. An analogous oscillation is observed in Jupiter's atmosphere (quasi-quadrennial oscillation *or QQQ*) tentatively explained in terms of gravity waves.

In addition, this regular *QPO* pattern on Saturn has to be matched with the alternating circulation pattern observed on the Saturn's North Pole (see Figs 8 through 12) - that, according to the argument of Gregori et al. (2025u) and references therein, seems to be explained only in terms of the e.m. interaction, rather than according to the better known standard atmospheric models that rely on thermodynamics and fluid dynamics.

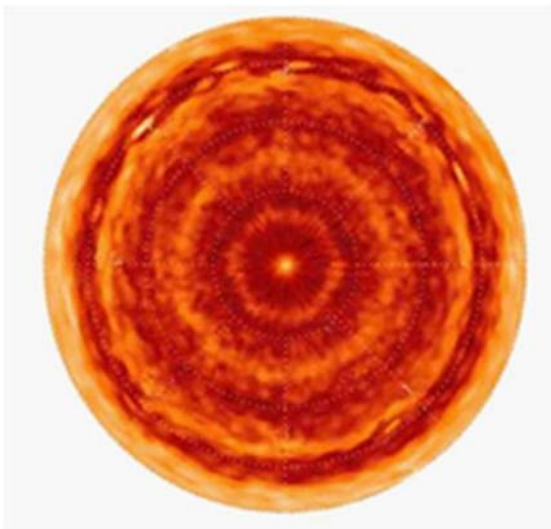


Fig. 10. "Saturn's North Pole, IR Cassini image. Saturn is a gaseous planet composed mainly of hydrogen and helium. This image was obtained during the dark winter. The pole is encircled by a hexagonal feature in its atmosphere, which is thought to be caused by a planetary (atmospheric) wave. Image obtained using the IR mapping spectrometer on board the Cassini orbiter spacecraft. Courtesy of: NASA/JPL-Caltech/University of Arizona. The Cassini-Huygens mission is a cooperative project of NASA, the ESA and the Italian Space Agency. Image Credit: NASA/JPL/GSFC/Oxford University/Science Photo Library ..." Figure and captions after Scott (2015). NASA and ESA copyright free policy.

Owing to this same physical mechanism, the identical storm-time also involved Saturn's moons that, in fact, also have an internal *TD* dynamo (see Tables 2 and 3 of Gregori et al., 2026a).

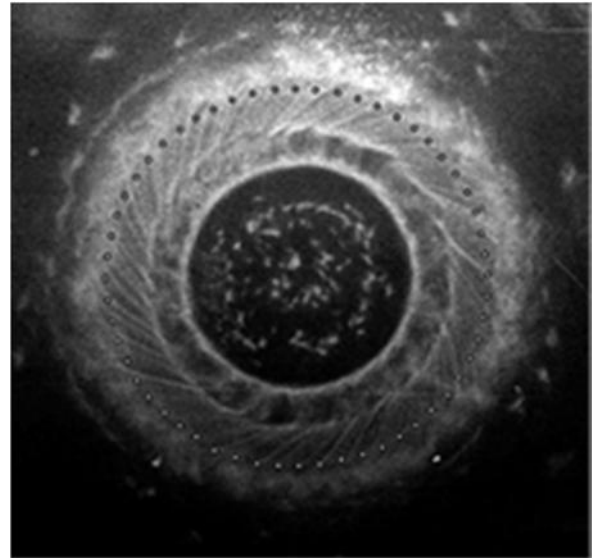


Fig. 11. "Cross-section of a dense plasma focus Birkeland current carrying $I = 174,000$ A. This image was captured by a witness plate placed in the discharge in a plasma lab. The spiral structure of the cross-section is visible. The 56-dot circular overlay shows the locations of the apparent spiral shaped paths of matter. Courtesy of A. L. Peratt (Peratt et al., 2007)." Figure and captions (simplified) after Scott (2015). With kind permission of *Progress in Physics* ("Open Access" academic journal).

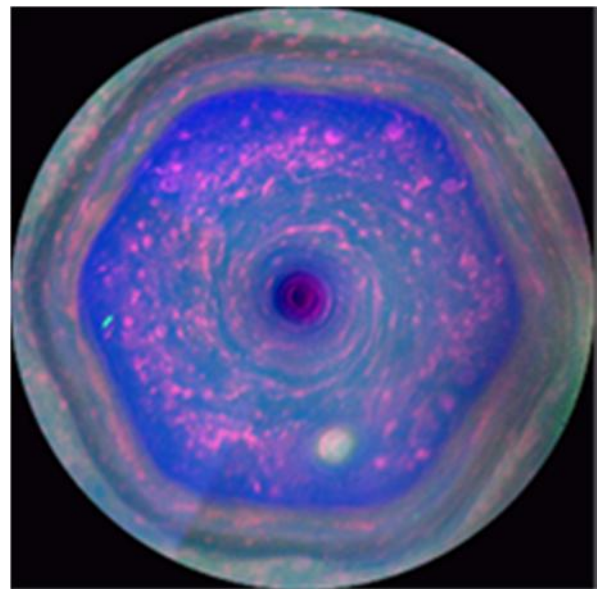


Fig. 12. "In full view: Saturn's streaming hexagon. This colorful view from NASA's Cassini mission is the highest-resolution view of the unique six-sided jet stream at Saturn's North Pole known as 'the hexagon'. Image obtained on December 10, 2012 and released December 4, 2013. Credit: NASA/JPL-Caltech/SSI/Hampton." Figure and captions after Anonymous (2018f). NASA copyright free policy.

“On Saturn’s largest moon, Titan, CH₄ storm clouds shifted up from the south toward the moon’s equator from 2004 to 2010. Their corresponding shift northward as the solstice approached was surprisingly slow; ... cloud models had expected the activity to happen years earlier. [The change of atmospheric dynamics is indicative of an anomalous injection of energy in the atmosphere. This is further supported by the following statement.]

But some action was sudden: in 2013, haze and trace hydrocarbons formerly found only in the north suddenly built up in the Titan’s south, indicating that its atmospheric circulation had changed direction due to the changing Sun exposure ...

Observations of how the locations of cloud activity change, and how long such changes take, give us important information about the workings of Titan’s atmosphere and also its surface, as rainfall and wind patterns change with the seasons too ...” (Lewin, 2017f; see Fig. 13).

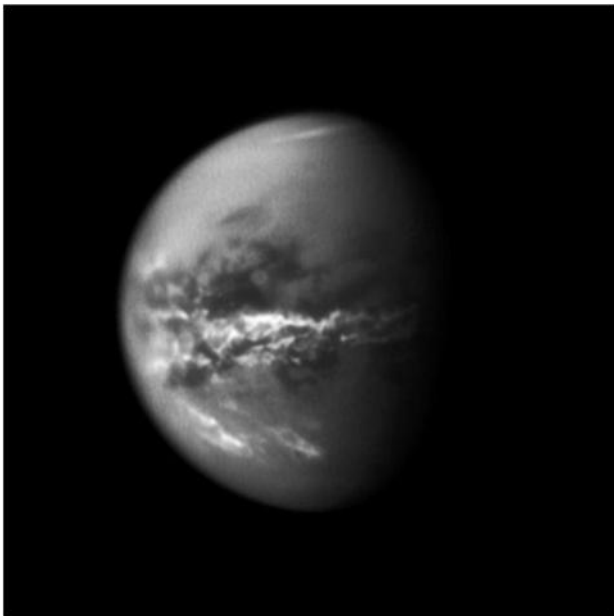


Fig. 13. “Storms on Saturn’s moon Titan changed as Saturn moved through equinox and toward solstice. In this 2011 image, CH₄ clouds can be seen concentrated near the moon’s equator. Credit: NASA/JPL-Caltech/SSI.” Figure and captions after Lewin (2017f). NASA copyright free policy.

Compared to the Earth’s, the meteorology of other planetary objects is quite different. For instance, Zubritsky (2015a) reports about the meteorology of Titan, relying on interviews with some scientists, including Carrie Anderson (at GSFC). She shows Figs 14 and 15 and comments on them as follows. The evidence envisages violent seasonal transitions that, therefore, ought to be particularly sensible to anomalous release of endogenous energy, as it ought to occur during every kind of MiniMax considered.

...Scientists have detected a monstrous new cloud of frozen compounds in the moon’s low- to mid-stratosphere - a stable atmospheric region above the troposphere, or active weather layer.

Cassini’s camera had already imaged an impressive cloud hovering over Titan’s South Pole at an altitude of about 300 km. However, that cloud, first seen in 2012,

turned out to be just the tip of the iceberg. A much more massive ice cloud system has now been found lower in the stratosphere, peaking at an altitude of about 200 km.

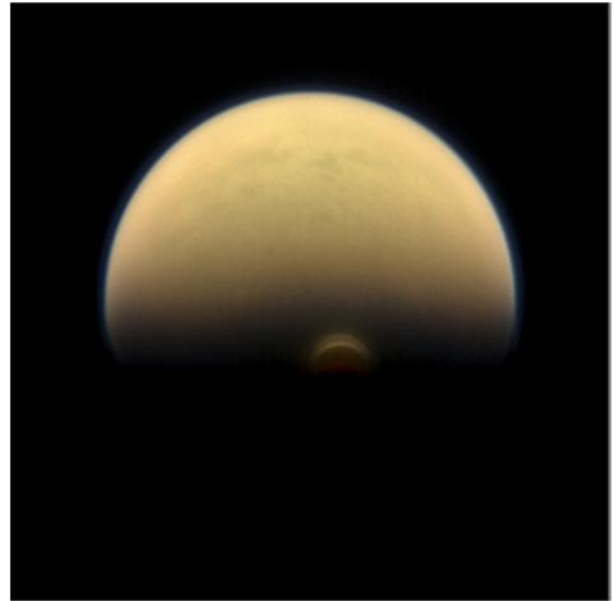


Fig. 14. “As winter sets in at Titan’s South Pole, a cloud system called the south polar vortex (small, bright ‘button’) has been forming, as seen in this 2013 image. Credits: NASA/JPLCaltech/SSI.” Figure and captions after Zubritsky (2015a). NASA copyright free policy.

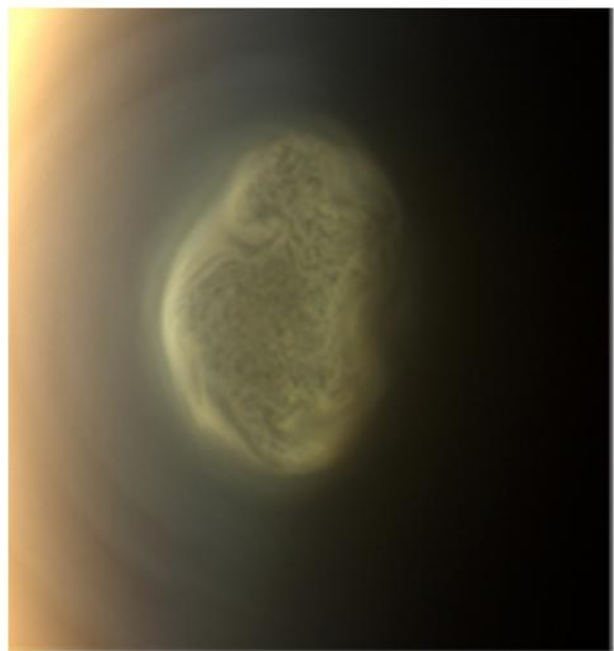


Fig. 15. “This 2012 close-up offers an early snapshot of the changes taking place at Titan’s South Pole. Cassini’s camera spotted this impressive cloud hovering at an altitude of about 300 km. Cassini’s thermal IR instrument has now detected a massive ice cloud below it. Credits: NASA/JPL-Caltech/SSI.” Figure and captions after Zubritsky (2015a). NASA copyright free policy.

The new cloud was detected by Cassini’s IR instrument - the Composite Infrared Spectrometer, or CIRS - which obtains profiles of the atmosphere at invisible thermal

wavelengths. The cloud has a low density, similar to Earth's fog but likely flat on top ...

[This is] the first time any spacecraft has seen the onset of a Titan winter ... each Titan season lasts ~ 7.5 years on Earth's calendar The ice clouds at Titan's pole don't form in the same way as Earth's familiar rain clouds.

For rain clouds, water evaporates from the surface and encounters cooler temperatures as it rises through the troposphere. Clouds form when the water vapor reaches an altitude where the combination of temperature and air pressure is right for condensation. [Concerning the water condensation process in the Earth atmosphere see Gregori and Leybourne (2026e).] The CH₄ clouds in Titan's troposphere form in a similar way.

However, Titan's polar clouds form higher in the atmosphere by a different process. Circulation in the atmosphere transports gases from the pole in the warm hemisphere to the pole in the cold hemisphere. At the cold pole, the warm air sinks, almost like water draining out of a bathtub, in a process known as subsidence.

The sinking gases - a mixture of smog-like hydrocarbons and nitrogen-bearing chemicals called nitriles - encounter colder and colder temperatures on the way down. Different gases will condense at different temperatures, resulting in a layering of clouds over a range of altitudes.

Cassini arrived at Saturn in 2004-mid-winter at Titan's North Pole. As the North Pole has been transitioning into springtime, the ice clouds there have been disappearing. Meanwhile, new clouds have been forming at the South Pole. The build-up of these southern clouds indicates that the direction of Titan's global circulation is changing ...

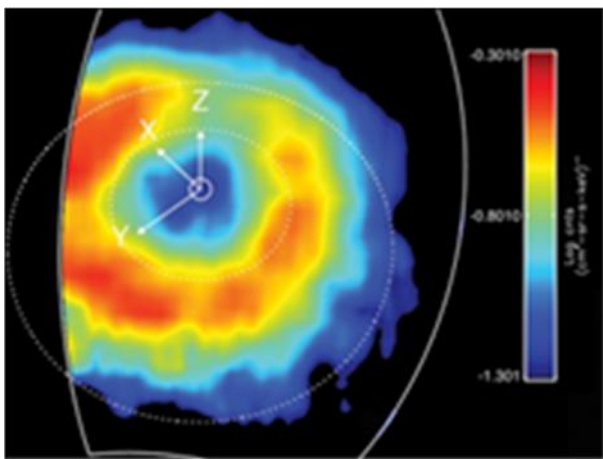


Fig. 16. "Saturn's ring current of energetic ions trapped in its **B** is shown in this false-color map from the Cassini spacecraft. The colors correspond to the intensities of the energetic neutral atoms emitted from the ring current. These neutral atoms are formed when trapped energetic positive ions take electrons from cold gas atoms, and are then able to escape Saturn's **B**. Credit: NASA/JPL/JHUAPL." Figure and captions after Zastrow (2015). AGU copyright free policy.

... From the ice cloud seen earlier by Cassini's camera, scientists determined that temperatures at the South Pole must get down to at least -150°C. The new cloud was found in the lower stratosphere, where temperatures are even colder. The ice particles are made up of a variety of compounds containing hydrogen, carbon and nitrogen.

Anderson and her colleagues had found the same signature in CIRS data from the North Pole, but in that case, the signal was much weaker. The very strong signature of the south polar cloud supports the idea that the onset of winter is much harsher than the end ..."

Always dealing with Saturn, also the 13 interchange events ought to be recalled (see Fig. 16) that have been reported by the Cassini mission's archives during 2005-2010. That is, these are exceptional events that ought to be representative of seldom occurring extreme conditions in interplanetary space. These events are likely to be the consequence of some anomalous state of solar activity. The MiniMax, which is a multiannual occurrence, is likely to be one facet of this extreme state of the Sun.

Uranus

Similar features have been observed on Uranus (Figs 17, 18 and 19). In fact, Uranus is an interesting case history. Howell (2014e) reports about a very anomalous and totally unexpected feature of Uranus (Fig. 18) observed on August 6, 2014. Compare this image with Fig. 19 that was observed on July 11 and 12, 2004.

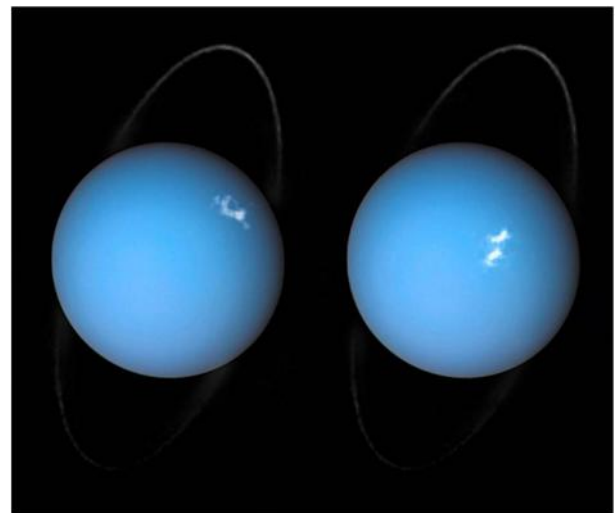


Fig. 17 - "The Uranus auroras are the white areas in this composite image via ESA/Hubble and NASA, L. Lamy / Observatoire de Paris." Figure and captions after Byrd (2017b). ESA copyright free policy.

"Uranus is finally having some summer storms, seven years after the planet reached its closest approach to the Sun, leaving scientists wondering why the massive storms are so late. [That is, as already stressed, the timing of seasons is not controlled by the spin-axis orientation with respect to the ecliptic ("external" way). Conversely, the seasonal timing on the large outer planets is controlled by endogenous energy release ("internal" way) that depends on the e.m. induction by the solar wind through the TD dynamo. This is shown in an impressive way by the Pluto/Charon binary system (see below).]

The usually quiet gas giant now has such 'incredibly active' weather that some of the features are even visible to amateurs, said Imke de Pater, the project's lead researcher

and an astronomer at the University of California, Berkeley

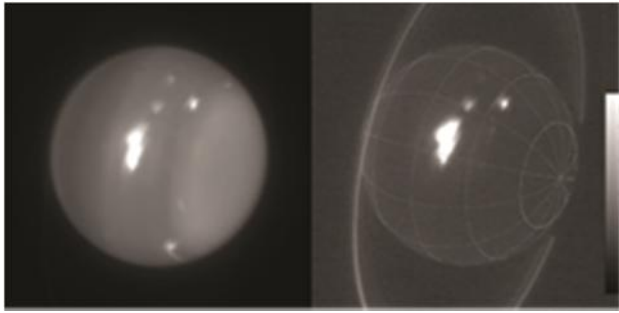


Fig. 18. “These IR images of the planet Uranus show a white spot that is actually a massive storm on the planet. This image was recorded by the Keck II telescope atop Mauna Kea in Hawai’i on August 6, 2014 in the 2.2 μm wavelength. Credit: Imke de Pater (UC Berkeley) and W. M. Keck Observatory images.” Figure and captions after Howell (2014e). NASA copyright free policy.

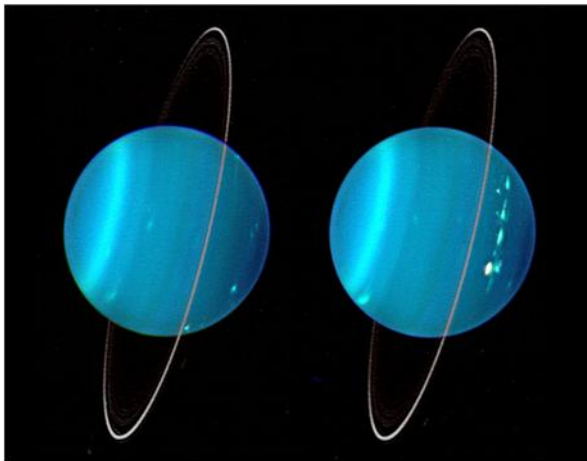


Fig. 19 – “Keck Telescope views of Uranus, (11 July 2004). An IR composite image of the two hemispheres of Uranus obtained with Keck Telescope adaptive optics. The component colors of blue, green, and red were obtained from images made at near IR wavelengths of 1.26, 1.62, and 2.1 μm respectively. The images were obtained on July 11 and 12, 2004. The North Pole is at 4 o’clock. Credit: Lawrence Sromovsky, University of Wisconsin - Madison/ W.W. Keck Observatory.” Figure and captions after Anonymous (2014s). NASA copyright free policy.

This is by far the most active weather de Pater’s team has seen on Uranus in the past decade, examining its storms and northern convective features. It also paints a different picture of the quiet planet Voyager 2 saw when the NASA spacecraft flew by in 1986.

Note, however, that 1986 was a solar minimum year, i.e., the Sun was (maybe) particularly quiet and the solar wind flow comparatively smoother and less scattered. In contrast, 2014 is the MiniMax year with an anomalous large sunspot, and this indicates an e.m. signal that, when analyzed by a Fourier algorithm, is of comparatively very low frequency.

Howell (2014e) quotes a co-investigator (Heidi Hammel): “this type of activity would have been expected in 2007, when Uranus’ once-every- 42 year equinox occurred and the Sun shined directly on the equator. But we predicted that such activity would have died down by now. Why we see these incredible storms now is beyond

anybody’s guess.” [In fact, compared to solar wind flow and to its variations, solar radiation plays an almost negligible role. This fact is evidenced by the following statements.]

Howell (2014e) comments as follows. “But here’s where the mystery comes in: as far as anyone can tell, Uranus has no source of internal heat. [In contrast, it has a great, violent internal TD dynamo. See Tables 2 and 3 of Gregori et al. (2026a).] Sunlight is thought to be responsible for changes in its atmosphere, such as storms. But the Sun’s light is currently weak in Uranus’ NH, so scientists are puzzled as to why that area is so active today.”

Another concern deals with Uranus atmospheric temperatures, as explained by Wendel (2016c) who refers to Fig. 20 and relies on an interview with Henrik Melin (University of Leicester).

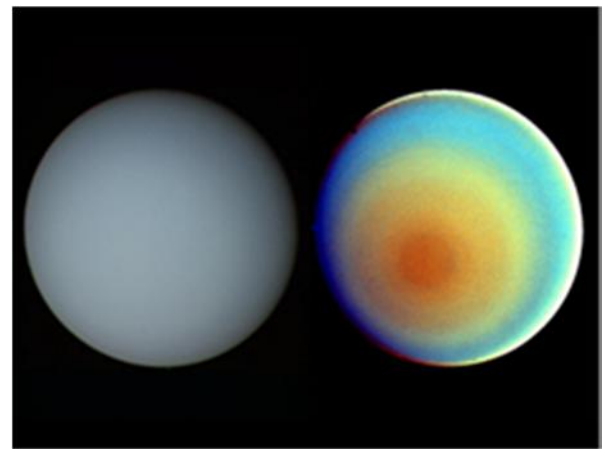


Fig. 20. “The Voyager 2 spacecraft snapped these (left) true-color and (right) false-color images of Uranus in 1986. Credit: NASA/JPL.” Figure and captions after Wendel (2016c). AGU copyright free policy.

“Models of Jupiter, Saturn, Uranus, and Neptune predict that the temperatures of their upper atmospheres ...should be around -73°C . However, when the two Voyager spacecraft zipped by those gas giants in the late 1980s, scientists discovered that the planets’ outermost atmospheres were much hotter than expected – nearing $> 700^{\circ}\text{C}$... [Note the enormous difference, which is clearly suggestive of the contribution by a relevant endogenous energy release, consistently with the intense internal TD dynamo.]

Although close monitoring has shown that Uranus’ upper atmosphere underwent consistent cooling over the past 20 years, measurements since 2014 ... revealed a reversal toward heating. [The endogenous energy source experiences time variation depending on the time changes of solar wind flow that control the efficiency of the internal TD dynamo.]

During this time, other observers detected a storm in the planet’s lower atmosphere. Could the two phenomena be related? [A greater input of energy into the atmosphere increases its dynamics and storminess.]

The fact that this turbulent weather phenomenon in the lower atmosphere occurs at the same time as there is significant heating in the upper atmosphere suggests that

[the storm] is an important mechanism' in that heating process, Melin said.

Melin suspects that the recently spotted Uranian storm could have generated enough heat to reverse the 20 year cooling trend in the upper atmosphere of the planet. Also, because storms occur all the time on Jupiter and Saturn, the disturbances might have a hand in maintaining high temperatures in their upper atmospheres as well, he suggested.

During the past 20 Earth years, the upper atmosphere of Uranus cooled from 750 to 550 K, but since 2013, it has heated by about 50 K per Earth year, Melin said. A Uranus year is 84 Earth years, so small variations in Uranus's atmospheric temperature while the planet orbits the Sun should take place gradually. The fact that the reversal happened relatively quickly means that 'something dramatic has changed', Melin said. [In fact, a crucial role is played by the endogenous energy source that is controlled by the whims of the solar wind flow.]

There are several mechanisms that can heat a planet, but none solve the mystery of the gas giants' so-called 'energy crisis', Melin explained. The Sun warms the gas giants, but because those planets are so large and far away, scientists know that solar photons don't supply enough energy to heat their upper atmospheres to current temperatures.

Scientific evidence suggests that Jupiter and Saturn hold extremely hot cores left over from their formation about 4.5 Ga ago, but the core of Uranus generates relatively little heat. [This is the same unconscious paradigm that reminds about the disproved "myth" of the Earth that, like every other planet, ought to cool in space like a Buffon's bronze cannon ball (see Gregori et al., 2026a).]

... Given the storm in Uranus's lower atmosphere, Melin suspects that another factor could be at work: low-amplitude 'acoustic waves'-also known as gravity waves-generated by huge, turbulent storms ...

Uranus is unique in that it has remained so very quiet [stormwise] for so long and that the appearance of these storms in 2014 correlates so well with the abrupt heating of the upper atmosphere', Melin said. [In fact, these time variations are very likely caused by changes of solar wind flow. In addition, the inclination of the spin axis of Uranus is likely to play a role.]

Astronomers have seen a similar effect before on Saturn ... In 2010, a huge storm erupted in Saturn's lower atmosphere, and scientists witnessed the evolution of a region of hot gases that rose into the upper atmosphere ...

However, scientists remain unclear as to how these planets' lower atmospheres interact with their upper atmospheres ... [in fact, a hot fluid exhalation occurs from the deeper layers of the planet] the 2014 storms do appear to have been bigger and brighter than anything we've seen before ..."

The explanation of these apparent paradoxes is given in the discussion associated to Tables 2 and 3 of Gregori et al. (2026a), and Uranus is to be expected to have a conspicuous internal TD dynamo, supplied by the large tidal pull on its fluid body.

The evidence of a large magnetosphere, which is originated by an intense planetary **B**, appears to be a most obvious self-consistency check of this whole interpretation. In any case, compared to solar wind flow variations, the variations of solar radiation play a role that is comparatively much smaller, in fact negligible, compared to what occurs in Earth's climate. On the other hand, the Uranus ionosphere is very sensible to large variations of the internal **B**, and this justifies the anomalous storm that, indeed, persists for a long time. That is, these storms are not a seldom occurring and more or less random event. Rather, they are a typical almost permanent feature when the Sun displays some peculiar anomalous behavior. The atmospheres of the large outer planets are therefore very effective natural sensors - and probes - suited to monitor the large-scale feature of the solar wind flow.

Howell (2014e) also specifies that "de Pater's team tracked eight large storms in Uranus' NH when observing the planet with the Keck II telescope between August 5 and 6 (2014). One storm stood out from the rest: shining in 2.2 μm , a wavelength sensitive to clouds in the tropopause (just below the stratosphere), it made up 30% of all of the light reflected from Uranus. Another storm, visible at 1.6 μm , could even be seen by amateur astronomers ...

Based on the colors and structure of the storm spotted by amateurs, professional astronomers believe it could hint at a vortex deeper in the atmosphere-similar to phenomena spotted on Jupiter, such as the Great Red Spot.

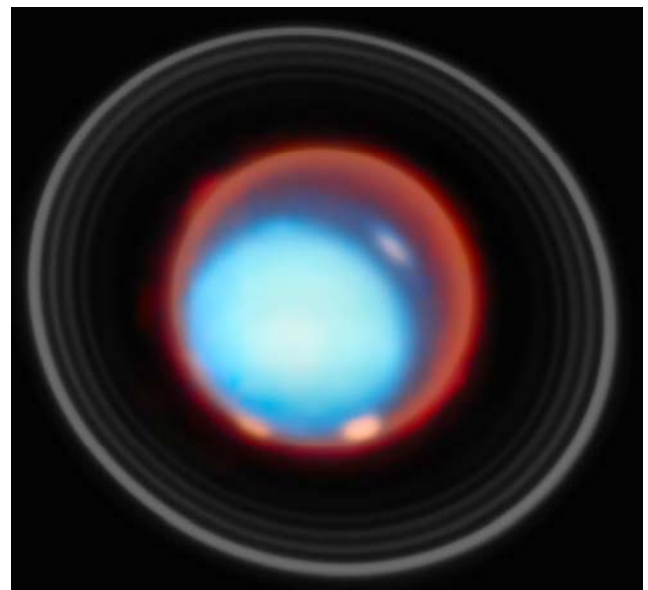


Fig. 21. "Webb has delivered the first detailed 3D view of Uranus's upper atmosphere, uncovering glowing auroras, heat peaks thousands of kilometers high, and the powerful influence of its tilted magnetic field. The data also confirm that the planet has been cooling for decades. Credit: ESA/Webb, NASA, CSA, STScI, P. Tiranti, H. Melin, M. Zamani (ESA/Webb)" Figure and captions after European Space Agency (ESA) (2026).

Follow-up observations with the Keck II telescope revealed that the storm was still raging, although it had changed its shape, and possibly its intensity.

Also contributing to the effort was the HST, which examined the entire planet of Uranus October 14 in several wavelengths. The observations revealed storms spanning several altitudes, over a distance of about 9,000 km ...”

A very recent finding is reported by Tiranti et al. (2026), announced by European Space Agency (ESA) (2026). We show Figs 21 and 22, borrowed after European Space Agency (ESA) (2026).

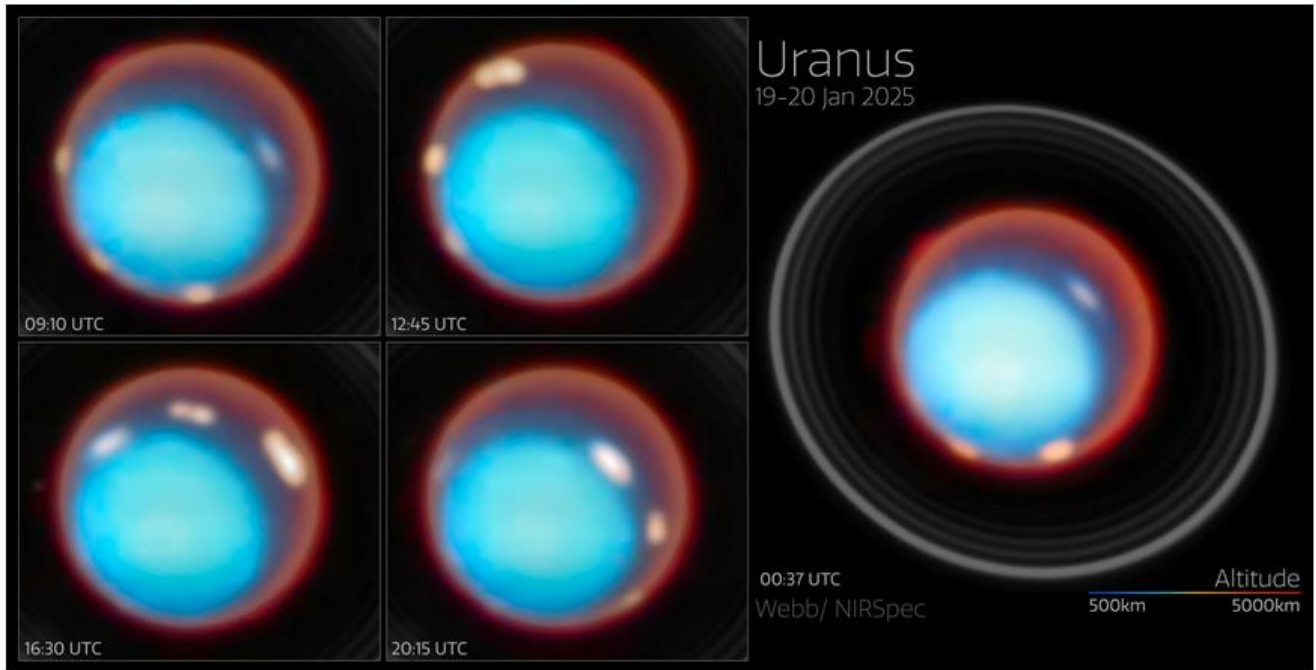


Fig. 22. “Two bright auroral bands were detected near Uranus’s magnetic poles, together with reduced emission and ion density in part of the region between the two bands (a feature likely linked to transitions in magnetic field lines). Credit: ESA/Webb, NASA, CSA, STScI, P. Tiranti, H. Melin, M. Zamani (ESA/Webb).” Figure and captions after European Space Agency (ESA) (2026).

Neptune

Similar inferences are provided by Neptune, which is concerned with two anomalous dark spots, one observed in the southern hemisphere (SH), and another one in the northern hemisphere (NH). Let us first refer to the SH dark spot.

“Voyager 2 in 1989 - and HST in 1994-saw similar features. But this dark spot, or vortex, is the first seen on Neptune in the 21th century” (Byrd, 2016t).

Reporting Weaver et al. (2016), in July 2015, both amateur astronomers and the largest telescopes reported new spots that scientists suspected were bright companions to some unseen, dark vortex. In 1989 *Voyager 2* flew by Neptune, and astronomers were surprised to observe a dark hole at southern latitudes in the cyan-colored atmosphere (see Figs 23 and 24) that later disappeared. However, *HST* observed in 1994, and anew on May 16, 2016, a new northern dark spot of comparable size (see Figs 25 and 26).

The dark vortices on Neptune are due to high-pressure systems. They usually occur with bright “companion clouds” that are also now observed. The occurrence of bright clouds is interpreted by means of a flow of ambient air when it is perturbed (by endogenous heat?) and diverted upward over the dark vortex. This phenomenon likely makes gases freeze into CH₄ ice crystals.

“Dark vortices coast through the atmosphere like huge, lens-shaped gaseous mountains ... And the companion clouds are similar to so-called orographic clouds that appear as pancake-shaped features lingering over mountains on Earth.”

New bright clouds were observed again on Neptune beginning in July 2015. Observations were carried out by amateur astronomers and by the *W. M. Keck Observatory* in Hawai’i. Astronomers guessed that these clouds might be bright companion clouds accompanying an unseen dark vortex. In any case, Neptune’s dark vortices typically can be observed only at blue wavelengths. Only *HST* has the sufficient high resolution needed for their observation on this distant planet.

The *Outer Planet Atmospheres Legacy (OPAL)* program is a long-term *HST* project that annually captures global maps of the outer planets. In September 2015, *OPAL* detected a dark spot close to the location of the bright clouds. The bright clouds had been monitored from the ground. When observing the vortex a second time, the new *HST* images confirmed that *OPAL* really detected a long-lived morphological feature.

In any case, the Neptunian dark vortices displayed a surprising diversity over the years, according to size, shape, and stability. They move in latitude, sometimes speeding up or slowing down, with no apparent regularity.

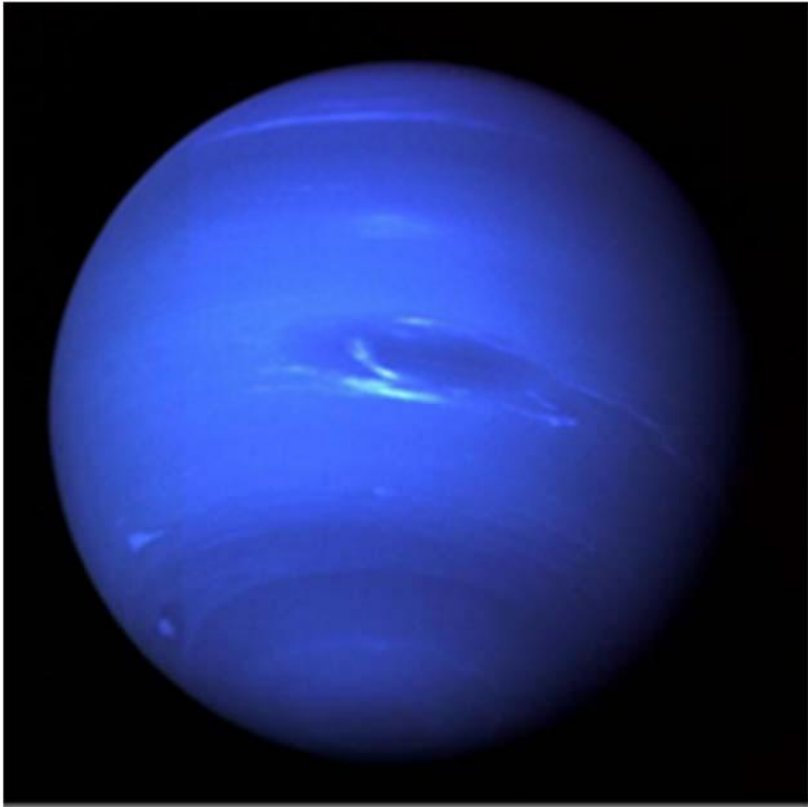


Fig. 23. "Neptune as observed by NASA's Voyager 2 spacecraft during its flyby in 1989. Credit: NASA/JPL." Figure and captions after Lewin (2015). NASA copyright free policy.

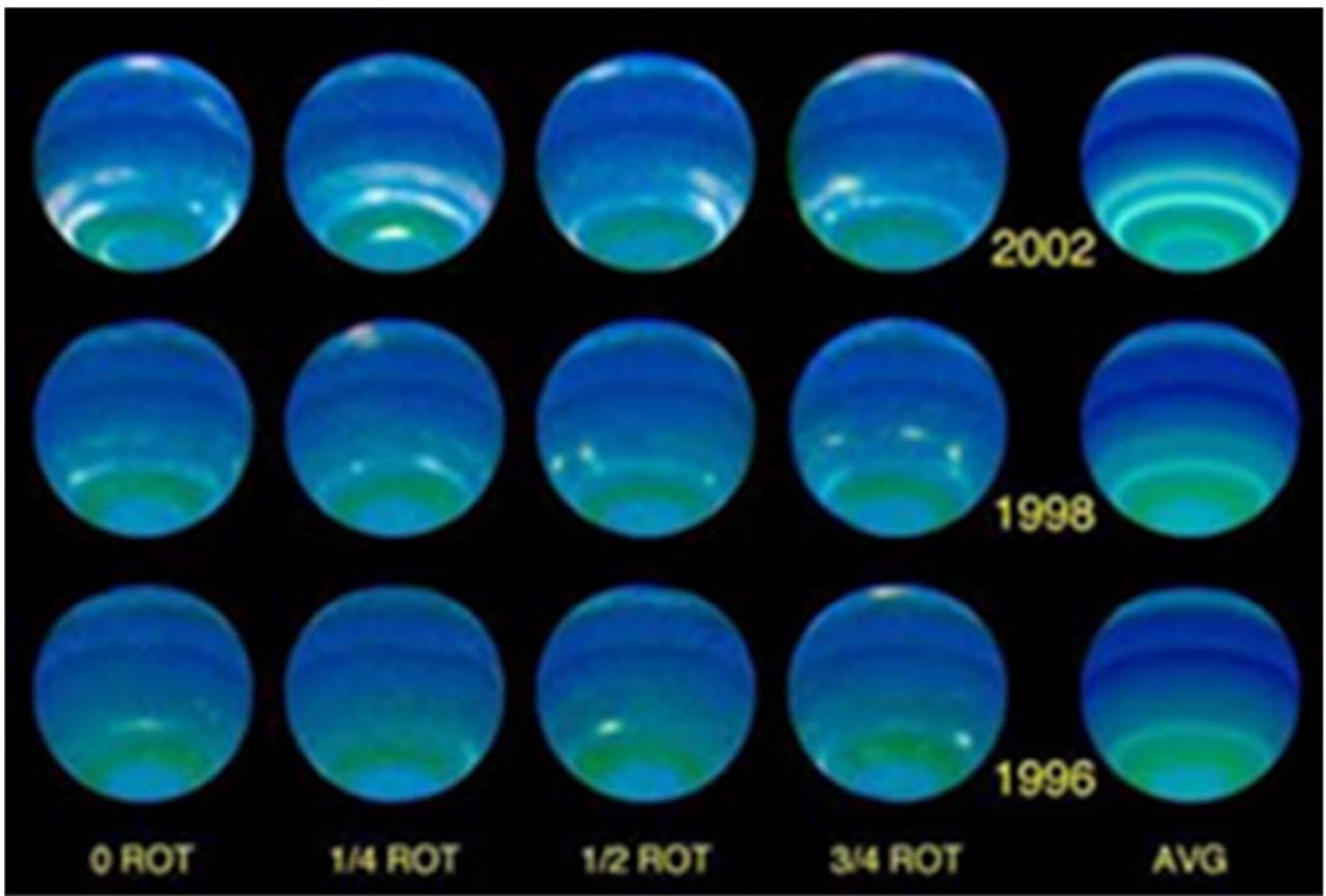


Fig. 24. "Several faces of the planet Neptune at each epoch: 1996, 1998 and 2002. Credit: NASA, L. Stromovsky and P. Fry (Univ. of Wisconsin, Madison)." Figure and captions after Anonymous (2003b). NASA copyright free policy.

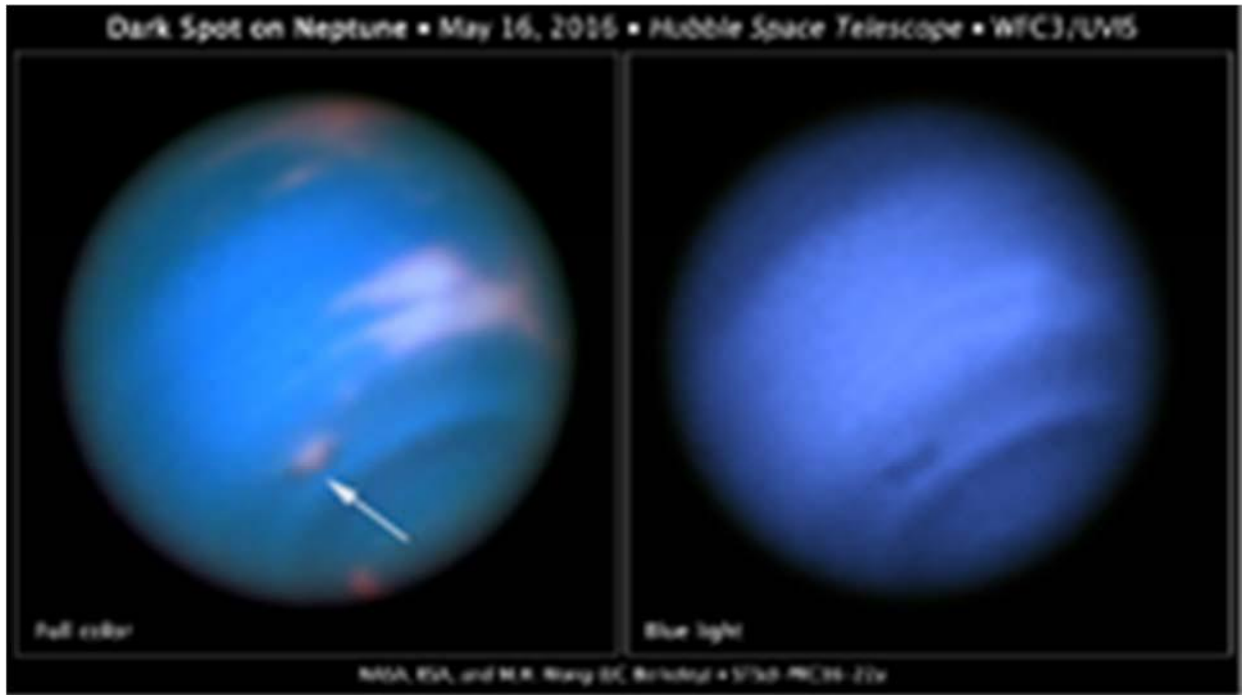


Fig. 25. “This new HST image confirms the presence of a dark vortex in the atmosphere of Neptune. The full visible-light image at left shows that the dark feature resides near and below a patch of bright clouds in the planet’s Southern Hemisphere (SH). The dark spot measures roughly 4,800 km across. Other high-altitude clouds can be seen at the planet’s equatorial region and polar regions. The image at right shows that Neptune’s dark vortices are typically best seen at blue wavelengths. Only HST has the high resolution required for identifying such weather features on distant Neptune. [See text.] Credit: NASA, ESA, and M.H. Wong and J. Tollefson (UC Berkeley).” Figure and captions after Weaver et al. (2016b). Reproduced according to NASA copyright free policy.

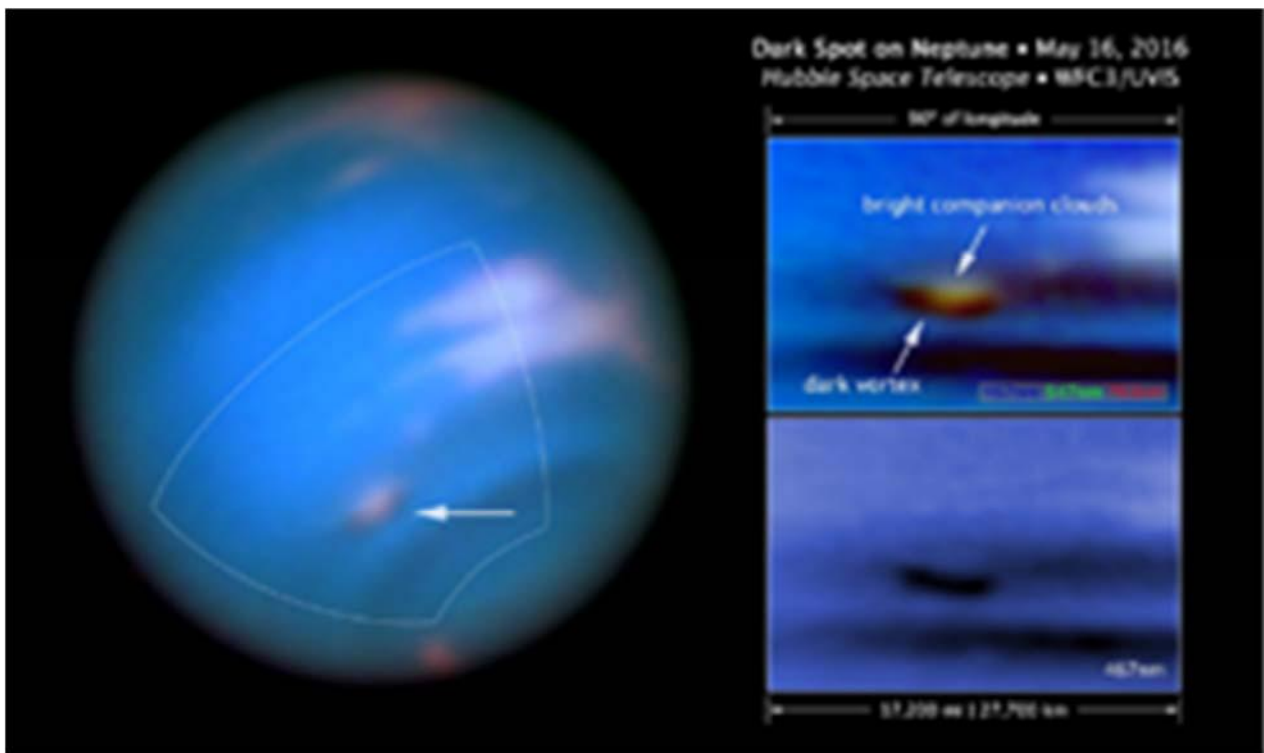


Fig. 26. “The full visible-light image at left shows that the dark feature resides near and below a patch of bright clouds in the planet’s Southern Hemisphere (SH) ...Other high-altitude clouds can be seen at the planet’s equatorial region and polar regions. The full-color image at top right is a close-up of the complex feature. Pancake-shaped clouds above the spot form when ambient air is perturbed and diverted upward over the vortex. The vortex is a high-pressure system. The image at bottom right shows that the vortex is best seen at blue wavelengths... [See text.] Credit: NASA, ESA, and M.H. Wong and J. Tollefson (UC Berkeley).” Figure and captions after Weaver et al. (2016b). NASA copyright free policy.

Compared to similar anticyclones observed on Jupiter, they evolve on much shorter timescales. In fact, the large Jovian storms evolved over decades. Maybe, the different space gradient of the solar wind flow plays a role, related to the different heliocentric distance of Jupiter and Neptune.

However, this guess should be suitably tested. In addition, the different unknown internal composition of every large planet can play a crucial role in the response of the internal TD dynamo.

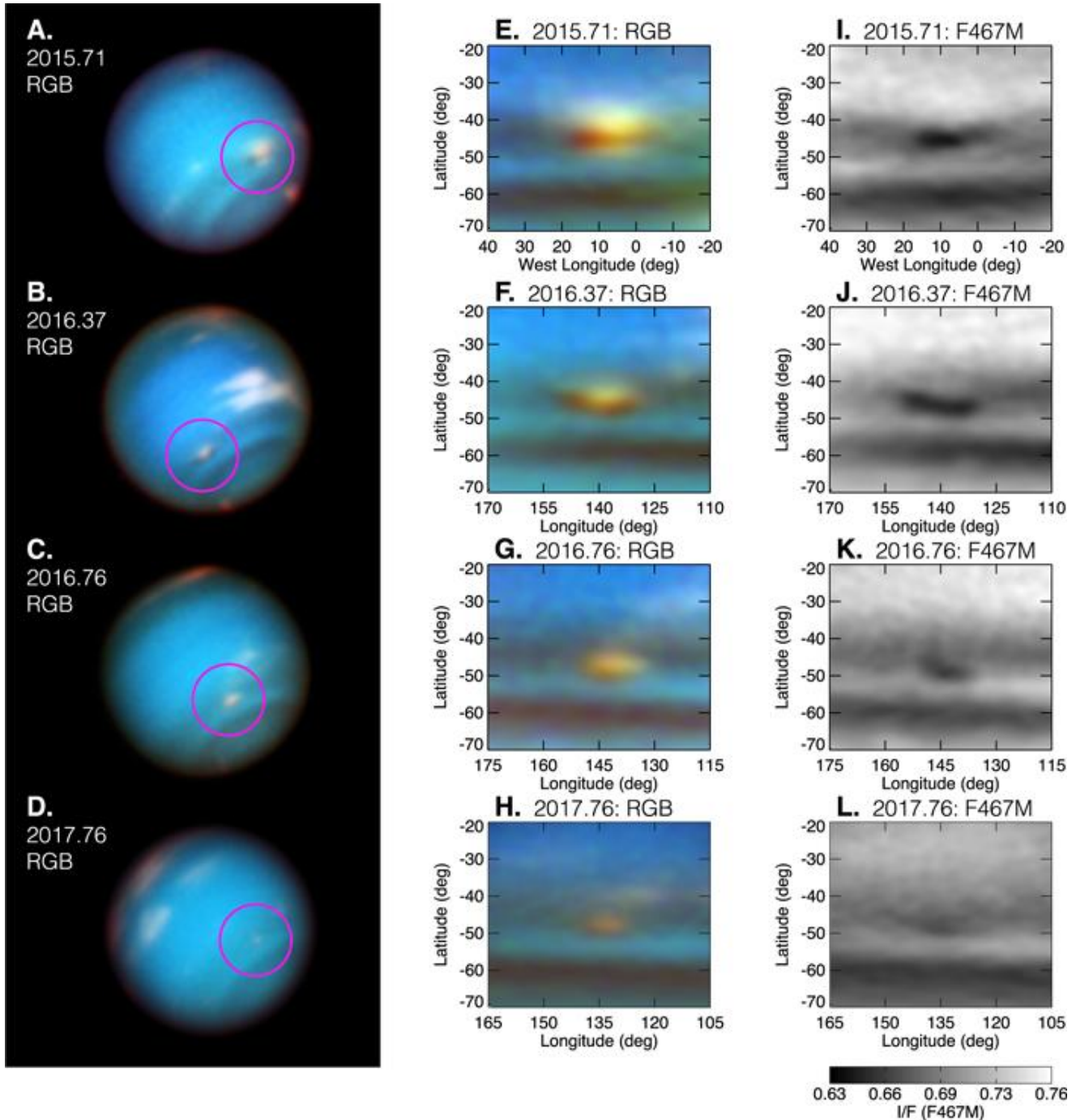


Fig. 27. “Gallery of SDS-2015 images and maps. [A, B, C, D] red/green/blue (RGB) composite images at four epochs ..., coadded from multiple frames ... [E, F, G, H] RGB cylindrical maps of the dark vortex at each epoch. [I, J, K, L] Blue (F467M) filter images show the dark vortex itself most clearly. The brightness scale is the same for all epochs. The F763M data (red channel in color maps) span I/F 0.08-0.35 on a square root stretch. The F547M data (green channel in color maps) span I/F 0.48-0.60 on a linear stretch. The F467M data (blue channel in color maps, greyscale in panels I-L) span I/F 0.63-0.76 on a linear stretch (see color-bar).” Figure and captions after Wong et al. (2018). Kind permission granted through © AAS and authors.

A more extensive analysis was carried out by Wong et al. (2018) who show Fig. 27 and summarize as follows their

inference. Note that I/F , or disk-center I/F , or the Minnaert albedo, is the limb-darkening corrected value related to the

contrast between the center of the dark spot and its boundary (see the original paper for definition).

“An outburst of cloud activity on Neptune in 2015 led to speculation about whether the clouds were convective in nature, a wave phenomenon, or bright companions to an unseen dark vortex (similar to the Great Dark Spot studied in detail by Voyager 2). The HST finally answered this question by discovering a new dark vortex at 45°S planetographic latitude, named SDS-2015 for ‘southern dark spot discovered in 2015’. SDS-2015 is only the fifth dark vortex ever seen on Neptune.

In this paper, we report on imaging of SDS-2015 using HST’s Wide Field Camera 3 across four epochs: 2015 September, 2016 May, 2016 October, and 2017 October. We find that the size of SDS-2015 did not exceed 20° of longitude, more than a factor of two smaller than the Voyager dark spots, but only slightly smaller than previous NH dark spots.

A slow (1.7 – 2.5° year⁻¹) poleward drift was observed for the vortex. Properties of SDS-2015 and its surroundings suggest that the meridional wind shear may be twice as strong at the deep level of the vortex as it is at the level of cloud tracked winds.

Over the 2015- 2017 period, the dark spot’s contrast weakened from about –7% to about –3%, while companion clouds shifted from offset to centered, a similar evolution to some historical dark spots. The properties and evolution of SDS-2015 highlight the diversity of Neptune’s dark spots and the need for faster cadence dark spot observations in the future.”

A very detailed image (Fig. 28) has been subsequently issued.

An anomalous “bizarre” huge storm has been observed on Neptune (Fig. 29), and this shifts the focus on anomalies in the NH. Howell (2017c) describes it as follows. *“The storm is about 9,000 km in length-about three-quarters Earth’s diameter - and is even huge compared to the size of Neptune: it spans nearly 30° in both longitude and latitude. When astronomers studied the storm between June 26-July 2, it appeared to get brighter.*

... Seeing a storm this bright at such a low latitude is extremely surprising ... Normally, this area is really quiet and we only see bright clouds in the mid-latitude bands, so to have such an enormous cloud sitting right at the equator is spectacular ...

The researchers wondered how the new storm was able to stay together across so many latitudes. Neptune the windiest planet in the Solar System has different winds at different latitudes, so the astronomers suggested the entire storm is anchored by a massive vortex ...

... The researchers also floated another theory: perhaps the system is a giant convective cloud ... Convective clouds have been spotted on other planets (such as Saturn in 2010) ... Although, if the system was a convection cloud, the researchers said they would expect the Neptune storm to have smeared out during a week of observations ...”

[Consider, however, the well know anomalous magnetosphere related to the low inclination of the rotation axis of Neptune. This implies a different response of the TD dynamo, and, in principle, also a possible difference of the

latitudinal distribution of endogenous heat exhalation. In any case, only an internal energy source can justify these huge convection patterns.]

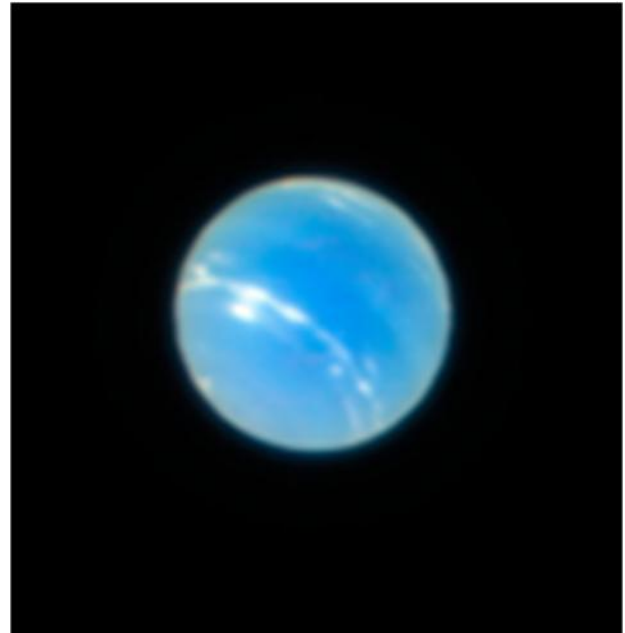


Fig. 28. “ESO Photo release eso1824. ESO’s Very Large Telescope (VLT) has achieved first light with a new adaptive optics mode called laser tomography - and has captured remarkably sharp test images of the planet Neptune, star clusters and other objects. The pioneering MUSE instrument in Narrow-Field Mode, working with the GALACSI adaptive optics module, can now use this new technique to correct for turbulence at different altitudes in the atmosphere. It is now possible to capture images from the ground at visible wavelengths that are sharper than those from the NASA/ESA HST.” Figure after Bartels (2018a), captions after Anonymous (2018h). ESO copyright free policy, granted through CC BY-04 license.

A significant witness of the anomalous storms on Neptune during MiniMax was given by Simon et al. (2019). Wall (2019g) while announcing this result claims that *“for the first time ever, astronomers have witnessed the birth of one of Neptune’s enormous ‘Great Dark Spot’ storms. Astronomers were studying HST images of a relatively small Neptune maelström that formed in 2015 when they noticed bright white clouds forming in a different locale on the ice giant. By 2018, a dark storm as wide as Earth had boiled up in that region ...”* (Fig. 30)

Simon et al. (2019) explains, in the plain language summary, that *“in 2018, a new Great Dark Spot was discovered on Neptune, nearly identical in size and shape as the one observed by Voyager 2 in 1989. The spot is in the NH and is drifting westward more slowly than the surrounding winds. Dark spots can only be identified in visible light, because of their strong absorption at blue wavelengths, and only the HST has sufficient spatial resolution to detect them.*

A search of global HST Neptune images from 2015 through 2017 reveals smaller clouds present at locations consistent with this storm, meaning it may take many years to form. If so, it may originate from much deeper in the atmosphere than previously thought ...”

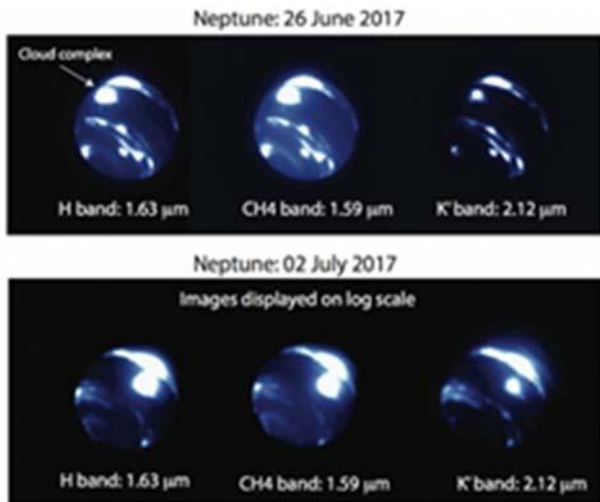


Fig. 29. “Researchers observing Neptune with the Keck Observatory spotted a massive, bright cloud complex crossing the planet’s equator. It brightened considerably between June 26 and July 2. Credit: N. Molter/I. De Pater, UC Berkeley/C. Alvarez, W. M. Keck Observatory.” Figure and captions after Howell (2017c). NASA copyright free policy.

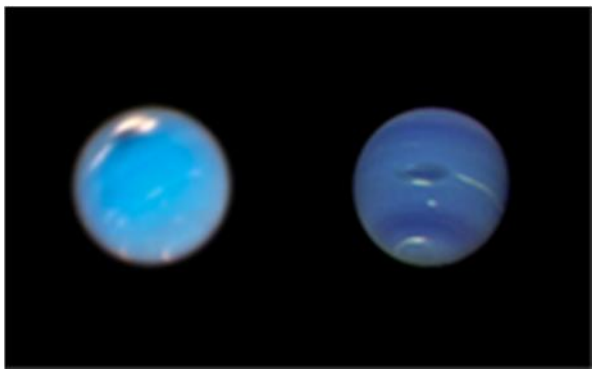


Fig. 30. “This composite picture shows images of storms on Neptune from the HST (left) and the Voyager 2 spacecraft (right). The HST image of Neptune, taken in September and November 2018, shows a new dark storm (top center). In the Voyager image, a storm known as the Great Dark Spot is seen at the center. It is $\sim 13,000 \times 6,600$ km in size. The white clouds seen hovering in the vicinity of the storms are higher in altitude than the dark material. (Image: © NASA/ESA/GSFC/JPL).” Figure and captions after Wall (2019g). NASA copyright free policy.

According to the interpretation that is here proposed, an anomalous B_{int} determines intense induced currents inside Neptune (as per Fig. 1). The increased endogenous Joule heat generates unusual convection patterns. The envisaged origin, which seems “much deeper in the atmosphere than previously thought”, is consistent with a trigger originated by the release of an increased endogenous energy, due to an intensified TD dynamo.

As far as Neptune is concerned, its images are available that were provided either by Voyager 2 (Fig. 23) or by the HST (Sromovsky et al., 2003; Fig. 24).

Sromovsky et al. (2003) comment that “HST observations in August 2002 show that Neptune’s disk-averaged reflectivity increased significantly since 1996, by

$3.2 \pm 0.3\%$ at 467 nm, $5.6 \pm 0.6\%$ at 673 nm, and $40 \pm 4\%$ in the 850 – 1000 nm band, which mainly results from dramatic brightness increases in restricted latitude bands. When 467 nm HST observations from 1994 to 2002 are added to the 472 nm ground-based results ... the combined disk-averaged variation from 1972 to 2002 is consistent with a simple seasonal model having a hemispheric response delay relative to solar forcing of ~ 30 years ($\sim 73\%$ of a full season).” [Consider, as mentioned above, that the seasonal modulation is associated to the internal TD dynamo, not to solar radiation.]

The dark spot on the NH is now observed also by ground-based telescopes (Irwin et al., 2023; illustrated by European Southern Observatory, 2023).

A recent image of Uranus and Neptune storms is shown in Fig. 31. Bartels (2019a) also comments that “the telescope regularly checks in on the two outer planets to see what’s happening in their atmospheres, and last autumn, HST captured incredible images of clouds on both worlds.

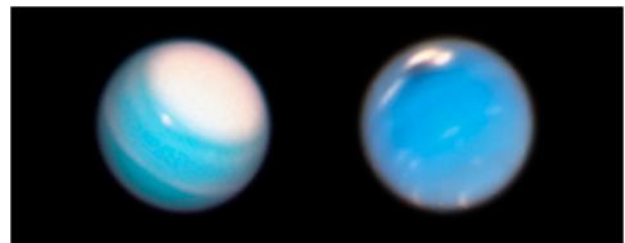


Fig. 31. “New HST observations of Uranus and Neptune track the planets’ atmospheres. (Image: © NASA, ESA, A. Simon (NASA GSFC), and M. H. Wong and A. Hsu (University of California, Berkeley).” Figure and captions after Bartels (2019a). NASA copyright free policy.

Uranus is currently deep into its summer season, and that shows in the giant, white cloud covering the planet’s North Pole, which currently points toward the Sun. As scientists have watched the Uranus summer progress - a season on this distant giant world lasts 21 Earth years - they have seen this massive cloud grow even bigger. The large polar cap is accompanied by a smaller, bright cloud of CH₄ ice.

On Neptune, where seasons last for 41 Earth years, it’s winter in the NH. That hemisphere is currently sporting a massive dark storm that stretches about 11,000 km across.

Scientists aren’t sure what phenomenon creates Neptune’s dark storms, although the tempests seem to pop up about twice a decade and disperse within about two years. Researchers suspect that the storms creep upward through the planet’s atmosphere, lifting the ingredients of deeper layers of the atmosphere to the top.

Near the dark storm currently on Neptune, HST spotted another atmospheric feature: sparkling white ‘companion clouds’, which scientists have spotted around dark storms in the past. Astronomers suspect that these bright clouds are full of CH₄ ice that’s been rapidly pushed upward and frozen.”

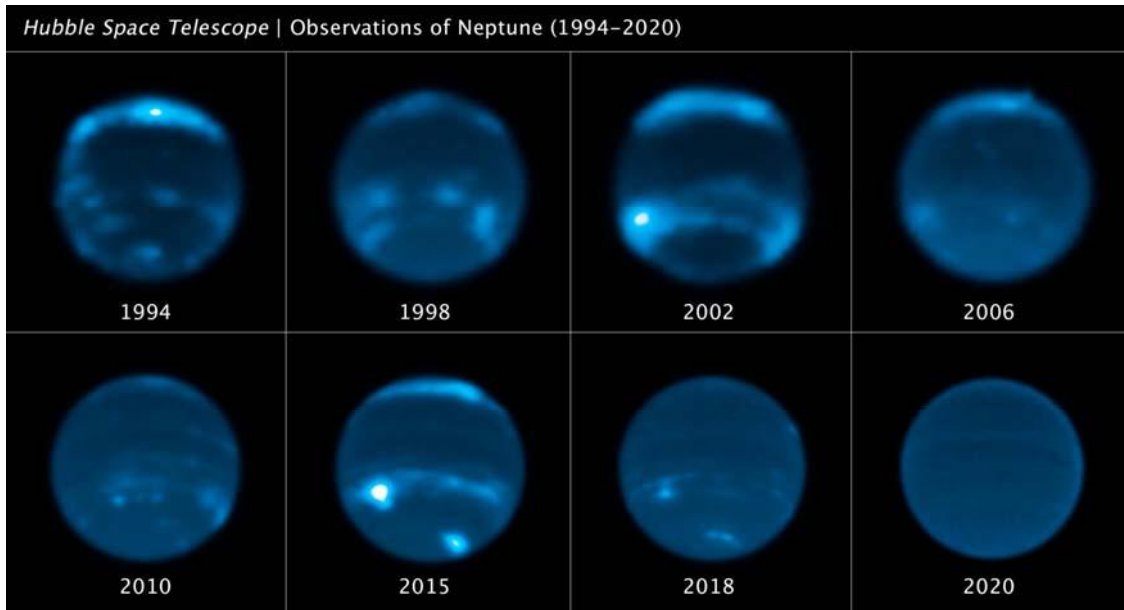


Fig. 32. “This sequence of HST images chronicles the waxing and waning of the amount of cloud cover on Neptune. This long set of observations shows that the number of clouds grows increasingly following a peak in the solar cycle - where the Sun’s level of activity rhythmically rises and falls over an 11 – year period. The chemical changes are caused by photochemistry, which happens high in Neptune’s upper atmosphere and takes time to form clouds. In 1989, NASA’s Voyager 2 spacecraft provided the first close-up images of linear, bright clouds, reminiscent of cirrus clouds on Earth, seen high in Neptune’s atmosphere. They form above most of the CH₄ in Neptune’s atmosphere and reflect all colors of sunlight, which makes them white. Hubble picks up where the brief Voyager flyby left off by continually keeping an eye on the planet yearly. Credit: NASA, ESA, Erandi Chavez (UC Berkeley), Imke de Pater (UC Berkeley).” Reproduced with NASA and ESA copyright free policy.

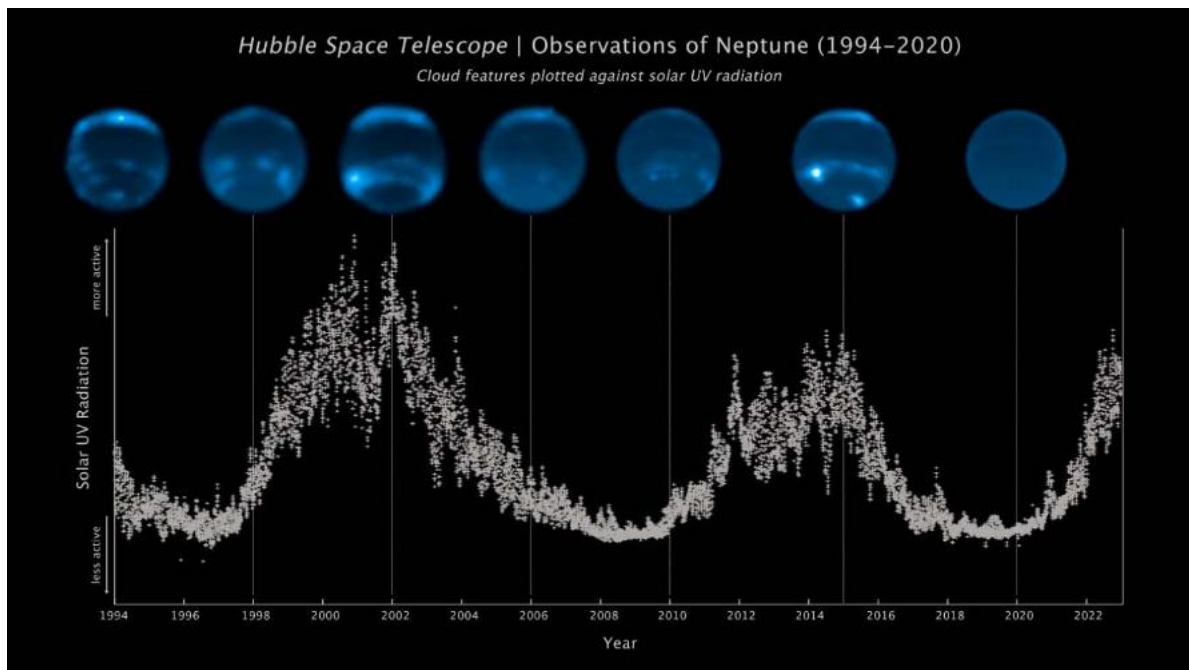


Fig. 33. “This sequence of HST images chronicles the waxing and waning of the amount of cloud cover on Neptune. This nearly-30 – year-long set of observations shows that the number of clouds grows increasingly following a peak in the solar cycle - where the Sun’s level of activity rhythmically rises and falls over an 11 – year period. The Sun’s level of UV radiation is plotted in the vertical axis. The 11 – year cycle is plotted along the bottom from 1994 to 2022. The Hubble observations along the top, clearly show a correlation between cloud abundance and solar peak of activity. The chemical changes are caused by photochemistry, which happens high in Neptune’s upper atmosphere and takes time to form clouds. Credit: NASA, ESA, LASP, Erandi Chavez (UC Berkeley), Imke de Pater (UC Berkeley).” Reproduced with NASA and ESA copyright free policy.

We stress, however, that the seasonal cycle is important on the Earth due to the modulation of solar e.m. radiation, while the solar wind is just an added, although less relevant,

trigger. In contrast, as already stressed, on the outer planets the solar e.m. radiation is negligible. Hence, also the seasonal modulation is definitely less important than on the

Earth. Hence, every seasonal change is perturbed by the erratic disturbances originated by the solar wind induction that controls Neptune's *TD* dynamo, and - through the sea-urchin spike mechanism - also Neptune's reflectivity, etc.

In fact, this is confirmed by a recent study by Chavez et al. (2023), illustrated by *Space Telescope Science Institute* (2023). They show Figs 32 and 33 that apply to dark spots observed either in the *SH* or in the *NH*.

However, also the polar polygonal vortex – well known in the case of Saturn (see Figs 10 and 12) - was observed on Neptune South Pole. According to Wall (2011), “*The Neptune squall was similar to a spinning storm discovered a few years earlier at Saturn’s South Pole, which even had a well-developed eye, just like an Earth hurricane. But, the Saturn polar vortex was much bigger than any hurricane found on Earth. Its eye alone measured ~ 4,000 km in diameter.*” See Fig. 34. The typical size of the eye of a terrestrial hurricane is just a few km.

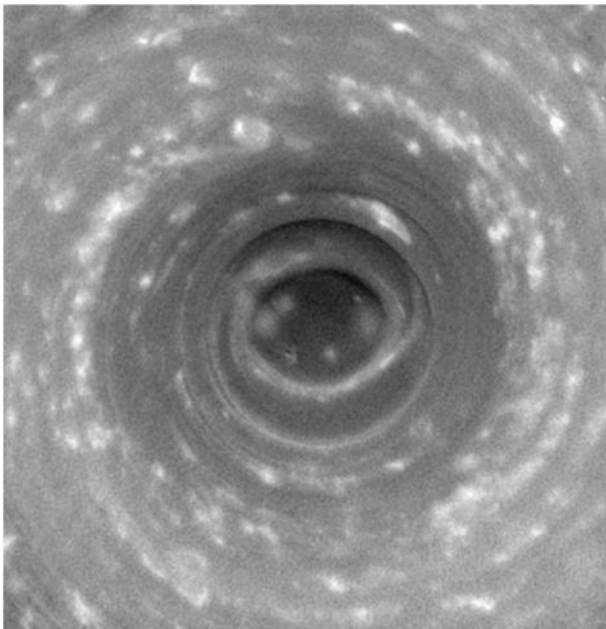


Fig. 34. “Cassini stares deep into the swirling hurricane-like vortex at Saturn’s South Pole, where the vertical structure of the clouds is highlighted by shadows. Such a storm, with a well-developed eye ringed by towering clouds, is a phenomenon never before seen on another planet. Credit: NASA/JPL/SSI.” Figure and captions after Wall (2011). NASA copyright free policy.

Pluto/Charon

Concerning the seasonal variation, a different comment is deserved for Pluto, and its Hadean seasonal cycle. Pluto’s orbit is very eccentric (aphelion ~ 120 AU, perihelion ~ 34 AU). Thus, during the Pluto’s year, which is ~ 248 Earth’s years long, the interaction with the solar wind changes by a substantial amount.

Hence, during some season a large endogenous heat is produced by the internal *TD* dynamo. Thus, huge oceans of liquid nitrogen melt, are crossed by large icebergs of floating water-ice. In contrast, during other seasons, the nitrogen oceans freeze, and the images show a large frozen

swamp with huge water-ice icebergs locked in it, like “floating hills”.

Therefore, the Pluto-Charon binary system with the 4 rocky mini-satellites, is an incredibly efficient natural laboratory to test the *TD* mechanism which is active inside planets, their satellites and the entire satellite systems of the Solar System.

Refer to mentions in Gregori and Leybourne (2026b) and, mostly, refer to the extensive discussion and several impressive figures in Gregori (2016a).

Conclusion

The stormy features of the outer planets, observed by space probes, or by ground-based telescopes or by orbiting telescopes, can be used like probes to monitor the behavior of the solar wind flowing at large heliocentric distances. This reminds us about the possible use of comets for this same purpose, although its feasibility must be ascertained. In fact, a comet is composed of plasma, which experiences convection. Hence, it develops a **B** through the Cowling dynamo (see Gregori et al., 2026d). Therefore, every comet develops a temporary magnetosphere (called “cometosphere”). The observed morphological features of comets can be interpreted (perhaps) as evidence of changes of their respective cometospheres. That is, if this guess is correct, comets are useful natural probes suited to monitor the solar wind flow throughout the space domain of the entire Solar System. This topic requires a long discussion that cannot be here anticipated.

As a final summary concerning the impact of MiniMax on the Earth, also seismic and volcanic activity seems to have largely increased during these same years, and - according to the Casey (2011) analysis - at present the very long trend of the Sun seems to be towards some new period analogous to the Maunder minimum. Therefore, it is crucial to understand the frequency that best affects the parameter that characterizes the role of the “internal” way compared to the “external” way, i.e.,

$$p_{int}(t) = \frac{w_{int}(t)}{w_{int}(t) + w_{ext}(t)} \quad (1)$$

defined in Gregori et al. (2026c). In this way, maybe, it is possible to issue some reasonable forecast for a better management of the consequent “global” climate change.

Zhou et al. (2007) used the sunspot time series derived by Solanki et al. (2004) from dendrochronological series and spanning the last 11,400 years before 1895. They searched for periodic and quasi-periodic fluctuations of secular solar activity on a thousand-year time scale (by means of Maximum Entropy Method and wavelet transform). Their results appear suggestive of possible quasi-periodic signals with periods close to ~ 1000 years and > 2000 years, and fluctuations with ~ 7000 years period.

Note, however, that the *TD* dynamo of every different planetary object is affected by an e.m. signal inside a given frequency band - that, in the case of the Earth, is controlled by an elongated duration of the solar minimum. On the other hand, the e.m. signals of comparatively either higher or lower frequency are not effective in the control of the *TD*

dynamo. Therefore, the millennial-scale variation of solar activity is effective in terms of climate only as far as it changes the intensity of the e.m. signal inside the given frequency band that is critical for *TD* dynamo operation inside every given planetary object.

A basic warning, however, is that no physical reason requires that these phenomena ought to be periodic. Human minds like “simplicity”, and a Fourier analysis is one way to satisfy the innate search for “simplicity”. The “myth” for the ability to “forecast” phenomena is typical of every society, which is either primitive or even highly technological and “scientific”.

However, the arrow of time always runs only in one direction. Everything evolves, everything is ageing. Hence, nothing can be strictly periodical. Therefore, we should search for trends and for multivariate relations between sets of different monitored quantities or parameters. That is, we must monitor the evolution of the natural system, much like we monitor the elapsing of time upon observing phenomena. This is the same gnoseologic definition of our perception of time (see, e.g., Gregori et al., 2022, 2022a, 2022b, 2022c, 2022d, 2022e, 2023, 2025w and references therein).

In contrast, “cycles” are a trickery originated by the intrinsic “simplicity” of the Fourier algorithm, while natural phenomena display trends, not cycles. “Cyclicality” only derives from some tool that is apparently suited to give an approximate description of the trend of phenomena.

As mentioned above, according to the rationale of the present study, the duration of the solar cycle ought (perhaps) to be likened to some kind of physical index related to the variation of the long-period spectrum of the solar e.m. signal, which affects the *TD* dynamo (mainly through the $\sim 22/6 = 3.666$ years period; or, maybe, also through the $\sim 40 - 45$ years period, or others?)

Summarizing, also these impressive “hurricanes” of the large outer planets, and the curious morphological features of the Pluto/Charon binary system, definitely seem to be an indirect, although clear support in favor of the *TD* dynamo mechanism extensively discussed in Gregori (2002) and Gregori and Leybourne (2021), which is a key driver for air-earth currents.

Acknowledgement

We want to acknowledge all co-workers that, during decades, in different ways and at different times, contributed to the exploitation of the analyses mentioned in the present study. We would also like to thank all for the warm encouragement we had from several outstanding scientists.

Funding Information

G. P. Gregori is retired since 2005. B. A. Leybourne is a semi-retired self-funded independent researcher.

Author's Contributions

This study derived from a long-lasting cooperation by both authors. The backbone draft was prepared by the first

author, although a large number of ideas resulted from the emergence of long-lasting discussions.

Ethics

This article is original and contains unpublished material. Authors declare that there are no ethical issues and no conflict of interest that may arise after the publication of this manuscript.

References

- Anonymous*, 2003b. Brighter Neptune suggests a planetary change of seasons, Space Telescope Science Institute, release, May 15, 2003
- Anonymous*, 2012k. Infrared hotspots in a monster Saturn storm, JPL/Caltech/Cassini/Resources, issued October 25, 2012
- Anonymous*, 2012l. Cassini: 15 years of exploration, JPL/Caltech/Cassini/Resources, issued October 30, 2012
- Anonymous*, 2014s. Solar system exploration. Planets. Uranus: gallery. NASA release, retrieved December 5, 2014
- Anonymous*, 2018f. Amazing Saturn photos from NASA's Cassini orbiter, Space.com, issued April 25, 2018
- Anonymous*, 2018h. Supersharper images from new VLT Adaptive Optics, ESO news, issued 18 July 2018
- Badman, S.T., P. Riley, S.I. Jones, T.K. Kim, R.C. Allen, C.N. Arge, S.D. Bale, C.J. Henney, J.C. Kasper, P. Mostafavi, N.V. Pogorelov, N.E. Raouafi, M.L. Stevens, J.L. Verniero, 2023. Prediction and verification of Parker Solar Probe solar wind sources at 13.3 R_{\odot} , Journal of Geophysical Research, Swolar Physics, 128 (4): e2023JA031359; DOI:10.1029/2023JA031359
- Baldwin, M.P., L.J. Gray, T.J. Dunkerton, K. Hamilton, P.H. Haynes, W.J. Randel, J.R. Holton, M.J. Alexander, I. Hirota, T. Horinouchi, D.B.A. Jones, J.S. Kinnery, C. Marquardt, K. Sato, and M. Takahashi, 2001. The quasi-biennial oscillation, Reviews of Geophysics, 39 (2): 179–229; DOI:10.1029/1999RG000073
- Bale, S.D., J.F. Drake, M.D. McManus, M.I. Desai, S.T. Badman, D.E. Larson, M. Swisdak, T.S. Horbury, N.E. Raouafi, T. Phan, M. Velli, D.J. McComas, C.M.S. Cohen, D. Mitchell, O. Panasenco and J.C. Kasper, 2023. Interchange reconnection as the source of the fast solar wind within coronal holes, Nature; DOI:10.1038/s41586-023-05955-3
- Bartels, M., 2018a. Telescope upgrade produces stunningly clear views of space, Space.com, issued Jul 18, 2018
- Bartels, M., 2019a. Hubble Telescope watches the weather on Uranus and Neptune, Space.com, issued February 08, 2019
- Bodu, R., H. Bouzigues, N. Morin, and J. P. Pffiffelmann, 1972. Sur l'existence anomalies isotopiques rencontrées dans l'uranium du Gabon, Comptes Rendus de l'Académie des Sciences, D275: 1731-1736
- Byrd, D., 2016t. A new dark spot on Neptune, EarthSky, issued June 26, 2016

- Byrd, D., 2017b. New views of Uranus' auroras and rings, EarthSky, issued April 12, 2017
- Byrd, D., 2018d. What will the sun do next?, EarthSky, Issued December 10, 2018
- Casey, J., 2011. Cold Sun, Trafford Publishing Bloomington, IN, pp: 184
- Chavez, E., I. de Pater, E. Redwing, E.M. Molter, M.T. Roman, A. Zorzi, C. Alvarez, R. Campbell, K. de Kleer, R. Hueso, M.H. Wong, E. Gates, P.D. Lynam, A.G. Davies, J. Aycock, J. McIlroy, J. Pelletier, A. Ridenour, and T. Stickel, 2023. Evolution of Neptune at near-infrared wavelengths from 1994 through 2022, Icarus; DOI:10.1016/j.icarus.2023.115667
- Choi, C.Q., 2015c. Mystery of Saturn's epic planet-encircling storms explained, Space.com, issued April 13, 2015
- Clavin, W., and M. Johnson, 2015. NASA telescopes detect Jupiter-like storm on small star, JPL News, issued December 10, 2015
- Dunn, W.R., G. Branduardi-Raymont, R.F. Elsner, M.F. Vogt, L. Lamy, P.G. Ford, A.J. Coates, G.R. Gladstone, C.M. Jackman, J.D. Nichols, I.J. Rae, A. Varsani, T. Kimura, K.C. Hansen, and J.M. Jasinski, 2016. The impact of an ICME on the Jovian X-ray aurora, Journal of Geophysical Research Space Physics, 121: 2274–2307; DOI:10.1002/2015JA021888
- European Southern Observatory, 2023. Mysterious dark spot on Neptune detected From Earth for the first time, SciTechDaily, issued August 25, 2023
- European Space Agency (ESA), 2026. Webb maps Uranus' upper atmosphere and finds a magnetic surprise, issued February 24, 2026
- Fermi, E., 1947. Elementary theory of the chain-reacting pile, Science, 105: 27-32
- Fischer, G., W.S. Kurth, D.A. Gurnett, P. Zarka, U.A. Dyudina, A.P. Ingersoll, S.P. Ewald, C.C. Porco, A. Wesley, C. Go, and M. Delcroix, 2011. A giant thunderstorm on Saturn, Nature, Letters, 475, 75–77; DOI:10.1038/nature10205
- Fletcher, L.N., G.S. Orton, P. Yanamandra-Fisher, B.M. Fisher, P.D. Parrish, and P.G.J. Irwin, 2009. Retrievals of atmospheric variables on the gas giants from ground-based mid-infrared imaging, Icarus, 200 (1): 154–175; DOI:10.1016/j.icarus.2008.11.019
- Fletcher, L.N., B.E. Hesman, P.G.J. Irwin, K.H. Baines, T.W. Momary, A. Sánchez-Lavega, F. Michael Flasar, P.L. Read, G.S. Orton, A. Simon-Miller, R.Hueso, G.L. Bjoraker, A. Mamoutkine, T. del Rio-Gaztelurrutia, J.M. Gomez, B. Buratti, R.N. Clark, P.D. Nicholson, and C. Sotin, 2011. Thermal structure and dynamics of Saturn's northern springtime disturbance, Science, 332 (6036): 1413–1417; DOI:10.1126/science.1204774
- Fletcher, L.N., B.E. Hesman, R.K. Achterberg, P.G.J. Irwin, G. Bjoraker, N. Gorius, J. Hurley, J. Sinclair, G.S. Orton, J. Legarreta, E. García-Melendo, A. Sánchez-Lavega, P.L. Read, A.A. Simon-Miller, and F.M. Flasar, 2012. The origin and evolution of Saturn's 2011–2012 stratospheric vortex, Icarus, 221: 560–586; doi:10.1016/j.icarus.2012.08.024
- Fletcher, L.N., S. Guerlet, G.S. Orton, R.G. Cosentino, T. Fouchet, P.G.J. Irwin, Liming Li, F.M. Flasar, N. Gorius, and R. Morales-Juberías, 2017. Disruption of Saturn's quasi-periodic equatorial oscillation by the great northern storm, Nature Astronomy, Letters,,1: 765–770; DOI:10.1038/s41550-017-0271-5
- Gladstone, G.R., J.H. Waite, Jr., D. Grodent, W.S. Lewis, F.J. Crary, R.F. Elsner, M.C. Weisskopf, T. Majeed, J.M. Jahn, A. Bhardwaj, J.T. Clarke, D.T. Young, M.K. Dougherty, S.A. Espinosa, and T.E. Cravens, 2002. A pulsating auroral X-ray hot spot on Jupiter, Nature, 415 (6875), 1000–1003; doi:10.1038/4151000a
- Gregori, G. P., and B. A. Leybourne, 2026e. The physics of electrical discharges – I. Small-scale phenomena - Fog - atmospheric precipitation – BLs. *New Concepts in Global Tectonics, Journal*, 14, (2): 129-152
- Gregori, G. P., B. A. Leybourne, and F. F. Bonavia, 2025u. Symmetries and polygonal patterns: a reminder, *New Concepts in Global Tectonics, Journal*, 13, (5): 711-730
- Gregori, G. P., B. A. Leybourne, and J. R. Wright, 2026d. Generalized Cowling theorem and the Cowling dynamo. *New Concepts in Global Tectonics, Journal*, 14, (1): 90-112
- Gregori, G. P., B. A. Leybourne, G. Paparo†, and M. Poscolieri, 2026a. The global Sun-Earth circuit. Present issue of *New Concepts in Global Tectonics, Journal*
- Gregori, G.P., 2002. Galaxy – Sun – Earth relations. The Origin of the Magnetic Field and of the Endogenous Energy of the Earth, with Implications for Volcanism, Geodynamics and Climate Control, and Related Items of Concern for Stars, Planets, Satellites, and Other Planetary Objects. A Discussion in a Prologue and Two Parts. *Beiträge zur Geschichte der Geophysik und Kosmischen Physik*, Band 3, Heft 3: pp. 1-471 [Available at <http://ncgtjournal.com/additional-resources.html>]
- Gregori, G.P., 2016a. The endogenous energy and the magnetic field of planetary objects: the Pluto/Charon binary system and its seasonal rejuvenation, *New Concepts in Global Tectonics, Journal*, 4, (3): 406-431.
- Gregori, G.P., and B.A. Leybourne, 2021. An unprecedented challenge for humankind survival. Energy exploitation from the atmospheric electrical circuit, *American Journal of Engineering and Applied Science*, 14 (2): 258-291; DOI:10.3844/ajeassp.2021.258.291
- Gregori, G.P., and B.A. Leybourne, 2025j. The energy supply to hurricanes. *New Concepts in Global Tectonics, Journal*, 13, (5): 731-786
- Gregori, G.P., and B.A. Leybourne, 2026b. The electrostatic Sun. Present issue of *New Concepts in Global Tectonics, Journal*
- Gregori, G.P., B.A. Leybourne, and J.R. Wright, 2026c. The solar cycle and MiniMax. Present issue of *New Concepts in Global Tectonics, Journal*
- Gregori, G.P., C.W. Monckton of Brenchley, W. Soon, R. Tattersall, A. D'Amico†, G. Zimatore, V.M. Velasco Herrera, B.A. Leybourne, and Z.A. Oziewicz †, 2022. Golden Ratio, Variational Principles, Cyclic and Wave phenomena, Quanta. In H.M. Colin Garcia, J.-deJ. Cruz

- Guzman, L.H. Kauffman, and H. Makaruk (eds), *Scientific Legacy of Professor Zbigniew Oziewicz, Selected Paper of the International Conference Applied Category Theory Graph-Operad-Logic* (August 25th to 27th, 2021), 2024 World Scientific Publishing Company; pp: 363-389; DOI:10.1142/9789811271151.0018
- Gregori, G.P., F.C. Wezel†, L.C. Gregori, B.A. Leybourne, W. Soon, and V. Straser, 2023. Archæology of the concept of “time” in the ancient Western, Eastern, and Far Eastern cultures The foundations of physics, *New Concepts in Global Tectonics, Journal*, 11 (1): 3-34
- Gregori, G.P., M.T. Hovland, B.A. Leybourne, S. Pellis, V. Straser, B.G. Gregori, G.M. Gregori, and A.R. Simonelli, 2025w. Air-earth currents and a universal “law”: filamentary and spiral structures - Repetitiveness, fractality, golden ratio, fine-structure constant, antifragility and “statistics” - The origin of life, *New Concepts in Global Tectonics, Journal*, 3, (1): 106-225
- Gregori, G.P., W. Soon, V. Straser, and B. A. Leybourne, 2022c. The foundations of physics and axiomatics. II - Algorithms and equations, and a comparison with Einstein’s theory of relativity. *New Concepts in Global Tectonics, Journal*, 10(3): 236-262
- Gregori, G.P., W. Soon, V. Straser, and B.A. Leybourne, 2022a. Golden ratio, fractals, and the arrow of time. Irreversibility vs. reversibility - Space, time, antitime - The foundations of physics. *New Concepts in Global Tectonics, Journal*, 10 (3): 158-201
- Gregori, G.P., W. Soon, V. Straser, and B.A. Leybourne, 2022b. The foundations of physics and axiomatics. I - Axioms. *New Concepts in Global Tectonics, Journal*, 10 (3): 202-235
- Gregori, G.P., W. Soon, V. Straser, and B.A. Leybourne, 2022d. The foundations of physics and axiomatics. III - Superluminal phenomena, mechanisms, matter-antimatter, cosmological implications. *New Concepts in Global Tectonics, Journal*, 10 (3): 263-283
- Gregori, G.P., W. Soon, V. Straser, and B.A. Leybourne, 2022e. The foundations of physics and axiomatics. IV - The geometrical representation of symmetries - Parity, emp, and charge (PEC) “meta-multiverse”. *New Concepts in Global Tectonics, Journal*, 10 (3): 284-299
- Herndon, J.M., 1980. The chemical composition of the interior shells of the Earth, *Proceedings of the Royal Society of London*, A372: 149-154
- Herndon, J.M., 1992. Nuclear fission reactors as energy sources for the giant outer planets, *Naturwissenschaften*, 79: 7-14
- Herndon, J.M., 1993. Feasibility of a nuclear fission reactor at the center of the Earth as the energy source for the geomagnetic field, *Journal of Geomagnetism and Geoelectricity*, 45: 423-437
- Herndon, J.M., 1994. Planetary and protostellar nuclear fission: Implications for planetary change, stellar ignition and dark matter, *Proceedings of the Royal Society of London*, A455: 453-461
- Herndon, J.M., 1996. Sub-structure of the inner core of the Earth, *Proceedings of the National Academy of Sciences*, 93, 646-648
- Herndon, J.M., 2003. Nuclear georeactor origin of oceanic basalt, $^3\text{He}/^4\text{He}$, evidence, and implications, *Proceedings of the National Academy of Sciences*, 100 (6): 3047-3050
- Herndon, J.M., 2008. *Maverick's Earth and Universe*, ISBN 978-971-4251-4132-4255, Trafford Publishing, Vancouver, pp: 276
- Herndon, J.M., 2010. Inseparability of science history and discovery, *History of Geophysics and Space Science*, 1: 25-41
- Herndon, J.M., 2010a. Impact of recent discoveries on petroleum and natural gas exploration: emphasis on India, *Current Science*, 98 (6): 772-779
- Herndon, J.M., 2014. Terracentric nuclear fission georeactor: background, basis, feasibility, structure, evidence and geophysical implications, *Current Science*, 106 (4): 528-541
- Hilton, D.R., and D. Porcelli, 2003. Noble gases as mantle tracers. In *The mantle and core*, Carlson, R.W., (ed.), Elsevier-Pergamon, Oxford, pp: 277-318. [Volume 2 of *Treatise on geochemistry*, Holland, H.D., and K.K. Turekian, (eds) (2nd ed., 2013, 9144 pp.)]
- Hilton, D.R., K. Grönvold, C.G. Macpherson, and P.R. Castillo, 1999. Extreme $^3\text{He}/^4\text{He}$ ratios in northwest Iceland: constraining the common component in mantle plumes, *Earth and Planetary Science Letters*, 173: 53-60
- Hollenbach, D.F., and J.M. Herndon, 2001. Deep-earth reactor: nuclear fission, helium, and the geomagnetic field, *Proceedings of the National Academy of Sciences*, 98: 11085-11090
- Howell, E., 2014e. Extreme storms on Uranus puzzle astronomers, *Space.com*, issued November 13, 2014
- Howell, E., 2017c. Surprise! New Neptune storm appears in a bizarre location, *Space.com*, issued August 3, 2017
- Imster, E., 2016f. Solar storms ignite Jupiter’s auroras, *Science Wire*, also *EarthSky*, issued Mar 24, 2016
- Irwin, P.G.J., J. Dobinson, A. James, M.H. Wong, L.N. Fletcher, M.T. Roman, N.A. Teanby, D. Toledo, G.S. Orton, S. Pérez-Hoyos, A. Sánchez-Lavega, L. Sromovsky, A.A. Simon, R. Morales-Juberías, I. de Pater, and S.L. Cook, 2023. Spectral determination of the colour and vertical structure of dark spots in Neptune’s atmosphere, *Nature Astronomy*; DOI:10.1038/s41550-023-02047-0
- Kuroda, P.K., 1956. On the nuclear physical stability of the uranium minerals, *Journal of Chemical Physics*, 25: 781-782
- Lamoreaux, S.K., and J.R. Torgerson, 2004. Neutron moderator in the Oklo natural reactor and the time variation of Alpha, *Physical Review D*, 69 (12): 121701(R); DOI:10.1103/PhysRevD.69.121701
- Lea, R., 2024. How auroras on Earth, Saturn and Jupiter could help forecast risky space weather, *Space.com News*, issued June 2nd 2024
- Lewin, S., 2015. Neptune's strange magnetic field stretches arms in new model (video), *Space.com*, issued July 08, 2015

- Lewin, S., 2017f. Saturn solstice: Cassini gets 'Ringside Seat' to dramatic seasonal changes, Space.com, issued May 25, 2017
- Li, Cheng, and A.P. Ingersoll, 2015. Moist convection in hydrogen atmospheres and the frequency of Saturn [rsquor]s giant storms, *Nature, Geoscience*, 8: 398–403; DOI:10.1038/ngeo2405
- Li, Cheng, I. de Pater, C. Moeckel, R.J. Sault, B. Butler, D. deBoer, and Zhimeng Zhang, 2023. Long-lasting, deep effect of Saturn's giant storms, *Science Advances*; DOI:0.1126/sciadv.adg9419
- Mathewson, S., 2018b. Jupiter's swirling clouds are mesmerizing in these views from Juno, Space.com, issued May 4, 2018
- Meshik, A.P., C.M. Hohenberg, and O.V. Pravdivtseva, 2004. Record of cycling operation of the natural nuclear reactor in the Oklo/Okelobondo area in Gabon, *Physical Review Letters*, 93 (18): 182302 [4 pp.]; DOI:10.1103/PhysRevLett.93.182302
- Molar Candanosa, R., 2015. Jupiter's Great Red Spot: a swirling mystery, NASA/GSFC release, issued August 4, 2015
- Murrell, M.T., and D.S. Burnett, 1982. Actinide micro-distributions in the enstatite meteorites, *Geochimica et Cosmochimica Acta*, 46: 2453-2460
- Newman, P.A., L. Coy, S. Pawson, and L.R. Lait, 2016. The anomalous change in the QBO in 2015–2016, *Geophysical Research Letters*, 43 (16): 8791–8797; DOI:10.1002/2016GL070373
- Osprey, S.M., N. Butchart, Jeff R. Knight, Adam A. Scaife, Kevin Hamilton, James A. Anstey, Verena Schenzinger, and Chunxi Zhang, 2016. An unexpected disruption of the atmospheric quasi-biennial oscillation, *Science*, 353 (6306): 1424–1427; DOI:10.1126/science.aah4156
- Pappas, S., 2018. These hellish storms on Jupiter are mesmerizing to watch, *Live Science*, issued April 3, 2018
- Peratt, A.L., John McGovern, Alfred H. Qoyawayma, Marinus Anthony Van der Sluijs, and Mathias G. Peratt, 2007. Characteristics of a high-current, Z-Pinch aurora as recorded in antiquity, Part II, Directionality and source. *IEEE Transactions of Plasma Science*, 35 (4): 778 – 807; DOI:10.1109/TPS.2007.902630
- Sánchez-Lavega, A., T. del Río-Gaztelurrutia, R. Hueso, J.M. Gómez-Forrellad, J. F. Sanz-Requena, J. Legarreta, E. García-Melendo, F. Colas, J. Lecacheux, L.N. Fletcher, D. Barrado-Navascués, D. Parker, and The International Outer Planet Watch (IOPW) Team, 2011. Deep winds beneath Saturn's upper clouds from a seasonal long-lived planetary-scale storm, *Nature, Letters*, 475: 71–74; DOI:10.1038/nature10203
- SCALE, 1995. A modular code system for performing standardized analyses for licensing evaluations, N.C.-Rev. 4, (ORNL/NUREG/CSD-2/R4), Volumes I, II, and III, April 1995. Available from Radiation Safety Information Computational Center at Oak Ridge National Laboratory as CCC-545
- Scott, D.E., 2015. Birkeland currents: a force-free field-aligned model. *Progress in Physics*, 11 (2): 167-179.
- Simon, A.A., M.H. Wong, and A.I. Hsu, 2019. Formation of a New Great Dark Spot on Neptune in 2018, *Geophysical Research Letters*, 46 (6): 3108-3113; DOI:10.1029/2019GL081961
- Solanki, S.K., I.G. Usoskin, B. Kromer, M. Schüssler, and J. Beer, 2004. Unusual activity of the Sun during recent decades compared to the previous 11,000 years, *Nature*, 431 (7012): 1084-1087; DOI:10.1038/nature02995
- Space Telescope Science Institute, 2023. Neptune's vanishing cloud mystery: astronomers discover a solar connection, *SciTechDaily*, issued August 19, 2023
- Sromovsky, L.A., P.M. Fry, S.S. Limaye, and K.H. Baines, 2003. The nature of Neptune's increasing brightness: evidence for a seasonal response, *Icarus*, 163 (1): 256–261
- Tiranti, P.I., H. Melin, L. Moore, E.M. Thomas, K.L. Knowles, T.S. Stallard, K. Roberts and J. O'Donoghue, 2026. JWST Discovers the Vertical Structure of Uranus' Ionosphere, *Geophysical Research Letters*; DOI: 10.1029/2025GL119304
- University of California – Berkeley, 2023. NASA's Parker Solar Probe plunges into fast solar wind and discovers its mysterious source, *SciTechDaily*, issued June 8, 2023
- University of California – Berkeley, 2023a. Megastorms on Saturn: 100-year-long storms challenge our understanding of gas giants, *SciTechDaily*, issued August 14, 2023
- Vogt, M.F., M.G. Kivelson, K.K. Khurana, R.J. Walker, B. Bonfond, D. Grodent, and A. Radioti, 2011. Improved mapping of Jupiter's auroral features to magnetospheric sources, *Journal of Geophysical Research*, 116 (A3): A03220; DOI:10.1029/2010JA016148
- Wall, M., 2011. Extraterrestrial hurricanes: other planets have huge storms, too, Space.com, issued on 26 August 2011 at 03:37 PM ET
- Wall, M., 2018e. Soar over Jupiter's monster polar storms with this stunning NASA video, Space.com, issued April 2, 2018
- Wall, M., 2019g. Birth of 'Great Dark Spot' Storm on Neptune seen for 1st Time (Photo), Space.com, issued 26 Mar 2019
- Weaver, D., R. Villard, and A. Parker, 2016a. Hubble discovers moon orbiting the dwarf planet Makemake, NASA Hubblesite News Release Number: STScI-2016-18, issued April 26, 2016
- Weaver, D., R. Villard, R. Sanders, and M. Wong, 2016. Hubble confirms new dark spot on Neptune, NASA – Hubblesite, issued Jun 23, 2016
- Weaver, H.A., M.W. Buie, B.J. Buratti, W.M. Grundy, T.R. Lauer, C.B. Olkin, A.H. Parker, S.B. Porter, M.R. Showalter, J.R. Spencer, S.A. Stern, A.J. Verbiscer, W.B. McKinnon, J.M. Moore, S.J. Robbins, P. Schenk, K.N. Singer, O.S. Barnouin, A.F. Cheng, C.M. Ernst, C.M. Lisse, D.E. Jennings, A.W. Lunsford, D.C. Reuter, D.P. Hamilton, D.E. Kaufmann, K. Ennico, L.A. Young, R.A. Beyer, R.P. Binzel, V.J. Bray, A.L. Chaikin, J.C. Cook, D.P. Cruikshank, C.M. Dalle Ore, A.M. Earle, G.R. Gladstone, C.J.A. Howett, I.R. Linscott, F. Nimmo, J.W. Parker, S. Philippe, H.J. Protopapa,, B.

- Reitsema,, T. Schmitt, M.E. Stryk,, C.C.C. Summers, H.H B. Tsang, O.L. Throop,, S. White, and A.M. Zangari, 2016b. The small satellites of Pluto as observed by New Horizons, *Science*, 351(6279); DOI:10.1126/science.aae0030
- Wendel, J.A., 2016c. What caused the sudden heating of Uranus's atmosphere?, *EOS, Transactions of the American Geophysical Union*, 97; DOI:10.1029/2016EO043473. Published on 13 January 2016
- Wong, M.H., J. Tollefson, A.I. Hsu, I. de Pater,, A.A. Simon, R. Hueso, A. Sánchez-Lavega, L. Sromovsky, P. Fry, S. Luszcz-Cook, H. Hammel, M. Delcroix, K. de Kleer, G.S. Orton, and C. Baranec, 2018. A new dark vortex on Neptune, *Astronomical Journal*, 155 (3): 117; DOI:10.3847/1538-3881/aaa6d6
- Zastrow, M., 2015. "Fingers" of plasma invade Saturn's magnetic field, *EOS, Transactions of the American Geophysical Union*, 96; DOI:10.1029/2015EO037417. Published on 15 Oct 2015
- Zhang, B., Z. Yao, O.J. Brambles, P.A. Delamere, W. Lotko, D. Grodent, B. Bonfond, J. Chen, K.A. Sorathia, V.G. Merkin, and J.G. Lyon, 2024. A unified framework for global auroral morphologies of different planets. *Nature Astronomy*, <https://doi.org/10.1038/s41550-024-02270-3>
- Zhou, Guangyan, Han Yanben, Yin Zhiqiang, Ma Lihua, and Han Yonggang, 2007. Quasi-periodic fluctuations of solar activity in scale of thousand years, *Progress in Geophysics*, (02); DOI:CNKI:ISSN:1004-2903.0.2007-02-016
- Zubritsky, E., 2015. NASA scientists identify missing wave near Jupiter's equator, NASA/GSFC release, issued April 17, 2015
- Zubritsky, E., 2015a. NASA's Cassini finds monstrous ice cloud in Titan's south polar region. NASA TV Cassini, issued November 11, 2015

Acronyms

- AGU* – American Geophysical Union
Caltech - California Institute of Technology
CICLOPS - Cassini Imaging Team and the Cassini Imaging Central Laboratory for Operations
CIRS - Composite Infrared Spectrometer
CXC - Chandra X-Ray Center
EGU - European Geosciences Union
ESA – European Space Agency
ESI – electric soldering iron (mechanism)
ESO – European Southern Observatory
GALACSI - The ground layer adaptive optics system for MUSE
GSFC – Goddard Space Flight Center
HST - Hubble Space Telescope
IC – inner core (of the Earth)
ICME - Interplanetary Coronal Mass Ejection
JHUAPL - Johns Hopkins University Applied Physics Laboratory
JPL – Jet Propulsion Laboratory
MORB – middle-ocean ridge basalt
MUSE - Multi-Unit Spectroscopic Explorer
NASA – National Atmospheric and Space Administration
NH – Northern Hemisphere
OPAL - Outer Planet Atmospheres Legacy
PSP - NASA's Parker Solar Probe
QBO - quasi-biennial oscillation
QPO - quasi-periodic oscillation
QOO - quasi-quadrennial oscillation
RGB - red/green/blue
SCALE software model – a module of a workbench for simulation engineers
SDS-2015 - southern dark spot discovered in 2015
SH – Southern Hemisphere
SSI - Space Science Institute
STScI - Space Telescope Science Institute
TD - tide-driven (dynamo)
UCL - University College London
VISIR - VLT Imager and Spectrometer for mid-Infrared
VLA - Karl G. Jansky Very Large Array
VLT - Very Large Telescope
AGU – American Geophysical Union

ABOUT THE NCGT JOURNAL

The NCGT Newsletter, the predecessor of the NCGT Journal, was begun as a result of discussions at the symposium “Alternative Theories to Plate Tectonics” held at the 30th International Geological Congress in Beijing in August 1996. The name is taken from an earlier symposium held in association with the 28th International Geological Congress in Washington, D. C. in 1989. The first issue of the NCGT Newsletter was December 1996. The NCGT Newsletter changed its name in 2013 to the NCGT Journal. Aims of the NCGT Journal include:

1. Providing an international forum for the open exchange of new ideas and approaches in the fields of geology, geophysics, solar and planetary physics, cosmology, climatology, oceanography, electric universe, and other fields that affect or are closely related to physical processes occurring on Earth from its core to the top of its atmosphere.
2. Forming an organizational focus for creative ideas not fitting readily within the scope of dominant tectonic models.
3. Forming the basis for the reproduction and publication of such work, especially where there has been censorship or discrimination.

